LARGE-SCALE INTEGRATION OF WIND POWER GENERATION ON POWER SYSTEM PLANNING

YUTONG ZHANG

Ph.D

The Hong Kong

Polytechnic University

2010

The Hong Kong Polytechnic University

Department of Electrical Engineering

LARGE-SCALE INTEGRATION OF WIND POWER GENERATION ON POWER SYSTEM PLANNING

YUTONG ZHANG

A thesis submitted in partial fulfillment of the requirements for the Degree of Doctor of Philosophy

April 2010

CERTIFICATE OF ORIGINALITY

I hereby declare that this thesis is my own work and that, to the best my knowledge and belief, it reproduces no material previously published or written or material which has been accepted for the award of any other degree or diploma, except where due acknowledgement has been made in the text.

_____(Signed)

Yutong ZHANG (Name of student)

ABSTRACT

Environment concerns and energy security yields no more time to further delay taking actions against mankind's largest challenge in the 21st century: man-made climate change. The recently rapid development in power electronics and energy conservation under the currently undergoing financial tsunami provide just the opportunity to develop wind generation, which is the most promising and booming one among all renewable energy. The integration of large amounts of wind generation into the existing power system brings in intensive researches into its impact on system reliability, stability and power quality. As a sustainable and renewable energy source, wind is the most promising one, the proportion of which is supposed to become much larger in the future as the era of burning cheap and abundant fossil fuel energy passed. But its variability and average predictability have constrained its full utilization. Research into the impacts of increasing wind penetration on system planning and operation has drawn a major attention recently.

The most obvious obstacle of wind utilization is its variability and average predictability. This unique characteristic must be paid attention to so as to deal with the emerging reliability and operation problems. A higher requirement for wind forecasting accuracy is raised because of the dramatically increased wind power generation capacity all over the world. Therefore, to achieve a high level of wind penetration, an accurate wind speed forecasting tool needs to be built. This thesis proposes a novel short term wind forecasting model based on Ensemble Empirical Mode Decomposition (EEMD) and combination of Support vector machines (Svm). The forecasting results have been compared with the results obtained from the reference models. Extensive tests with historical wind data obtained from meteorological stations in Hong Kong and UK verified that the proposed model is indeed able to produce forecasting results with the highest

accuracy among all the reference models. With the assistant of preliminary applications, the crucial roles that wind speed forecasting tool plays are specified and analyzed, i.e. saving system reserve and improving wind trading price. It has been shown that with a greatly improved forecasting accuracy, a robust wind forecasting tool would improve the wind power integration in both economic and technical aspects.

Increasing amounts of grid-connected wind farms would also be a big challenge in system operation and security since high wind penetration level exert a great influence on system plan and operation. Thus with increasingly installed wind generation into the present electricity networks, it is a big concern to evaluate the wind penetration limit of an existing electric power system since high level of wind penetration will cause various problems.

Under the definition of instantaneous wind power penetration, wind penetration level is the ratio of the wind power output to the total load demand at some specific moment. This type of penetration is also called output penetration. This thesis presents a method of estimating the wind penetration maximum by analyzing the self-organized criticality (SOC) of power system, based on the complexity system theory. SOC is based on the idea that complex behavior can develop spontaneously in certain many-body systems whose dynamics vary abruptly, i.e. the nonlinear dynamics of a complex system under disturbances organized the global system state near to the state that is marginal to major disruptions, often as cascades. In a modern power system, interconnections of power system do not only provide convenience, like enhancing the capability of the electricity network to absorb wind power, but also cause problems. Power systems with strong transmission networks and robust interconnections to neighboring systems are expected to show a superior capability of absorbing large amount of wind power. With the assistant of the slightly modified IEEE

30-bus system and 118-bus system, case studies have revealed the self-organized criticality of the power system as being companied by the increased ratio of the wind power output to the total load demand, i.e. the instantaneous wind power penetration.

Furthermore, under the definition of capacity penetration, wind penetration level is the installed wind generation capacity normalized by the total generation capacity on the system. From the viewpoint of utilities, wind power fluctuations could be considered as a negative stochastic load disturbance sources, which would result in more complicated and uncertain load variations, i.e. lead to a great influence on the frequency control of power systems. Automatic Generation Control (AGC) is one of the key control systems required for a successful operation of interconnected power systems. The primary objective of AGC is to maintain the frequency of each control area and to keep the tie-line power close to the scheduled values by regulating the power outputs of AGC generators to accommodate fluctuating load demands. AGC performances in the normal interconnected power system operation are usually monitored and assessed by interchange power flow, system frequency and other guideline standards all the time. This thesis also focuses on the impacts of wind penetration on the AGC system and estimation of the wind penetration as limited by NERC's new AGC performance standards, CPS1 and CPS2. With the realistic simulations based on the representative and historical system data from the China Southern Power Grid power system, it has been revealed that both CPS1 and CPS2 have been deteriorated as being companied by the increasing installed wind generation capacity normalized by the total generation capacity on the system, i.e. the installed capacity penetration.

ACKNOWLEDGEMENT

First and foremost, I would like to express my sincere gratitude and appreciation to my supervisor, Dr. Kevin Ka Wing Chan, for his invaluable guidance and constant encouragement throughout the challenging path towards a doctoral degree. His enthusiasm and guidance were strong sources of inspiration. He is always available for me in spite of his busy schedule and duties. It has been an honor to work under his supervision.

Obtaining a degree called Doctor of Philosophy is a life changing experience. I honestly never thought it would be this intellectually challenging, but fun and satisfying. I have a wonderful time at my department, Electrical Engineering Department.

I am grateful to all staffs of the Department of Electrical Engineering for their support and help. I would like to acknowledge the help that I received from my friends and coworkers as well.

I reserve special thanks to my father, my mother, my fiancée and other family members who encourage me so much in life and helped me become the person I am today. They are always being supportive. They shower me with love and care, which is why I feel so lucky to have been blessed with the family I have.

TABLE OF CONTENTS

LIST OF FIGURES, TABLES, AND ABBREVIATIONS

LIST OF FIGURES

LIST OF TABLES

LIST OF ABBREVIATIONS

WTGs	Wind Turbine Generators
EEMD	Ensemble Empirical Mode Decomposition
Svm	Support vector machine
EMD	Empirical Mode Decomposition
IMFs	Intrinsic Mode Functions
WFs	Wind Farms
AGC	Automatic Generation Control
CSG	China Southern Power Grid
NARI	Nanjing Automation Research Institute
EMS	Energy Management System
PI	Proportional Integral
LFC	Load Frequency Control
CPC	Control Performance Criteria
ACE	Area Control Error
NERC	North American Electric Reliability Council
CCTF	Control Criteria Task Force
WSCC	Western Systems Coordinating Council
TSR	Tip Speed Ratio
WECS	Wind Energy Conversion System
MOS	Model Output Statistics
NWP	Numerical Weather Predictions
ANN	Artificial Neural Networks
MAPE	Mean Absolute Percentage Error
RMSE	Root Mean Squared Error
SVR	Support Vector Regression

KKT	Karush–Kuhn–Tucker
RBF	Radial Basis Function
SNR	Signal to Noise Ratio
FOH	Forced Outage Hours
SH	Service Hours
LOLE	Loss of Load Expectation
MCP	Market Clearing Price
VaR	Value-at-Risk
CVaR	Conditional Value-at-Risk
CF	Compliance Factor
EMS	Energy Management System
WRF	Weather Research and Forecasting
LNG	Liquefied Natural Gas
ED	Economic Dispatch
UC	Unit Commitment
NCL	Nonconforming Load

CHAPTER I INTRODUCTION

1.1 BACKGROUND AND MOTIVATION

The ongoing and deepening global financial tsunami has extraordinarily hard hit the whole economic and society to the greatest extent. Instead of energy security and environment concerns, financial crisis is the major concern at the moment, and somehow hinder the renewable energy projects. Although the glorious efforts that United Nations made to urge all countries to sign climate accord do not seem quite promising, energy security and environment concerns gives no more time. Besides, the not yet completely disappeared global financial tsunami provides just the change to move away from fossil fuels and ultimately achieve a cleaner economy.

Energy security has become one of the most heatedly discussed topics nowadays thanks to the rising cost and uncertainty of energy. The concern over energy security is not derived only from an exceedingly tight oil market and high oil prices, but it is also from the dwindling stock of other fossil fuel energy. The affordability of traditional fuel energy is one of the most important reasons why the world economy is still relatively stable until now. For a long time, cheap energy, fossil fuels, drives the global economy. However, these cheap fossil fuels do carry a heavy environmental price tag. Extracting fossil fuels despoils the landscape. Burning fossil fuels pollutes the air. And the carbon emissions from burning fossil fuels have proved to be the main cause of the climate change. Global warming is a warning for us to slow down this uncertain tradeoff.

Energy uncertainty and environmental concerns propel us to rethink about using fossil fuel energy and looking for alternatives. Some countries have undertaken much research into nuclear energy, which might be an option. But nuclear energy also causes a series of problems, such as safety, pollution and so

forth. So it is more and more believable that renewable energy will become a considerable potential for increasing security of energy supply. Among all kinds of renewable energy, wind power has emerged as a leading renewable energy technology.

Wind power, among all renewable resources, is the most promising and booming one because of its relatively low cost and mature technology when being compared with the others. Intensive researches have been done to enhance the large amounts of wind integration into the existing power systems. With the increasing wind power capacities, power system planners and operators are facing lots of new challenges because of its unique characteristics, like variability and average predictability. However, both Dr Barack Obama and Ms Barbara Finamore have guaranteed that this is just the time to tackle the transition from a high-carbon to a low-carbon economy, i.e. developing green energy to create new jobs and to pull back the economy [1]. For China, slower energy demand also provides an opportunity to move away from coal and ultimately achieve a greener economy.

China, with a total installed capacity stepping forward from No. 10 in 2004 (764 MW) to No. 6 in 2006 (2,599 MW) in the global ranking, shows an average annual growth rate of over 46% during the last 10 years [2, 3]. China is the second energy consumption country currently due to her rapid economic growth since the 1990s. Besides, with a huge population, China is definitely becoming a super energy consumption country. To deal with this increasing level of energy consumption and the deteriorating state of the environment, Chinese central government has made wind development a high priority. China is rich in wind, with a wind reserve of about 3.2GW, mostly located in the coastal regions and northwest provinces. Thus there is a great potential for China to develop wind energy. Also, Chinese government has the ambition of reaching a wind capacity

of 40 GW by 2020, 100 GW by 2030, and 400 GW before 2050. However, fitting a large amount of wind generation into the existing grid causes lots of technical and economic problems.

The integration of large amounts of wind generation into the existing power system brings in intensive research into its impacts on system reliability, stability and power quality. Wind can only provide reliable energy when the other conditions, like weather, are cooperating. This may cause operation and security problems when substantial amount of wind generation is added to the present electricity system. In other words, more actions and better services are demanded.

The biggest challenge to incorporate large amounts of wind power generations into the existing power system is its variability. Although variability is nothing new in electricity world, it still exerts great influence on power system reliability because of high reliability requirements. A robust tool for wind speed forecasting will improve the wind power integration in both economic and technical aspects.

Wind forecasting is important in ensuring power system reliability and reducing cost of the whole power system in terms of dealing with variable-output generation. A well-performed wind forecasting model will help a lot to “avoid last-minute deployment of expensive reserve power by minimizing the probability of an unexpected gap between scheduled and actual system load”. Different types of prediction in terms of short or long time scale will bring benefits to generation dispatch in electricity market and system security in different aspects. Application of long-term wind prediction allows planning the connection or disconnection of wind turbines and conventional generators [4].

Short-term wind prediction, on the other hand, seems to be more attractive. Some previously applied wind forecasting models includes: statistical wind

forecasting models, ANN wind forecasting models and fuzzy logic wind forecasting models. Short term forecasting is not only useful for all producers who generate wind power to make up schedules, but also helpful for dispatchers to enhance system operation security. The groups participating in electricity markets benefit from wind power prediction in many aspects as well.

The intermittency of wind turbine output may cause stability problems when substantial amount of wind generation is added to the present electricity system. Furthermore, most of the WTGs (Wind Turbine Generators) are asynchronous generators and those synchronous WTGs are actually connected to the grid via some electronic converters, which are quite different from the way conventional generators connected to the grid. The above analysis implies that rotor angle stability might not be an issue when large amounts of WTGs are installed and integrated into the existing electricity network except that the new installation of large amounts of wind turbines will change the power flow patterns, which might cause new stability problem. As a matter of fact, some studies even showed that transient rotor-angle stability could be improved by replacing those conventional generators with WTGs, which might be WTGs' advantages.

However, with voltage stability, in regions with large amounts of wind generation, those wind turbines could have a significant impact on voltage stability following a network fault, or even when the nearby generators are switched on/off due to generation and load mismatch, which may only cause a slight voltage drop. So adequate and fast reactive and voltage controls are required. Although some wind power plants have the ability to control and regulate voltage at or near the point of interconnection to transmission grid, yet something must be pay attention to is that the voltage control applied here should be special. Among all kinds of wind turbines, DFIGs are getting increasing important for its potential reactive power control capability and relatively low

price. The different control strategies of DFIGs are discussed in paper [5-9].

Also, with frequency instability, since DFIGs and generators with full converter interface do not contribute to system inertia because the mechanical frequency and the electrical frequency are totally decoupled, which may lead to frequency instability, particularly in smaller power systems with high penetration of wind generator, like some island or a highly dependent electricity network via only weak connection to the other part of the grid. [10, 11] provide the strategy of applying some special control to creative virtual inertial to contribute to system frequency stability when subject to disturbances. The impacts of different WT technologies on power system frequency stability are discussed in [12-14]. As increasingly WTGs installed into the existing power system networks, the impacts of WTGs on power system frequency are getting more and more attentions.

Because of the variable characteristics of the wind speed and wind direction, and the fact that the output of wind turbines is proportional to the cube of wind speed and depends on wind turbine characteristics, the generation of WTGs would vary largely with the wind. This fluctuant power will affect the power quality of the imbedded grid, such as voltage fluctuation and flicker. There are also some other power quality problems caused by integration of large amount of wind power, like voltage dip [15-20], harmonics [21-23], etc.

1.2 PRIMARY CONTRIBUTIONS

New issues arisen because of large amounts integration of wind power into existing power system need to be addressed by new strategies and better actions. The main objective of this research is to develop new methodologies for assistance to new actions in order to deal with problems caused by adding a good

deal of wind generation into the power system.

To be more specific, the contributions of this thesis are summarized into the following aspects:

(1) This thesis proposes a novel short-term wind forecasting model based on Ensemble Empirical Mode Decomposition (EEMD) and Support vector machine (Svm). The results from Empirical Mode Decomposition (EMD) and EEMD are compared. The methodology developed uses EEMD to identify the intrinsic wind oscillatory modes by their characteristics time scales in the data empirically, and then decompose the wind speed time-series accordingly into different intrinsic mode functions (IMFs) with corresponding frequencies and the residue component. Svm would be combined and used to forecast the IMFs and the residue component. Then Svm would be applied to reconstruct individual forecasting results, which would yield the final result. Based on the corresponding results, the expected impacts of wind speed forecasting with improved accuracy are specified and analyzed. To be more specific, the system reserve requirement is lowered and the wind trading price is improved. A small case study is then carried out to illustrate that the integration of large amounts of wind power into the present power system needs to be supported by robust wind forecasting techniques.

(2) From the viewpoint of utilities, these wind power fluctuations are usually considered as ‘the negative stochastic load disturbance sources’ and would lead to more complicated and uncertain load variations which would have a great influence on the frequency control of power systems. With the recent rapid development in power electronics and increasing demand pressure for

generation with low-carbon emission, more and larger wind farms (WFs) would be grid-connected with increasing penetration levels and contributed more significantly to the system operation and stability. Automatic Generation Control (AGC) is one of the key control systems required for the successful operation of interconnected power systems. This thesis focuses on the impacts of increased levels of wind penetration on the AGC system and estimation of the wind penetration as limited by the new NERC AGC performance indices.

(3) The amount of wind power that can be assimilated by the grid without major problems is highly dependent on 'the nature of the electrical power system itself'. From a system level viewpoint, the third main contribution of this thesis is to evaluate the wind power penetration level by analyzing the self-organized criticality of power system with increasing wind penetration. Based on the complexity system theory, the global state of a system with SOC characteristics would spontaneously vary abruptly to major disruptions under disturbances. The proposed algorithm is implemented on the slightly modified IEEE 30-bus system and 118-bus system. Not only to simulate the power system SOC mechanism under a high wind penetration level, a new AC-based OPF blackout model with consideration of wind integration is proposed to quantify the wind penetration limit and give some good inspirations for power network optimization. Finally, preliminary results specify the corresponding instantaneous power penetration level for both IEEE 30 and IEEE 118 systems as well.

1.3 ORGANIZATION OF THIS THESIS

This thesis consists of seven chapters.

Chapter 1 mainly states the background and motivation of the research, followed by the organization of this thesis and a list of publications of the research work.

Chapter 2, a brief literature review on the application of conventional strategies assisting the integration of wind energy into the existing modern power system, presents a description on the state of the art of the methodologies adopted in this thesis. Also, the theoretical foundations of the novel methodologies and strategies based on new developed mechanisms in this thesis are presented in details. Furthermore, some development progresses in the real electrical engineering industry all over the world are highlighted.

In Chapter 3, wind speed distribution and other characteristics, as well as wind related modelling, are presented in details. Wind speed is a typical time series, which could be forecasted by many models based on historical data. Also, its statistical characteristics could be assessed and analyzed. The unique characteristics of wind must be considered when building wind related modelling.

In Chapter 4, a novel short term wind forecasting model based on EEMD and combination of Svm is proposed and fully described. The most obvious obstacle of wind utilization is its variability and average predictability. This unique characteristic must be paid attention to so as to deal with the emerging reliability and operation problems. To achieve a high level of wind penetration, an accurate wind speed forecasting tool needs to be built. The forecasting results has been compared with those obtained from the reference models. The case study followed would prove that, with a greatly improved forecasting accuracy, a robust wind forecasting tool would improve the wind power integration in both

economic and technical aspects.

In Chapter 5, a new wind power penetration estimation scheme with consideration of AGC control is developed based on the new NERC standards and NARI's novel control strategy. This scheme provides an effective way for utilities to quantify the proper wind power penetration level. The detail China Southern Power Grid (CSG) power system models, which would be adopted as the simulation study in this chapter, have been implemented a hierarchical AGC system developed by Nanjing Automation Research Institute (NARI). And the AGC strategy under NERC's CPS adopted in the Energy Management System (EMS) is an improved proportional integral (PI) control. This control scheme has been proved effective in maintaining frequency quality and providing power support to interconnected control area during emergency. The penetration level of WFs on the CSG power system would be fully studied via realistic simulations based on the representative system data and historical load data.

Chapter 6 presents a method of estimating the wind penetration maximum by analyzing the self-organized criticality of power system. Based on the complexity system theory, the global state of a system with SOC characteristics would spontaneously vary abruptly to major disruptions under disturbances. With the assistant of the slightly modified IEEE 30-bus system and 118-bus system, these two case studies has revealed the self-organized criticality of the power system as being companied by the increased ratio of the wind power output to the total load demand, i.e. the instantaneous wind power penetration.

In Chapter 7, the main contributions of this thesis are finally concluded. Also, some possible directions for future research work are presented.

1.4 LIST OF PUBLICATIONS

1. Yutong Zhang, Ka Wing Chan, "The Impact of Wind Forecasting in Power System Reliability", DRPT 2008, The Third International Conference on Electric Utility Deregulation and Restructuring and Power Technologies, April 06-09, 2008 International Conference Hotel of Nanjing, Nanjing, P.R.China.

2. Yihong Wang, Ka Wing Chan, Shengwei Mei, Yutong Zhang, " A Novel Criterion on Judging Long-term Vogtage Stability", DRPT 2008, The Third International Conference on Electric Utility Deregulation and Restructuring and Power Technologies, April 06-09, 2008 International Conference Hotel of Nanjing, Nanjing, P.R.China.

3. Yutong Zhang, Ka Wing Chan, "Rotor Speed Stability Analysis of Grid Connected Wind Energy Conversion Systems", International Conference on Advances in Power System Control, Operation and Management APSCOM 2009, IET, 8-11 Nov 2009, Kowloon Shangri-la Hotel, Hong Kong.

4. Fei He, Yihong Wang, Ka Wing Chan, Yutong Zhang, Shengwei Mei, "Optimial Load Shedding Strategy Based on Particle Swarm Optimization", International Conference on Advances in Power System Control, Operation and Management APSCOM 2009, IET, 8-11 Nov 2009, Kowloon Shangri-la Hotel, Hong Kong.

5. Yutong Zhang, Bin Zhou, Ka Wing Chan, and Tao Yu, "Investigation of Impact of Wind Power Fluctuations on AGC Performance", International Conference on Electrical Engineering, ICEE 2010, July 11-14, 2010, Paradise

Hotel, Busan, Korea.

6. Yutong Zhang, Deyou Yang, Ka Wing Chan, Peng Zhang, and Guowei Cai, “Short-term Wind Forecasting Based on EMD and Statistical Models”, International Conference on Electrical Engineering, ICEE 2010, July 11-14, 2010, Paradise Hotel, Busan, Korea.

7. Peng Zhang, Deyou Yang, Ka Wing Chan and Yutong Zhang, “Self-adaptive Wide-area Damping Control Based on SSI and WAMS”, International Conference on Electrical Engineering, ICEE 2010, July 11-14, 2010, Paradise Hotel, Busan, Korea.

8. Ye Tian, Bin Zhou, Yutong Zhang, and Ka Wing Chan, “Investigation on the Use of GPGPU for Fast Sparse Matrix Factorization”, International Conference on Electrical Engineering, ICEE 2010, July 11-14, 2010, Paradise Hotel, Busan, Korea.

9. Yutong Zhang, Ka Wing Chan, Deyou Yang, “Short-term Wind Forecasting Based on EEMD and Combination of Svm”, submitted to IEEE Transactions on Sustainable Energy, Manuscript ID - TSTE-00117-2010, under review.

10. Yutong Zhang, Ka Wing Chan, Bin Zhou, “Estimation of Wind Penetration as Limited by NERC's Control Performance Standards”, submitted to IEEE Transactions on Sustainable Energy, Manuscript ID: TSTE-00068-2010, under revision for second review.

11. Yutong Zhang, Ka Wing Chan, Fei He, “Estimation of Instantaneous Wind

Power Penetration by the Self-Organized Criticality", submitted to IEEE Transactions on Sustainable Energy, Manuscript ID: TSTE-00102-2010, under revision for second review.

CHAPTER II LITERATURE REVIEW AND DEVELOPMENT PROGRESS

2.1 LITERATURE REVIEW

It is generally well known that power system planning covers two parts, power system expansion planning and power system operation planning. Electrical power system planning covers the planning for electricity generation, transmission, and distribution systems in the sense that the planning would meet the expected energy consumption economically with proper extent of safety margin.

Among all the renewable energy, wind power is generally accepted as the most promising one since it does not only has those merits shared by all green energy, but also has some other excellent features, such as easy and quick installations, relatively low cost, and so on. Therefore, wind would be the major technology adopted to deal with energy security and environment issues in the future though it has characteristics of undispatchable, intermittent power output, etc, which are obviously going to cause some new challenges to power system planners.

Furthermore, major issues concerned with power system planning, especially those need to be addressed in the event of high level of wind power penetration, would be discussed. Furthermore, some specific terms and standards, which play crucial roles in presenting the contributions of this thesis, would be discussed in details. These sub-topics include, wind forecasting, NERC's new control performance standards, the philosophy of self-organized criticality, and wind penetration level.

2.1.1 POWER SYSTEM PLANNING

Electrical power system planning is not only a technical/engineering problem to solve, but also an economic one, which involves intensive financial investments. The two parts of power system planning, power system expansion planning and power system operation planning, would be discussed in details respectively.

2.1.1.1 EXPANSION PLANNING

Traditionally, power system planning means the expansion planning of electrical power system, which is mostly dealt with forecasting techniques and optimization methodologies [24]. The aim of power system expansion planning is to solve issues regarding the development and expansion of generation units and transmission and distribution networks, in the long run, in order to meet the requirements of the expected load growth in the sense of both reliability and economy. Power system expansion planning consists of two parts, power generation expansion planning and transmission network expansion planning. The former planning cycle lies in the time range of twenty years or more and the latter one is with the forward planning cycle of five to fifteen years. For the power generation section, issues like site selection, type of power plant, and capacity need to be considered and determined. While for the transmission network expansion planning, issues such as type of transmission mode, voltage level, and so on is ought to be analyzed and decided. Once both of the expansions planning sections are finished, financial analysis would be necessary to guarantee that the whole plan is not only economically feasible, but also 'least-cost'.

2.1.1.2 OPERATION PLANNING

The same as expansion planning of electrical power system, forecasting techniques and optimization methodologies would be generally applied to solve operation planning issues as well, only with short time horizon. According to [25], the power system operation planning could be divided into three categories with different time horizons as follows:

(1) Short-Term Operation Planning, from one day to one week;

(2) Mid-Term Operation Planning, from a few months to one year;

(3) Long-Term Operation Planning, from two years to five years.

Operation planning of electrical power system is developed to solve those gap problems between power system planning issues and power system operation issues [26]. The objective of power system operation planning is to find the optimum operation scheme for the existing system capacity in the best possible manner, i.e. to achieve a minimum operation cost under an acceptable degree of reliability.

2.1.1.3 POWER SYSTEM PLANNING WITH WIND POWER GENERATION

Nowadays, the operation planning of electrical power system is required to meet not only the single objective of meeting a set of pre-determined security criteria with highest economical efficiency, but also other objectives such as minimizing the total emissions.

Referring to minimizing the total emissions, green energy would be the first choice to consider for power system planners. Among all kinds of renewable energy, wind energy is a massive power source with relatively mature technology and quick installation procedures, and hence has become one of the renewable energy with the most development prospect. Here, the major issues regarding the power system planning with significant wind power generation would be briefly

addressed. The specific sub-topics, which would be further studied in details in this thesis, will be identified as well.

The unique features of wind resource itself and wind turbine based energy conversion system need to be specially considered in power system planning. Major issues regarding the power system planning with significant wind power generation covers a wide area, in which much previous research work has been done to assist the industry practice. These planning aspects include:

(1) Site selection and relating issues

Site selection would be the first problem being come across by power system planners. Wind resources at different locations would have different characteristics, which could be used to determine what type of wind turbine shall be adopted, the maximum capacity, and the other related issues. [27] carried out an assessment for wind farm site selection, taking account into the economic benefits. Together with the wind farm site selection, another issue needed to be considered is how to plan the wind turbine installations under some specific space constraints. [28] pointed out that, in order to maximize the overall energy output per unit land area, large rating wind turbine installations would lead to a better utilization.

(2) Network infrastructure reinforcement

Good wind resources usually located in remote areas. This means additional transmission / distribution networks need to be built in order to deliver the wind power electricity generation to the load center. This wind integration related expansion planning problem involves huge financial investment and so has to be taken good care of. Especially when a large generation capacity wind farm is connected via a weak transmission / distribution network, the corresponding electricity transmission system might have bottleneck problems. In [29], this transmission capacity limitation problem is dealt with reliability and cost/benefit

analysis by comparing various transmission reinforcement alternatives.

(3) Reactive compensation

Another important issue needed to be addressed is that wind turbine based generators often absorb reactive power when generating electricity since induction generators are usually applied. This sink of reactive power makes proper reactive power compensation planning necessary [30]. [31] proposed an capacitor planning optimization scheme for a power system with wind generations. It has also been proved in [30] that it would be enough to only provide reactive power support inside the wind plant while it would be necessary to provide reactive power compensation in the neighboring transmission networks too.

(4) Energy storage system

Apart from more accurate wind forecasting techniques, energy storage systems might be a good choice to deal with the wind generation intermittency issue. As discussed in [32], as an energy buffer, battery energy storage system could ease the wind power output fluctuations to achieve an optimum power system operation planning with the assistance of proper short-term wind forecasting.

(5) Reserve Margin

Output variations and unpredictability are the biggest challenge that power system planners need to face. As large amounts of wind power generation being added to the existing power system, the system reserve requirements would increase. Better and robust wind forecasting tool would help power system planners to minimize the reserve requirement [33].

(6) Wind penetration level

For each wind farm location candidate, the maximum possible wind generation capacity could be estimated by different criteria. For the whole power

system, there is also a maximum limit for the wind power generation. However, at different angles, wind penetration could be totally different. The wind penetration level estimation is the key contents of this thesis. The state-of-art of wind penetration level estimation would be fully discussed in 2.1.5 while some novel wind penetration level estimation methodologies would be developed in Chapter 5 and 6.

(7) Financial consideration

No matter which sub-area the power system planners are dealing with, economic benefit analysis and financial feasibility study must be executed to decide whether the plan is profitable and feasible. [34] implements a financial assessment method on an Indian wind site, especially considering the operation and maintenance cost whilst [35] concentrates on the market constrained optimal planning problems for multiple wind sites.

(8) The other planning issues

The other wind project related planning issues include the maintenance schedule of wind farm equipments, seasonal management of wind-hydro power systems, and so on, which are mainly on the power system operation planning side.

To sum up, power system planning with significant wind power generation need to take the unique features of wind resource itself and wind turbine based energy conversion system into account. Obviously, the most unique feature is that the output of wind power generation is uncertain and not easy to forecast, which means accurate wind forecasting would be desired. As discussed before, wind forecasting is related to power system planning issues like reserve margin, energy storage system installations, and so on. Since wind forecasting is so crucial, the state-of-art in this area would be fully discussed in 2.1.2. Furthermore, short-term wind forecasting would be another key content of this thesis, which

would be studied in Chapter 4.

Except for the two key components of this thesis, namely wind forecasting and wind penetration level estimation, the other two objects would be discussed in details in the following in this chapter, NERC's new performance standards and the philosophy of self-organized criticality. These two objects are both crucial since they are applied as the criteria to estimate the corresponding wind penetration level limits.

2.1.2 WIND FORECASTING

Among all the challenges engineers would face when trying to incorporate large amounts of wind power generations into the existing power system, the variability and hard-to-forecast is the biggest one. Although variability is nothing new in electricity world, yet it still exerts great influence on power system reliability because of the high reliability requirements. In order to improve the wind power integration in both economic and technical aspects, a robust tool for wind speed forecasting would be desired.

Wind power generation is highly related to meteorological variables, which would be provided as crucial for wind power forecasting. Obviously, wind speed is definitely the most directly linked item. Therefore, wind speed forecasting is an essential prerequisite for wind power forecasting, which is not only important in ensuring power system reliability, but also helpful in the sense of reducing cost of the whole power system operation in terms of dealing with variable-output generation. A perfectly- performed wind forecasting tool would help "avoid last-minute deployment of expensive reserve power by minimizing the probability of an unexpected gap between scheduled and actual system load" to a great extent. Different types of forecasting would have different time scale, which, in many aspects, have benefits to power dispatch and system security.

Application of long-term wind forecasting allows planning the connection or disconnection of wind turbines and conventional generators [4]. Short-term wind forecasting, on the other hand, seems to be more attractive. Methodologies generally used in the area of wind forecasting include numeric weather forecasting methods, statistical methods, and artificial intelligence (AI) [36].

The mechanism of a statistical wind forecasting tool is to directly analyze the wind speed time-series and find the relationship between the forecasting results and wind generation outputs [37]. For statistical methods, the simplest and well-known one of forecasting wind is the simplistic persistence method [38]. For example, when doing one-hour-ahead wind forecasting, this approach uses the past hour wind speed (or wind power) as the forecast for the next hour. This method does not give the impression of a forecasting methodology. But it is not only nearly costless, but performs reasonably well. The persistence method is a very simple model stating as follows:

$$P(t+l) = P(t) \tag{2.1}$$

where $P(t)$ is the production at time t and l is the look-ahead time. This model is popularly called the "what-you-see-is-what-you-get" (WYSIWYG) model. There are a lot of other statistical methods could be applied to wind forecasting. Yet one class of models among them appears to be more attractive. This class of models are called autoregressive integrated moving average model (ARIMA). This class of models normally comprises three components, autoregressive, integrated, and moving average component. Among them, the integrated part is proved that it cannot provide significant improvements on wind speed/power forecast [39]. So the moving average model (MA), the autoregressive model (AR), and the autoregressive moving average model (ARMA) are several commonly used probabilistic models for time series analysis, and all of them are feasible models for wind speed/power forecasting. In [40], an AR-generalized autoregressive

conditional heteroskedasticity (GARCH) model was developed to forecast the probability density function of wind generation output. This method has been applied to five wind farm locations in UK and showed strong potential. To obtain more accurate forecasting results, some much more complicated and robust models were built. In [41], an advanced statistical wind speed forecasting model was built. It separates the wind speed time-series into three subgroups based on their magnitude and forecasts each one respectively. Statistical models, like ARMA models, perform very well in forecasting stationary time series since there are no needs to explore the production background of the time series, which is not the case in wind forecasting. Furthermore, forecasting accuracy by statistical models would be greatly compromised with the increasing forecasting lead time because almost all of statistical forecasting methods try to tune the model parameters by analyzing the difference between the forecasting value and the actual input wind speed. Another disadvantage of using statistical wind forecasting technology is that they are usually not portable, i.e. this site-depending model needs to be tuned or even re-built every time for each specific wind farm.

On the other hand, Artificial Intelligence (AI) models seem to be more attractive in dealing with non-stationary time series. Different from statistical methods, artificial intelligence methods are more being described as a learning approach, i.e. 'let the data speak for themselves' in a non-statistical approach. This feature would make AI technology a better tool to deal with non-stationary time series forecasting, e.g. wind forecasting. In [42], a high order Artificial Neural Networks (ANN) model, the so-called Recurrent Neural Network, was built for wind speed forecasting, and the forecasting results have been implemented into a control system for the optimal operation and management of the power system. A fuzzy model for wind forecasting considering spatial correlation was built in [43]. Spatial correlation [43] is a measure of the tendency for places that are near to

each other to have more similar (positive correlation) or dissimilar (negative correlation) values of their statistics. This fuzzy logic wind forecasting tool has been applied in Eastern Crete in Greece and showed significant improvement when being compared to the persistence method. In [44], an novel AI model was proposed. This adaptive neuro-fuzzy inference wind forecasting model make fuzzy system and neural network complement for each other to serve for wind forecasting. As the most advanced learning machine, Svm is generally accepted as a preferable alternative of ANN. Svm models for wind and other time series forecasting were proposed in [45] and [46], in which the Svm models outperformed the multilayer perceptron model and ANN model, respectively.

When performing wind forecasting, many variables except wind speed, such as wind directions, temperature, air pressure, and so on, need to be considered. The wind forecasting model in [47] is a hybrid model with Bayesian clustering by dynamics (BCD) and support vector regression (SVR), which would solve the commonly encountered data non-stationary and model robustness problems. Among all the models built previously aiming at short-term wind forecasting, in [43] and [48], the spatial correlation factor was considered, which would contribute to developing a robust and accurate wind forecasting tool. However, spatial correlation models require quite long historical data and wind information of different sites and its correlations, which may not be readily available and also high computational cost would be involved. Therefore, this model would not be further considered in this thesis.

Short term forecasting is not only useful for all producers who generate wind power, but also helpful for system operation security, especially for the quantification for system reserve when with large amount of wind power penetration [36]. Reserve requirements for conventional units with large-scale wind power are quantified in [49], in which wind and load forecast error and ramp

rates of traditional thermal power plants are taken into account. As reported in [50], the spinning reserve and production costs increase with increasing amounts of intermittent generation and emissions are reduced accordingly. Transmission planning issues regarding adding large-scale wind farms are analyzed in [51] and [52]. Also, groups participating in electricity markets benefit from wind speed forecasting in many aspects. For example, the forecasting errors in the Spain electricity market were taken into account in [53]. It showed that the error costs could be as high as 10% of the whole generation revenues. Other applications include the sale of wind energy in spot market, the optimization of wind power and other energy resources, and the programming of short period maintenances, etc.

2.1.3 NERC'S NEW CONTROL PERFORMANCE STANDARDS

Increasingly more wind farms (WFs) would be grid-connected because of the recent rapid development in power electronics and more and more demand pressure for generation with low-carbon emission. Increasing higher level of wind penetration would contribute more significantly to the system planning and operation. From the viewpoint of utilities, these wind power fluctuations are usually considered as the negative stochastic load disturbance sources [54, 55] and would lead to more complicated and uncertain load variations which would have a great influence on the frequency control of power systems. Automatic Generation Control (AGC) is one of the key control systems required for the successful operation of interconnected power systems [56]. This thesis would focus on the impacts of increased levels of wind penetration on the AGC system and estimation of the wind penetration as limited by the AGC performance indices.

Primary frequency regulation and Automatic Generation Control (AGC) are the key Load Frequency Control (LFC) functions required for the successful operation of interconnected power systems. The primary objective of AGC is to maintain the

frequency of each control area and to keep tie-line power flow close to the scheduled values by regulating the power outputs of AGC generators to accommodate fluctuating load demands. AGC performances in the normal interconnected power system operation have always been monitored and evaluated by interchange power flow, system frequency and other guideline standards [57]. Generous resources were provided by the System Control Subcommittee to the power engineering community to encourage researches related to AGC [58]. Prepared under the auspices of the Electric Power Research Institute, basics that are applicable to modern power system and AGC were presented to assist those interested research parties [59]. The control area's AGC performance in normal interconnected power system operation had been monitored and evaluated by Control Performance Criteria (CPC), A1 and A2 criteria, since 1960s [60]. Both A1 and A2 criteria are based on a term called Area Control Error (ACE), which could be defined as 'the difference between scheduled interchange and metered control area boundary flow, plus a factor proportional to the difference between prevailing and scheduled interconnection frequency' [61]. A1 criterion requires that 'ACE return to zero within ten minutes of previously reaching zero'. A2 requires that 'the average ACE for each of the six ten-minute periods during the clock hour is within specific limits', referred to as *Ld*. The value of *Ld* was specified by North American Electric Reliability Council (NERC). The NERC's Control Criteria Task Force (CCTF) was formed in mid-1980. NERC addressed the criticisms of A1 and A2 with 'technical justification, modification, or replacement with new criteria'. These updated new standards were results of continuous analytical studies, which were reported in details in [62]. Continued enhancement of these schemes are expected through some novel practices with new developed logic algorithms and process control technology [63].

However, over the years, it was highly believed that good A1 and A2 control area performance do not necessarily indicate a satisfactory interconnected system operation. With solid technical foundation, it is believed that a new control performance standards, CPS1 and CPS2 [64], would not suffer from such criticism. The new standards were designed in the way that the system control performance was evaluated without prescribing how control would be accomplished, which 'allows control areas to tailor their own algorithms to maintain the necessary control of area interchange flows and interconnection frequency while minimizing non- productive adjustments of generation'. Therefore, this new standards would make generators to be operated in a more efficient way. In addition, minimum maintenance would be achieved because of less wear and tear. These new control performance standards also provide a method of controlling the system frequency features [65].

On 1 February 1997, the old A1 and A2 standards were replaced by the North American Electric Reliability Council (NERC) with a new control performance standards, CPSl and CPS2 [66]. All the Western Systems Coordinating Council (WSCC) control areas discarded automatic time error control from AGC since October 1997 [67]. Control areas in NERC began to adopt CPS for control performance evaluation on 1 February 1998. 'Each control area is required to monitor its control performance and report its compliance with CPS1 and CPS2 to NERC at the end of each month.' In the beginning, several pioneer control areas took advantage of this new strategy in evaluating control performance with some greatly improved efficiencies [64]. In 2005, NERC published the new Control Performance Standards document (Standard BAL-001) on its Official Website [68].

2.1.4 SELF-ORGANIZED CRITICALITY (SOC)

The philosophy of self-organized criticality was firstly introduced in 1987 by Bak, Tang and Wiesenfeld [69]. It is based on the idea that complex behavior can develop spontaneously in certain many-body systems whose dynamics vary abruptly, i.e. the nonlinear dynamics of a complex system under disturbances organized the global system state near to the state that is marginal to major disruptions, often as cascades [70].

The research into the failure data of North America illustrates that the scale of power system blackout has the power law characteristics [71]. This instanced that the complex electric power transmission systems obey self-organized criticality like dynamics since power law distribution is a typical token of self-organized criticality [72, 73].

As a general tendency, interconnections of power system do not only provide convenience, like enhance the capability of the electricity network to absorb wind power, but also cause problems. For example, cascading events are highly likely to occur in large and heavily stressed power systems. Modern electricity network is such a system since the transmission system are running more and more closely to their operating limits due to the increasing consumption and economical tradeoff. Therefore, as important as the state of individual components, the global system state needs to be analyzed as well from a system level viewpoint.

To prevent power system suffering from cascading failures and loss of loads, many models revealing the self-organized criticality of power system have been explored. These models include, the CASCADE model based upon load transfer [74], branching process model [75], Hidden failure model [76], OPA model [77], the Manchester model based on load cutting and AC flow [78], and so on. Among all these models, only the Manchester model applies AC flow. Neither the CASCADE model nor the Branching process model sufficiently describes the

necessary elements of a typical power system except for describing the network characteristics.

In this thesis, reactive power and voltage aspects have to be considered when accounting wind power into power flow analysis. DC models, such as Hidden failure model and OPA model, assumes that the angle differences between nodes could be neglected, which is not the case under high wind penetration level. Although based on AC flow, Manchester Model assumes that the generator output is fixed, i.e. the failure scale is overstated.

Based on the OPA model and Manchester model, [79] proposes another AC model, which simulates the cascading failures and depicts the power system evolution process. Not only to simulate the power system SOC mechanism under a high wind penetration level, a new AC-based OPF blackout model with special consideration of wind integration is proposed in this thesis to quantify the wind penetration limits and give some good inspirations to power network optimization.

2.1.5 WIND PENETRATION LEVEL

A few terms need to be defined before estimating the wind penetration levels. There are several definitions for wind penetration under specific conditions.

(1) Installed capacity penetration:

This is the installed wind generation capacity normalized by the total generation capacity on the system, including wind generation capacity.

(2) Instantaneous wind power penetration:

This is the ratio of the wind power output to the total load demand at some specific moment. This kind of penetration is also called output penetration.

(3) Energy penetration:

This is the electricity transformed from wind energy fed into an electrical system, normalized by the total electricity consumption in the whole

electrical system over a given period.

As could be seen from the above definitions, at different angles, wind penetration could be totally different. In this thesis, the first two definitions would be adopted and estimated in different cases, which would be described in detail in the following chapters.

The amount of wind power that could be assimilated by the grid without major problems is highly dependent on the nature of the electrical power system itself [80]. Power systems with strong transmission network and robust interconnections to neighboring systems are expected to show a superior capability of absorbing large amount of wind fluctuations [81]. Denmark is an outstanding case with a wind power penetration limit of 50% or so, a wind energy penetration level of about 16.2%, and an installed wind capacity penetration level of around 29.0% [82]. For the enabling of a substantial amount of wind power integration, intensive researches have been done to assist the determination of the wind penetration limit. A method of quantifying wind penetration was applied based on the amount of fluctuating power that could be filtered by wind turbine generators and thermal plants [83]. The results yield a penetration level of 50% when being estimated conservatively and a bold attempt of 90% when the smoothing capability was vastly improved. The transmission capacity of an existing transmission system considering a large amount of wind integration was estimated according to its thermal limitations [84]. Furthermore, the frequency response between fixed speed generator and doubly-fed induction generator was compared with frequency stability analysis as well. The wind penetration level could also be limited by N and N-1 criteria [85], in which, it is shown that wind turbine-generators should be equipped with fault ride-through (FRT) capabilities to increase the maximum penetration level. The FRT capability of a wind turbine-generator is its ability to remain stable and connected on-line when the voltage in the grid is temporarily

reduced due to a fault or load change in the grid. In [86], wind penetration level limit is assessed by maintaining an acceptable voltage stability condition for the system. The assessment of penetration limit in isolated electricity grids were reported in [87, 88], in which some simple but efficient methods for quantifying the maximum penetration level in autonomous systems were illustrated, like the situation in an island [89].

However, as more and more wind power generation being integrated into the existing power system, higher voltage level connected to the grid is becoming a trend. Also, as mentioned before, power systems with strong transmission network and robust interconnections to neighboring systems are expected to show a better capability of absorbing wind power generation [81]. Therefore, the upper limit on wind power penetration will definitely rise when interconnectivity strategy is adopted. Until now, few researches have been done to analyze the relationship between the wind penetration level limit and the robustness of the corresponding electricity network. Although some previous research did consider the integration of large amounts of wind power generation into the grid rather than just an island system, yet the application was limited to a quite small test system [83]. Besides, only coal-based thermal power plants were considered when developing the power system model. These extremely important factors would be taken account into and fully studied in the following chapters.

2.2 WIND DEVELOPMENT PROGRESS AROUND THE WORLD

It has been witnessed that wind power was developed really fast in the last several tens of years. From small-scale experimental testing systems that originally often used as a concept demo to large-scaled wind farms that directly connected to the power grid, the wind turbine based generators are becoming

larger and larger in size. Also, to accommodate more and more wind power generation that integrated into the existing electricity networks, power system planners and operators have overcome many technical and economic challenges. Especially since 2004, wind generation, the most promising and mature technology, is booming dramatically. Experiences around the world have proved that the integration of large amounts of wind power generation into the model electricity network is possible. More than that, wind energy is becoming the driving force for not only the climate protection and economic development, but also the creation of future-proof jobs.

The three main markets, Europe, North America, and Asia, are dominated by the United States, Germany, and China respectively, a situation of tripartite confrontation.

2.2.1 US

The U.S. wind industry is definitely one of the most booming ones all over the world. The U.S. government has taken many strategies and policies to push the research on the development of wind energy, which subsequently stimulated the wind industry. Billions of dollars were invested on various wind energy related projects. In the meantime, various preferential policies were offered by the U.S. government to support the development of wind industry, such as tax exemptions and reductions, and so on.

Though until 2004, the electricity generated from wind in U.S. only accounted less than 1% of its total power consumption, it is still believed that the wind industry in U.S. would be quite promising. According to American Wind Energy Association, after 2007, U.S. overtook Germany as the largest wind power user in the world. Most especially, nearly 10,000 MW of new installed wind generating capacity is achieved by the end of 2009. The total installed wind

generating capacity in U.S. is now over 35,000 MW, ahead of Germany, which had an installed capacity of 16,800 MW [90]. This is a huge achievement comparing with the situation by the end of 2000, when U.S. only have an installed wind generating capacity of 2,600 MW. With the continuously strong installations of wind farms, the U.S. department of Energy put forward a report, which entitled a projection of 20% wind energy by 2030.

2.2.2 GERMANY

In the sense of making use of wind energy to generate electricity and developing wind industry, Germany is the most advanced country all over the world. Germany is believed to be the most advanced country in the development of wind technology and industry since wind power currently supports about 7.5 percents of the total electricity consumption of this country, which let the other countries be too far to catch up with Germany in this industry. Until 2007, Germany was the largest user of wind power in the world. With an installed wind generating capacity of more than 22,300 MW, Germany is ahead of U.S. by 5,700 MW [90].

Installed capacity is not the only achievement Germany made. German manufacturers and suppliers eventually win markets overseas. Nearly 28% of the world's quota, which is a turnover of about 22.1 billion Euros, was contributed by German wind industry related manufacturers and suppliers in 2007. The export quota in 2007 increased by more than 9% compared to the one in 2006. Together with installation, another turnover of more than 7.6 billion Euros from wind operation and maintenance services is achieved by the German wind industry. Furthermore, this industry also contributes a lot for creating more employment opportunities.

The German government has pledged to support the wind industry with

preferential loan and tax preference. Furthermore, electricity generated by renewable energy would be unconditionally purchased by German power companies at a support price set by the government. However, the German government still wishes that, in the future, even without the preferential loan and tax preference provided by the government, electricity generated by wind energy or other renewable energy would be able to compete with the other conventional ones.

2.2.3 DENMARK

Speaking of wind industry, the first country would be thought of was Denmark, who has always being a pioneer in developing wind power. In 2007, wind power provided almost 20% of electricity production in the whole country, which is an achievement that the other countries would not keep up with [91]. Even in the long term, this significantly higher proportion is not that easy to be surpassed by any other countries.

Denmark government set a good example for the other countries of how government support could make an alternative energy source, in this case, wind, commercially possible and viable, even promising. The Denmark government provides not only subsidies and electricity tax repayment for privately owned wind turbines to stimulate demand, but also sufficient funding for research and development. In Denmark, private wind turbines are allowed to be directly connected to the national grid after some technical tests, which would overcome one of the main drawbacks of wind energy, variations. This policy does not only stimulate the demand, but also make the fluctuations to be averaged and thus provide relatively constant electricity.

Prosperous wind industry development in Denmark does not only make Denmark less dependent on imported energy supply and reduce the pollution of

the environment, but also play an important role in earning foreign exchange. Nowadays, nearly half of the wind turbines all around the world are with Danish trademarks.

As a country with a quite small territory, Denmark is connected by transmission line to other European countries. As a result, Denmark does not need to install additional peak-load plant or add more reserve to balance its wind power variations. However, additional electricity purchases from its neighbor countries would be necessary. The Denmark government has already proposed an even bolder and more ambitious plan to further strengthen the national power grid in order to integrating more wind power generations into the existing Danish power system.

2.2.4 SPAIN

Among all European countries, the battle for Europe wind domination has always being between Spain and Germany. Currently, after the United States, Germany and China, Spain is the world's fourth biggest producer of wind power generated electricity. Until the end of 2008, Spain has reached a wind power generating capacity of 16,740 MW with an increase of 1,600 MW for year 2008 [92]. On 10 November 2009, thanks to the over five hours' strong winds, over 53 percents of the Spain's power came from wind energy, which means for the first time, the instantaneous wind power penetration level in Spain reached to more than 50% [93].

Compared to other leading countries in wind industry, Spanish wind turbine manufactures are good at making bigger size of turbines but with less turbine weight. Not only leading in the wind related equipments manufacturing, the Spain Government has proposed a target of 20,000 MW in installed wind generating capacity by 2010.

2.2.5 CHINA

At the end of 2009, only after the Unites States and Germany, China has become the third largest wind power producer in the world with an installed wind electricity generating capacity of 25,100 MW [94]. Under the still ongoing global financial crisis, the wind industry development in China is far from being hindered, but rose as a new key force to pull back the country's economy. New developed industry needs support from the government. Except for tax preference and the other preferential policy, the National People's Congress permanent committee has passed a law, which requested the corresponding Chinese energy companies to purchase all the electricity produced by wind energy with absolutely no strings attached [94].

China has mass and long coastline with huge wind resources that could be transformed into electricity. With intensive and enormous amount of investment in wind industry, preferential policies offered by the government, and unique geographical advantages, not surprisingly at all, China is the country with fastest-growing wind industry.

2.3 SUMMARY

In this chapter, a literature review on the application of conventional strategies assisting the integration of wind energy into the existing modern power system is presented with a description on the current state of the art on the methodologies adopted in this thesis. Furthermore, the development progress in the power industry in different countries around the world including USA, Germany, Denmark, Spain and China is briefly described with practical experiences being highlighted.

CHAPTER III WIND CHARACTERISTICS AND RELATED MODELING

3.1 INTRODUCTION

The recently rapid development of wind energy could assist in significantly reducing the combustion of conventional fossil fuel, i.e. producing energy with much lower carbon emission. Due to the current energy security challenges and increasingly growing environmental consciousness, it would be extremely imperative to develop green and renewable energy. Wind is one of most leading and promising clean energy techniques nowadays. Growth in wind generation all over the world is driven not only by the greatest challenges facing humanity, environmental concerns, but also by the rapidly updated understanding of the wind resource. When actually transforming wind energy into electricity in the real electrical engineering world, it would be very important to analyze the statistical characteristics and other crucial features of the wind for purposes like forecasting the energy output generated from a wind energy conversion system. For instance, it is important to verify that the methodology applied for analyzing and measuring wind would, to a great extent, yield an estimation of the energy produced that is close to the actual wind energy captured since wind is varying all the time.

Due to the intermittency characteristics of wind, it would cause some technical and economical problems when integrating a large amount of wind power into the existing electricity networks. In order to analyze the impacts on power system plan and operation brought by large amounts of wind generation integration in depth, the unique characteristics of wind must be considered, especially when building the wind related models.

In this chapter, the key properties of wind resource would be discussed.

Furthermore, the wind related models considering the unique characteristics of wind would be introduced and described.

3.2 WIND RESOURCES

From a meteorological point of view, records collected from weather stations were the only resource where historical wind data could be measured and collected. However, with the fast booming of wind industry, historical data collected from weather stations would not be sufficient, especially when considering the commercial and large amounts integration of wind generation produced by multi-megawatt class wind turbine based generators. This is because that the meteorological data itself is lack of detailed information about wind speed and characteristics variations with the alteration of the height of the wind turbines, the local wind conditions of a particular terrain, and so on.

With the extremely rapid development of wind industry all over the world in the past several decades, researchers and engineers in those leading countries of wind industry have done extensive wind measurement and analysis work, taking account of the unique characteristics of wind resources and application of wind turbines. This preliminary work regarding wind resources would be the first step for a successfully planning of any wind farms intending to connect to the power grid.

3.2.1 CAUSES OF WIND ENERGY

Wind energy is originally generated from solar energy. Basically, the earth atmosphere is like a huge heat engine, which extracts binding energy from the sun and delivers this energy to earth in the form of light. This radiation from the sun mostly is then absorbed by the earth surface. Some of the radiation is afterwards

reflected to the earth atmosphere above. The earth surface is with different terrains and landscapes, such as mountains, lake, desert, and so on. Also, the solar energy absorbed by earth surface would vary with respect to different geographic distribution, the time of the day and the annual distribution, which would produce different temperature, density and pressure. Thus, the air masses and pressures would vary from one place to another temporarily. Air within the region with higher pressure would flow to the region where the air pressure is relatively low. Thus, the difference in air pressure is the direct cause of wind flow. Several factors played an important role in determining the wind characteristics include solar radiation, air pressure, temperature, land surface roughness, and so on.

There are typically three forms of wind flow patterns:

(1) **General Circulation of Atmosphere:** General circulation of atmosphere is caused by solar radiation and earth rotation.

(2) **Sea-Land Breeze:** Sea-land breeze, in the coastal areas, is with reference to the wind direction alternations of breezes between land and sea, i.e. onshore wind and offshore wind, which is caused by the day and night temperature changes.

(3) **Mountain-Valley Breezes:** The wind directions of mountain-valley breezes alter because of the temperature changes between days and nights, i.e. anabatic wind and katabatic wind.

3.2.2 UNIQUE CHARACTERISTICS OF WIND

Compare with coal, natural gas and other forms of fossil fuel generated energy, i.e. traditional energy, wind energy has many merits, which could be summarized as:

(1) Wind is free. Thus, wind farms need no fuel.

(2) Wind produces no waste or greenhouse gases.

(3) Developing wind generation is a good method of supplying energy to remote areas.

(4) The most important reason is that wind is "comprehensively cheap" when comparing with other renewable sources.

However, wind is never impeccable. The following are the demerits of using wind energy:

(1) Wind is not always available - some days, there is no wind at all.

(2) Suitable areas for wind farms are often expensive.

(3) Covering the landscape with wind turbines could be unsightly.

(4) Wind farms could be noisy, either in the way could be heard, or in the way that could affect television reception.

Among all the weaknesses of utilizing wind energy, the following two should be addressed carefully:

Variability and Fluctuation: Due to constantly changing of airflow, wind varies from seconds to seconds, which would lead to fluctuated wind power output. Variability and fluctuation, as well as the unpredictable characteristics of wind, would be the biggest drawback of wind. This unique feature has adverse effects on power systems stability and security, power quality, power system reliability, and the planning of the electricity networks.

Low Energy Density: Air mass density is quite low, only one eight hundreds and sixteenth of the water mass density. Low air mass density implies that it would be very difficult to capture wind energy and turn it into other form of energy.

Another one of the most important phenomena needs to pay attention to in the process of wind turbine installation in the real industry world is that wind speed would increase with the altitude. When wind moves against the earth

surface, wind speed would be slowed down because of frictions between flowing air masses and earth surface. According to [95], wind speed would be undisturbed between the range of 600 and 2000 m, which is called the atmospheric boundary layer, above ground under different conditions.

3.2.3 WIND TURBINE BASED GENERATORS

Most of the wind power generators are based on induction machines, which would not contribute much to the power system frequency regulation and require reactive power support. Therefore, wind farm should be connected to some network with super ability of absorbing power fluctuations. Unfortunately, wind farm usually locate at those remote areas and mostly connect to the network on the distributed level or sub-transmission level, which are not originally designed to deliver a lot of power to the grid. Therefore, constraints like the thermal limits, voltage quality and stability need to be taken care of when there is a large-scale wind power integration. Wind farm modeling is crucial when analyzing the power system stability, reliability and power quality with large amount of wind power being integrated into the existing grid.

There are mainly four types of induction generator based modern wind turbines occupying the industry and academic circle nowadays.

(1) Cage rotor induction generator

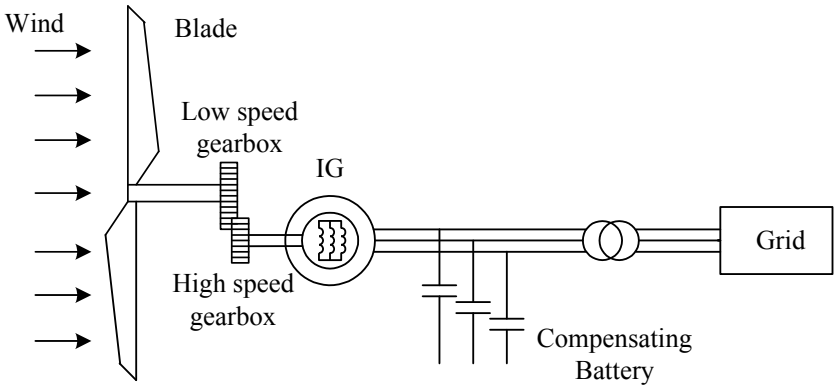

Fig. 3.1 Cage rotor induction generator

Mostly, cage rotor induction generator as shown in Fig.3.1 would be directly connected to the grid. The low turbine rotor rotational speed would be turned into a high rotational speed of the induction generator via the gearbox. The output of the generator would be related to the variation of the speed and the slip. This kind of generators would have high starting currents, which would be limited by some thyristor soft-starters. In addition, capacitor banks would be used to provide reactive power compensation. This type of induction generator based wind turbines is simple and cheap. It is also called fixed speed wind turbine.

(2) Wounded rotor induction generator with rotor resistance control

The slip of this type of induction generators is proportional to the resistance of the rotor windings. Therefore, the generator speed could be varied in the range of 10% or so by varying the slip, i.e. the rotor windings. Thus, it is also called limited variable speed wind turbine.

Both the above two types of wind turbines would be operated at a super-synchronous speed in order to generate electricity. The reactive power compensation could be achieved by capacitor banks or other kinds of power electronic equipments, such as SVC and so on.

(3) Doubly fed induction generator (DFIG)

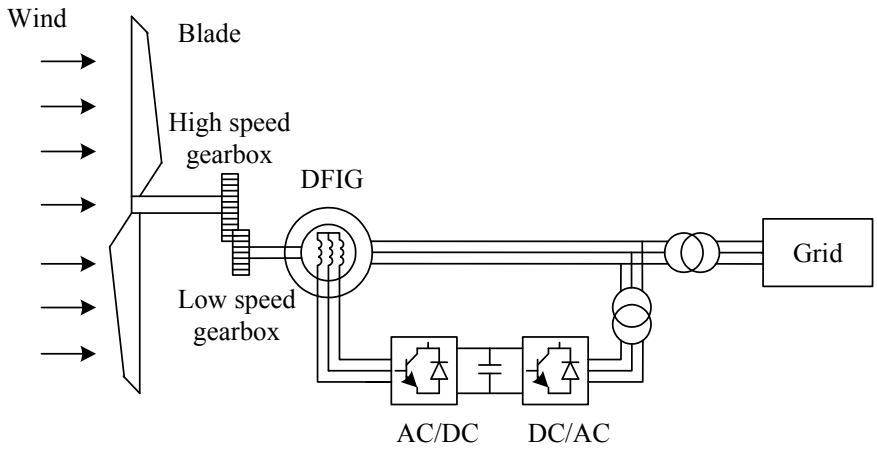

Fig. 3.2 Doubly fed induction generator

The stator of a DFIG as shown in Fig.3 would be directly connected to the grid and thus would be the main path for the energy transfer to the grid. While the rotor of the generator is connected to the grid by electronic converters through slip rings, which enable around 30% of the rotor speed variation. The above analysis implied that the nominal power of the power electronic converter system could be around 30% of the wind turbine since only part of the power generated would be fed via power electronic converter, which would be the greatest advantage of DFIGs.

(4) Full rate power electronic interfaced generators

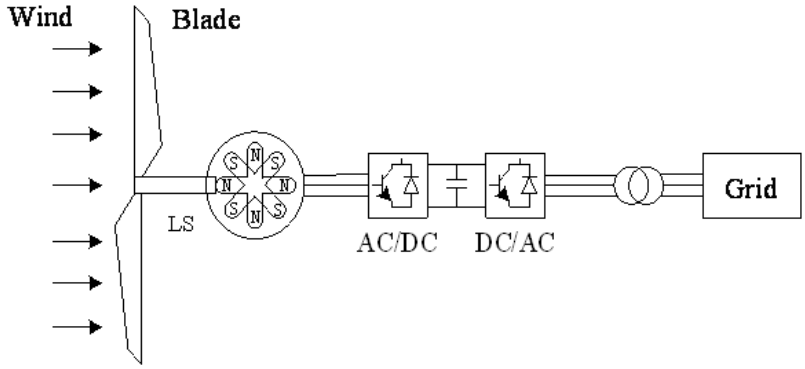

Fig. 3.3 Full rate power electronic interfaced generator

By using a full rated power electronic system as shown in Fig. 3.3, the generator would be totally decoupled from the AC work. The converter at the grid side controls the active and reactive power output, which is its advantage because of the improvement of the dynamic response. However, this type of induction generator has not been applied widely because it is much more expensive.

3.2.4 CONTROL CONCEPT OF WIND TURBINE

Like the design of other prime movers, wind turbines would be designed in a way that it would generate electricity at a minimum cost. In practice, this also means that sometimes it would be necessary to give up some of the excess

energy in order to prevent the wind turbine from damaging itself. Thus, every kind of wind turbines would be designed with power control.

There are three commonly used control strategies in modern wind generation industries: pitch control, stall control, and active stall control. Generally speaking, any type of control strategy, or a combination of any two of them, could be adopted for a fixed speed wind turbine. While for a variable speed wind turbine, pitch control would be the one adopted.

These three commonly used control concepts are introduced in details as follows:

(1) Pitch control: A wind turbine with the ability of pitch control could adjust the power performance coefficient C_p by turning the angle of its rotor blades according to the specific environment. These blades could be either turned out the wind when the wind generation is too high or turned into the wind when the wind generation is becoming too low.

Adopting this type of control strategy would allow the wind turbines to perform efficient power control, assisted start-up and emergency stall. However, there are also some pitfalls as well. For instance, there would be extra complexity due to the pitch mechanism and strong generation output fluctuations when the wind speed is relatively high.

(2) Stall control: Among all these three types of control concepts, stall control is quite popular since it is very simple, robust and cheap as well. Contrary to the pitch controlled turbine, for stall control, the blades are locked onto the hub at a fixed angle. Therefore, this type of power control would be provided by the aerodynamic performance of the blades. The rotor stalls would act once the wind speed exceeds the cutout wind speed, i.e. shutting down the WECS. Compared to pitch control, there would be less power fluctuations by applying slow aerodynamic power control, i.e. stall control. This type of control would not be

desired at low wind speeds due to its low efficiency. Besides, the maximum steady state power would vary with air density and grid frequencies. The other disadvantages of adopting this control method include no assisted start-up and so on.

(3) Active stall control: At lower speed, active stall control is kind of acting like a pitch control, i.e. tuning the angle of the blades would achieve the stall control. However, when under high wind speed, the blades would enter into a deeper stall state, i.e. the blades would be tuned to the direction just opposite to that of the wind turbine adopting pitch control scheme. The attack angle of the blades would be increased to a stall situation instead of pitching the blades out of the wind.

A smoother generation would be achieved without strong output fluctuations when wind turbines are equipped with active stall as in the case of simple pitch control. By using this control strategy, the variations in air density would be compensated. For active stall control, the incorporation of pitch mechanism makes wind turbines much easier to perform emergency stops and to start-up.

3.3 WIND RELATED MODELING

The output of a wind turbine based wind energy conversion system is relating to many factors, such as wind speed distribution, wind turbine modeling, electric generator modeling, etc.

To analyze the impact of large amounts of wind power integration on power system stability and power quality, the static and dynamic behavior of the complete wind farm has to be modeled accurately.

A complete model of a wind farm should include a number of detailed wind turbines. However, the computation and analysis of a large number of detailed

wind turbines based generators could be time-consuming and impractical. Therefore, a method called turbines aggregation needs to be adopted. How many turbines should be aggregated depends on every specific situation. When analyzing the impacts on local stability, a detailed model of every single wind generator with mechanical components and controller devices has to be taken into account. Otherwise, an aggregated wind farm model with a number of wind turbines would save the calculation time.

3.3.1 WIND SPEED STATISTICS

Wind speed distribution is one of the most important characteristics of wind. This crucial feature provides valuable information for not only the evaluation of the performance of WECS and the wind energy potential, but also the environmental and structural analysis and design. Therefore, it is always a desirable objective to develop a proper statistical model, which could perfectly describe the wind speed frequency distribution.

There are several probability distributions which could be used to describe the wind speed feature on a specific site, including the *Weibull* distributions [96], the *Rayleigh* distributions [97], the *Chi-2* distributions [98], the *Lognormal* distributions [99], and so on. The two most commonly used ones are the *Weibull* distributions and the *Rayleigh* distributions. The *Weibull* distribution has two parameters and thus is more versatile. On the other hand, since the *Rayleigh* distribution has only one parameter, it is simpler to use. In this thesis, the *Weibull* distribution would be introduced in details.

Given a time series of wind speed *v1*, *v2*, …, *vn*, the wind speed is considered to be distributed as a Weibull distribution, i.e. its probability density function is as follows:

$$p_{df}(v) = (\frac{k}{c})(\frac{v}{c})^{k-1} e^{-(\frac{v}{c})^k} \tag{3.1}$$

where v is the wind speed, k is the shape parameter and c is the scale parameter. So once the two specific parameters, c and k, are known, the mean wind speed and the standard deviation of the wind speed could be determined. In other words, c and k could be used to describe the wind characteristics at any site.

For example, if the shape parameter (k) = *2* and the scale parameter (c) = *7*, the wind speed probability density function would be Weibull (7, 2), which is plotted as the below figure,

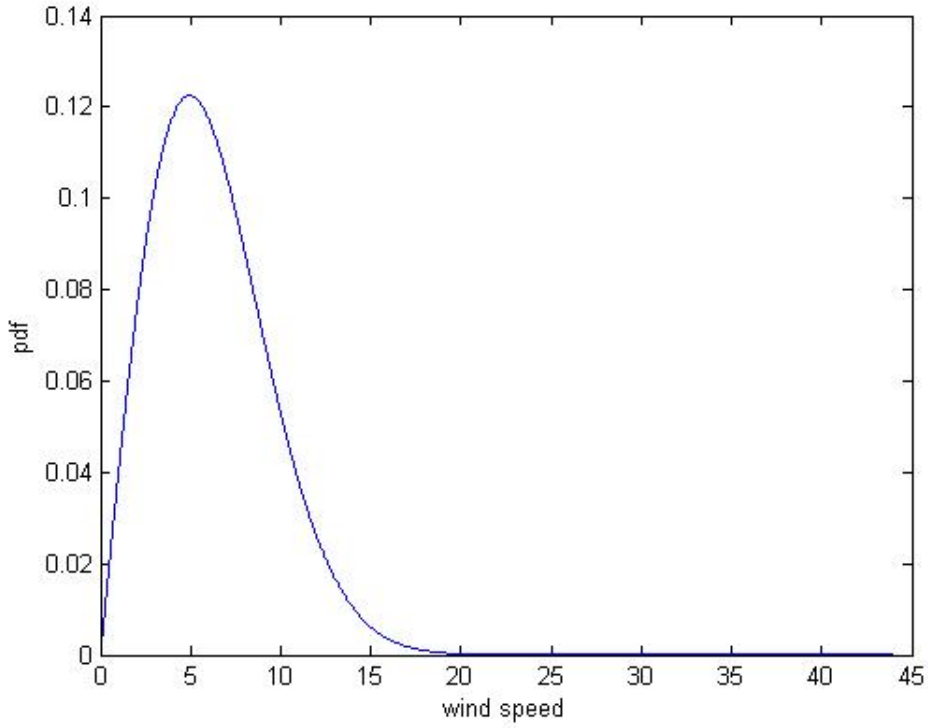

Fig. 3.4 Wind speed probability density function example

Wind data in a short period, a few hours or even one or two days, usually would not be well fitted by a Weibull or any other statistical function. However, if it is for some long period, several months to a few years or more, the Weibull distribution usually fits the observed wind historical data quite well.

Wind speed probability density function gives a good expression to the statistic characteristics of wind resource. Therefore, it is an essential parameter when planning wind farm integration.

3.3.2 WIND VELOCITY MODEL

For the purpose of accurately describing wind and its unique characteristics, a wind speed model consisting of four components would be usually adopted as follows [100]:

$$v_w = v_{wM} + v_{wG} + v_{wR} + v_{wN} \tag{3.2}$$

where v_{wM} is the mean wind velocity in m/s, which is also called the base wind velocity, v_{wG} is the gust wind component in m/s, v_{wR} is the ramp wind component in m/s, and v_{wN} is the noise wind component in m/s.

Equation (3.2) indicates that the turbulent wind velocity component are comprised of three parts; among them v_{wG} and v_{wR} are deterministic parts while v_{wN} is the stochastic part to forecast the occurrences of wind turbulence and the correlation of wind turbulences at different locations in a wind farm. These four wind velocity components would be described in details as follows:

(1) The base wind velocity could be obtained from the parameters of the Weibull distribution as follows:

$$v_{wM} = c \cdot \Gamma[1 + \frac{1}{k}] \tag{3.3}$$

where c and k are the scale parameters and shape parameters of the Weibull distribution, $\Gamma(\cdot)$ is the gamma function.

(2) To perform dynamic studies, the essential mission is to model the gust wind component, which could be used to express sudden changes of wind. This could be described by the equation as follows:

$$v_{wG} = \begin{cases} 0 & t < T_{G0} \\ v_{\cos} & T_{G0} < t < T_{G0} + T_G \\ 0 & t > T_{G0} + T_G \end{cases} \tag{3.4}$$

where

$$v_{\cos} = \frac{MaxG}{2}\{1 - \cos 2\pi[(t / T_G) - (T_{G0} / T_G)]\}$$

T_G = gust period in s

T_{G0} = gust starting time in s

$MaxG$ = gust peak in m/s

t = time in s

(3) The ramp wind velocity component could be used to simulate those step wind velocity changes, ramps of either positive or negative slopes, which could be describe as follows:

$$v_{wR} = \begin{cases} 0 & t < T_{R0} \\ v_{ramp} & T_{R0} < t < T_{RMax} \\ 0 & t > T_{RMax} \end{cases} \tag{3.5}$$

where

$$v_{ramp} = R_{Max}(1 - \frac{t - T_{RMax}}{T_{R0} - T_{RMax}}) \quad \text{m/s}$$

R_{Max} = ramp maximum in m/s

T_{R0} = ramp start time in s

T_{RMax} = ramp max time in s

(4) The last wind velocity component, the noise wind component, is used to approximate the random component of wind velocity, which could be expressed as follows:

$$v_{wN} = 2\sum_{i=1}^{N}[s_V(\omega_i)\Delta\omega]^{\frac{1}{2}} \cos(\omega_i t + \varphi_i), \quad t < 0 \tag{3.6}$$

where

$$\omega_i = (i - \frac{1}{2})\Delta\omega$$

φ_i = A random variable with uniform probability density on the interval 0 to 2π

Function $s_V(\omega_i)$, the spectral density function could be described as follows:

$$s_V(\omega_i) = \frac{2K_N F^2 |\omega_i|}{\pi^2[1 + (\frac{F\omega_i}{\mu\pi})^2]^{\frac{4}{3}}} \tag{3.7}$$

where K_N is the surface drag coefficient, which is usually 0.004, F is the turbulence scale, μ is the mean speed of wind at reference height (ft/s). According to the previous studies, $N = 50$ and $\Delta\omega = 0.5 - 2.0 rad/s$ would be adopted for obtaining accurate results.

To sum up, these four components provide sufficient and reasonable flexibility for the study of one or a group of wind generators.

3.3.3 WIND TURBINE MODEL

The mathematic expressions of wind turbine are expressed as in [71].

The mechanical output power of the wind turbine could be modeled as follows:

$$P_m = \frac{1}{2}\rho A v^3 C_p(\lambda, \beta) \tag{3.8}$$

where P_m is the aerodynamic power captured from wind; ρ is the density of air, Kg/m^3; A is the area that the wind power can be obtained; C_p is the power coefficient; v is the wind speed; β is the blade pitch angle; and λ is the tip speed ratio (TSR).

Here, C_p, the power coefficient of the turbine, the percentage of power in the wind that converted into mechanical energy, would be provided by the manufacturer to describe the characteristics of the wind turbine [101], which could be describe as follows:

$$C_p(\lambda, \beta) = C_1\left(\frac{C_2}{\lambda_i} - C_3\beta - C_4\right)e^{\frac{-C_5}{\lambda_i}} + C_6\lambda \tag{3.9}$$

$$\frac{1}{\lambda_i} = \frac{1}{\lambda + 0.08\beta} - \frac{0.035}{\beta^3 + 1} \tag{3.10}$$

where λ_i is the intermediate variable defined in equation (3.10); and C_1 to C_6 are constants for different wind turbine types.

The wind speed versus power curve of a typical wind turbine is shown in Fig. 3.5.

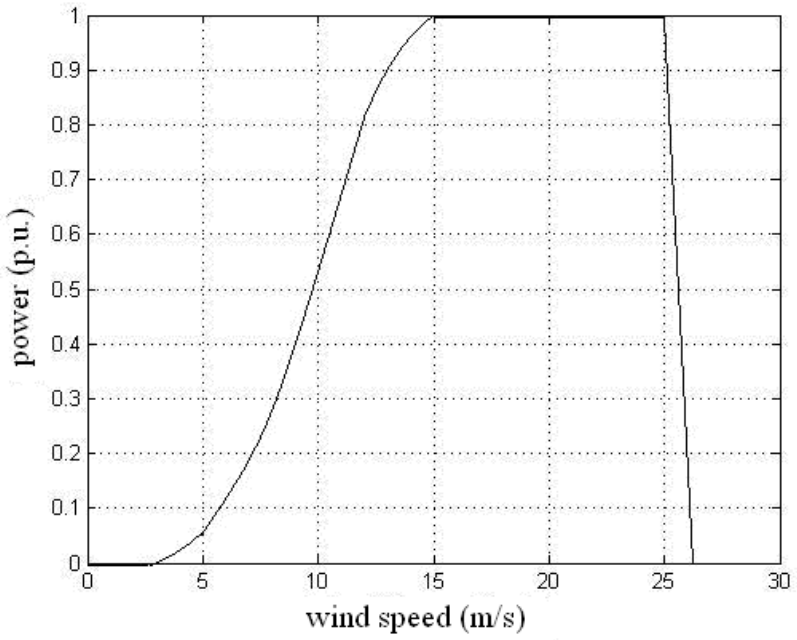

Fig. 3.5 Typical wind speed and power curve of a wind turbine.

3.3.4 DRIVE TRAIN MODEL

For the mechanical model of wind turbine based generators, some wind turbine design with dynamic structure would contribute to the interaction between the turbine and the system [102]. Therefore, the drive train would be taken into account. For the drive train model, it has been commonly accepted that the mechanical dynamics could be neglected since their responses are considerably slower than the electrical dynamics, especially for those turbines with huge inertia. Therefore, the modeling of the rotational system could be expressed as follows:

$$J_{WG}\frac{dw_r}{dt} = T_W - T_G - Dw_r \tag{3.11}$$

where J_{WG} is the turbine mechanical inertia plus the corresponding generator mechanical inertia; w_r is the angular rotor speed, T_W is the mechanical torque; T_G is the generator electromagnetic torque; and D is the friction coefficient [Nm/rad].

Specifically, the drive train model should be represented by the two-mass

model since the torsion oscillations in the shaft systems of the wind turbines excited by a short-circuit fault in the transmission system need to be simulated [103]. The two-mass model could be characterized as follows:

$$\begin{cases} 2H_{tur}\dfrac{d\omega_{tur}}{dt} = T_{tur} - K_s\theta_s - D_{tur}\omega_{tur} \\ 2H_{gen}\dfrac{d\omega_{gen}}{dt} = K_s\theta_s - T_E - D_{gen}\omega_{gen} \\ \dfrac{d\theta_s}{dt} = \omega_0(\omega_{tur} - \omega_{gen}) \end{cases} \tag{3.12}$$

where H_{tur} and H_{gen} are the rotor inertia constant of the wind turbine and generator respectively; K_s is the shaft stiffness; D_{tur} and D_{gen} are the rotor damping of the wind turbine and generator respectively; θ_s is the angle displacement between those two mass; T_{tur} and T_E are the mechanical torque of the wind turbine and the electromagnetic torque of the generator; ω_{tur} and ω_{gen} are the rotor speed of the wind turbine and generator; and ω_0 is the synchronizing speed.

3.3.5 INDUCTION GENERATOR MODEL

In order to investigate the impact of large amounts of wind power integration on power system stability and power quality, it is necessary to consider the modeling of the wind farm first of all. There would be a lot of possible interconnection structures for wind farms and different wind turbine technologies applied. Therefore, the most common connection characteristics from the stability or power quality of view and the most promising wind turbine based generators need to be paid attention to.

DFIGs are considered to be the most promising wind turbine based generator because of its good characteristics and reasonable cost. The greatest difference between DFIG and normal asynchronous one is that the rotor circuit of DFIG is connected to some external voltage source via the slip ring, which

determines that the rotor voltage u_{rd} and u_{rq} is not zero. Therefore, the output of active and reactive power could be controlled by varying the value of external voltage source. The favored way of representing a DFIG for the purpose of simulation, analysis and control would be the utilization of direct and quadrature axes, i.e. dq axes, which would create a reference rotating synchronously with the stator flux vector [56].

3.3.5.1 STATIC MODEL

The static model representing DFIG can be deduced as follows:

$$\dot{U}_s = R_s\dot{I}_s + jX_s\dot{I}_s + jX_m(\dot{I}_s + \dot{I}_r) \tag{3.13}$$

$$\frac{\dot{U}_r}{s} = \frac{R_r}{s}\dot{I}_r + jX_r\dot{I}_r + jX_m(\dot{I}_s + \dot{I}_r) \tag{3.14}$$

The equivalent circuit is as shown Fig. 3.6,

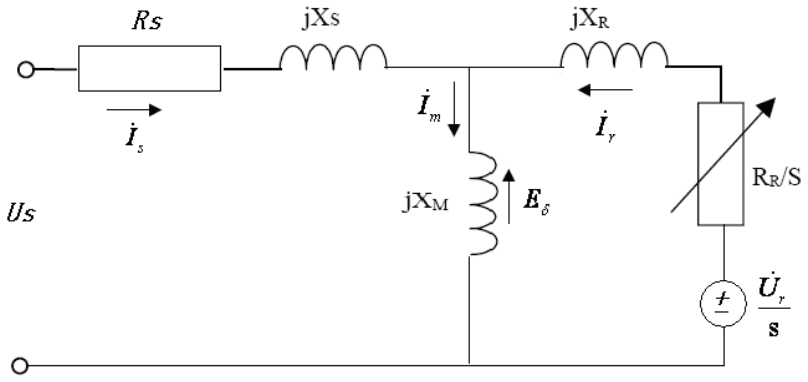

Fig. 3.6 The equivalent circuit of DFIG

From the figure above, the following equations could be obtained:

$$E_\delta = \dot{U}_s - (R_s + jX_s)\dot{I}_s \tag{3.15}$$

$$\dot{I}_m = \dot{E}_\delta \Big/ jX_m \tag{3.16}$$

$$\dot{I}_r = \dot{I}_m - \dot{I}_s \tag{3.17}$$

$$\dot{U}_r = s\dot{E}_\delta + (R_r + jsX_r)\dot{I}_r \tag{3.18}$$

The stator voltage $\dot{U}_s$ and current $\dot{I}_s$ are related with rotor voltage $\dot{U}_{\mathrm{r}}$ and current $\dot{I}_r$, the active and reactive power on the stator side can be controlled by $\dot{U}_{\mathrm{r}}$ and I_{m}.

3.3.5.2 DYNAMIC MODEL

The dynamic model of DFIG can be represented as follows:

$$\begin{cases} u_{sd} = \dfrac{d\psi_{sd}}{d_t} - \omega_s \psi_{sq} + R_s i_{sd} \\ u_{sq} = \dfrac{d\psi_{sq}}{d_t} - \omega_s \psi_{sd} + R_s i_{sq} \\ u_{rd} = \dfrac{d\psi_{rd}}{d_t} - s\omega_s \psi_{rq} + R_r i_{rd} \\ u_{rq} = \dfrac{d\psi_{rq}}{d_t} - s\omega_s \psi_{rd} + R_r i_{rq} \end{cases} \tag{3.19}$$

where, ω_s is the rotating speed of the axes, i.e., the synchronous speed

And the flux linkage equations are as follows:

$$\begin{cases} \psi_{sd} = L_s i_{sd} + L_m i_{rd} \\ \psi_{sq} = L_s i_{sq} + L_m i_{rq} \\ \psi_{rd} = L_r i_{rd} + L_m i_{sd} \\ \psi_{rq} = L_r i_{rq} + L_m i_{sq} \end{cases} \tag{3.20}$$

where $L_s = L_{aa} - L_{ab}$, $L_r = L_{AA} - L_{AB}$, $L_m = \dfrac{3}{2} L_{aA}$.

For DFIG, the rotor voltage u_{rd} and u_{rq} is not zero, and the control of DFIG is realized by controlling the value of external voltage source via a converter.

With the electromagnetic power developed by DFIG, the transient stator electromagnetic power is,

$$p_s = \frac{3}{2}(u_{sd} i_{sd} + u_{sq} i_{sq}) \tag{3.21}$$

$$p_s = \frac{3}{2}[R_s(i_{sd}{}^2 + i_{sq}{}^2) + \omega_s(i_{sq}\psi_{sd} - i_{sd}\psi_{sq}) + (i_{sd}\frac{d\psi_{sd}}{dt} + i_{sq}\frac{d\psi_{sq}}{dt})] \tag{3.22}$$

In equation (3.22), the first item is the copper loss, the second item is the

electromagnetic power, and the third item is the power item when considering the transient process, which could be treated as zero if ignoring the transient process.

The reactive power absorbed or developed by the stator can be written as,

$$Q_s = \frac{3}{2}(u_{sq}i_{sd} - u_{sd}i_{sq}) \tag{3.23}$$

Likewise, the electromagnetic power of rotor should be,

$$p_r = \frac{3}{2}(u_{rd}i_{rd} + u_{rq}i_{rq}) \tag{3.24}$$

$$Q_r = \frac{3}{2}(u_{rq}i_{rd} - u_{rd}i_{rq}) \tag{3.25}$$

So the total electromagnetic power of the DFIG is,

$$p_{DFIG} = p_s + p_r \tag{3.26}$$

Since for DFIG, there is the following equation,

$$p_r = -sp_s \tag{3.27}$$

the electromagnetic torque for DFIG can be written as,

$$\begin{aligned} T_e &= \frac{p_{DFIG}}{\omega_r} = \frac{p_s - sp_s}{\omega_r} = \frac{(1-s)p_s}{\omega_s} \\ &\approx \frac{(1-s)\frac{3}{2}\omega_s(i_{sq}\psi_{sd} - i_{sd}\psi_{sq})}{(1-s)\omega_s} = \frac{3}{2}(i_{sq}\psi_{sd} - i_{sd}\psi_{sq}) \end{aligned} \tag{3.28}$$

The protection system of the DFIG should also be included in the whole modeling. There should be at least three protection scheme included, low/over voltage protection, low/over speed protection, and so-called cross-bar protection.

3.4 SUMMARY

The output of a wind turbine based wind energy conversion system is relating to many factors, such as wind speed distribution, wind turbine modeling, electric generator modeling, and so on.

Theoretically, a complete model of a wind farm should include a number of detailed wind turbines. However, the computation and analysis of a large number of detailed wind turbines based generators could be time-consuming and impractical. Therefore, a method called turbine aggregation needs to be adopted. How many turbines should be aggregated depends on every specific situation. In this thesis, an aggregated model shall provide a fairly good approximation of the wind farm performance since it is for interconnection studies.

However, there are some certain situations that a detailed model is required. For instance, when analyzing the impact on local stability for faults occurred at or near to the wind farm, a detailed model is preferred.

CHAPTER IV KEY TO OVERCOME VARIATIONS: WIND FORECASTING

4.1 INTRODUCTION

Wind, as the most promising and booming renewable technology, has been chosen as the major energy source for sustainable development in many countries. Wind is perfect for fighting against energy security and environment concerns. However, its variability and average predictability may cause both technical and economic problems. Research into the impact of increasing wind penetration on system planning and operation has drawn a major attention.

Variability is nothing new in a modern electrical power system, but obviously, comparing with the relatively predictable load variations, the output variations of a wind energy conversion system (WECS) is much harder to predict. Especially, in order to achieve the ambitious green energy projections, high level of wind penetration is eventually going to be realized in many countries and regions, which will certainly exert great influences on power system planning and operation. Viewed from this perspective, well-performed wind forecasting is extremely desired so as to ensure the power system reliability and reduce the whole power system operation cost. On the other hand, electricity market is the trend nowadays. In order to follow this trend, wind forecasting will also be the key for wind farm owners to enter the competitive market and optimize their market operation to achieve a higher trading price.

In terms of different forecasting time scales, there are three types of forecasting applications, long-term, medium-term, and short-term wind forecasting. Wind forecasting could also be categorized by the forecast models applied, such as statistical models, physical models, hybrid models, and so on. These different types of forecasting models have their own scope of application

regarding different time scales, which will bring benefits to generation dispatch in electricity market and system reliability in different aspects.

This chapter would introduce and study wind forecasting technique in a reasonable structure. First, the crucial role of wind forecasting will be reviewed and evaluated, i.e. why wind forecasting is desired. Thereafter, all important factors regarding wind forecasting are discussed and analyzed. Furthermore, this chapter proposes a novel short-term wind forecasting model based on Ensemble Empirical Mode Decomposition (EEMD) and Support vector machine (Svm). The time series decomposition results from both Empirical Mode Decomposition (EMD) and EEMD would be demonstrated and compared. The methodology developed uses both EMD and EEMD to identify the intrinsic wind oscillatory modes by their characteristics time scales in the data empirically, and then decompose the wind speed time-series accordingly into different intrinsic mode functions (IMFs) with corresponding frequencies and the residue component, which would be further forecasted respectively by some specific wind forecasting technology. Therefore, in order to obtain a more accurate wind forecasting result, it is crucial to have a good decomposition method. It would be shown during the decomposition testing that EEMD decomposition would yield components with more obvious periodicity and smoother instantaneous frequency curve. Especially, when dealing with real wind speed times series, EEMD decomposition even yields one more IMF component. Svm would be then adopted and used to forecast every IMF respectively and the residue component. Finally, Svm would be applied to reconstruct all the individual forecasting results, which would yield the final result. The forecasting results has been compared with the one obtained from those reference models, not only the simplest persistence model, but also some more complicated models, i.e. EMD-ARMA model, and Svm model itself, which was developed previously and already yielded much better results than those from

persistence methods. Finally, the study illustrates that the proposed model yields a high accuracy, which would optimize the integration of wind power in both technical and economical aspects, like system reserve level reduction, energy trading optimization.

4.2 WHY WIND FORECASTING IS REQUIRED?

Electricity is the foundation of global economy and they are inter-dependable. Traditionally, electricity has been generated by thousands of power stations burning fossil fuels, mainly coal, oil and gas. Based on the energy uncertainty and environment concerns mentioned above, the development of renewable electricity generating systems is pursued to meet the electricity demand.

However, as mentioned in previous chapters, wind power generation is variable in output. Although variability is not a new concern in electricity world, yet still, it will have some influences on the power system supply and operation, especially when with high wind power penetration. Therefore, forecasting of wind speed/power becomes the most essential issue of adding large wind power generating system to the existing system, i.e. “prediction is the key to variability”.

Wind prediction could be categorized into long-term and short-term by different time scales. Some statistical or physical models have been applied for daily, weekly, or even monthly time series, which belong to the first category. Yet some other models could be applied for much shorter time scale, from a few seconds to a few hours, which are so called short-term prediction. Different types of prediction in terms of short or long time scale will bring benefits to generation dispatch in electricity market and system security in different aspects.

Forecasting wind power contributes significantly to cutting down the costs of

the whole power system in terms of dealing with variable-output generation. A well-performed forecast will help a lot to "avoid last-minute deployment of expensive reserve power by minimizing the probability of an unexpected gap between scheduled and actual system load".

Application of long-term wind prediction allows planning the connection or disconnection of wind turbines and conventional generators, which brings about low spinning reserve and optimal operating cost.

Short-term wind prediction, on the other hand, seems to be more attractive. Short term forecasting is not only useful for all producers who generate wind power, but also helpful for system operation security, especially when with large amount of wind power penetration. The groups participating in electricity markets benefit from wind power prediction in different aspects, which can be seen in Table 4.1:

	BENEFITS
Energy Supplier	Supply and demand balance would be better matched. More accurate generation estimations would be submitted to the operation centre. A lower charge would be requested by the TSO.
Wind Farm Owner	More accurate information about expected wind generation to the energy supplier.
Operators of Distribution System	More accurate information on expected power flows leads to better network management, which would cut down operational costs.
Operators of Transmission System	More accurate information on expected power flows would not only lower the operational costs but also the investments on strengthening networks, i.e. cutting down the total cost.

Table 4.1 Benefit from wind power prediction in different aspects

4.3 WIND DATA

Wind data can be obtained from meteorological office or wind farm. Wind speed data and wind farm output data can be obtained to forecast wind. There are two advantages by using wind speed data rather than wind farm output data. One is that a far longer period of wind observations is available from wind speed measurements than from wind farm measurements. The other one is the wind speed measuring sites are usually all over the country, like UK, United States, and China, which provides a more uniform view of wind characteristics throughout the country, and also allows the wind patterns of all regions to be examined.

4.4 FORECASTING METHODOLOGY

There are different approaches to forecast wind power production. Some of the forecast tools rely more on physical method, yet others on statistical method. In some systems, a combine of both these method was applied and has obtained some better results.

4.4.1 PHYSICAL METHOD

In short, the physical models try their best to use physical considerations to reach a better prediction of the wind speed/power. Then Model Output Statistics (MOS) will be applied to reduce the remaining error.

Two basic inputs will be introduced to a physical model, “dynamic input and static input.” The first input contains numerical weather predictions (NWP) obtained from some meteorological services and the on-line measurements for applying to the MOS. And the second one illustrates the wind farm installation, which consists of the number of turbines, power curve, and so on. It also

describes the prediction terrain, which involves roughness, layout of the turbines, etc.

Fig. 4.1 shows the main operating chain of a physical model [104] which provides a picture of the basic steps of using a physical prediction method.

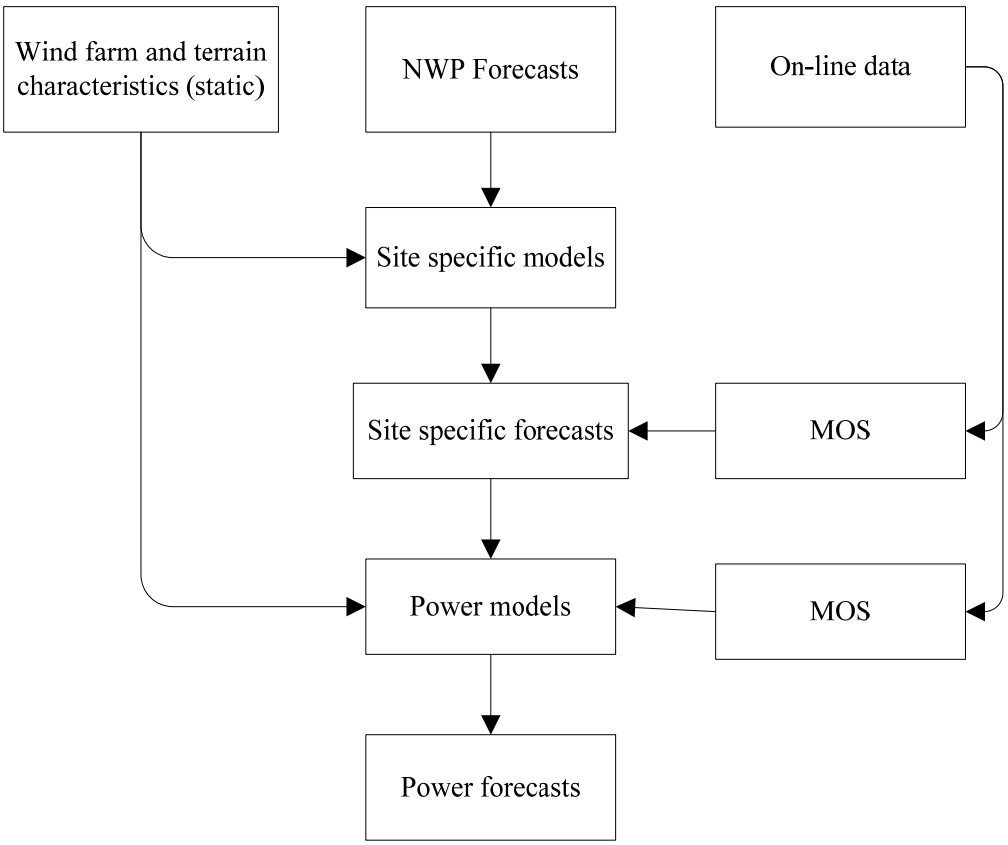

Fig. 4.1 Operating chain of a physical wind forecasting model

4.4.2 STATISTICAL METHOD

The statistical method is another option, which requires the NWPs and online data as its direct input, rather than the site specific and power curve model establishing. The only aim of statistic models is trying to establish the relationship between a set of variables including NWPs and the on-line measured data. By combining of alternative statistical models, a better performance is witnessed by getting most out of the advantages of each model.

4.5 WIND FORECASTING MODEL

This chapter would mainly focus on short-term prediction of wind power. A few commonly used wind forecasting models would be introduced in details with examples.

4.5.1 NUMERICAL WEATHER PREDICTION MODELS

This group is based more on numerical weather prediction (NWP) methods, which are more suitable for longer-term prediction of wind speed (more than six hours). The NWP model will instantly provide wind estimate, the expected wind speed and direction in a future point. Such models are similar to those used by national meteorological agencies. Both Risø's predictor and the Previento model from the University of Oldenburg provide good examples about short-term wind speed prediction of single wind farms using NWP models. For instance, the figure below shows the main process for Previento model to predict wind speed/power for single farms [4]:

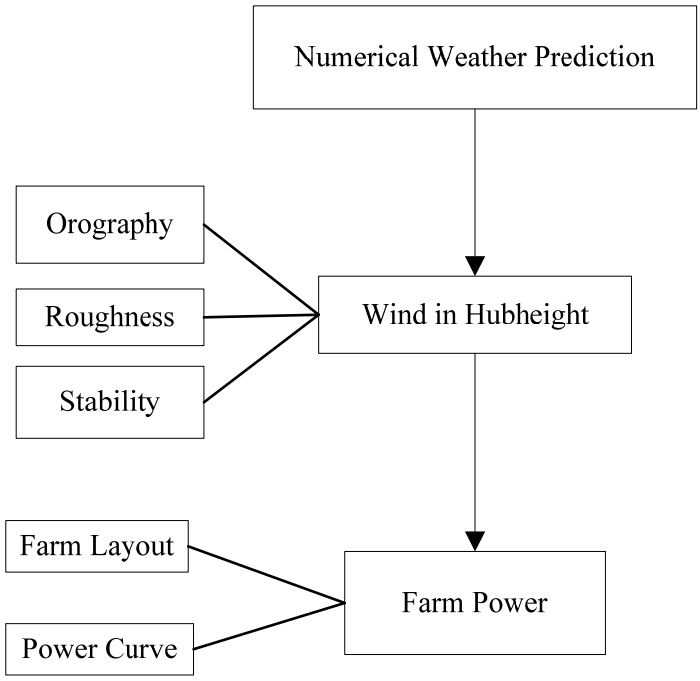

Fig 4.2 Main process for Previento model

4.5.2 THE OTHER WIND FORECASTING MODELS

The other categories are based on some other statistical models, such as artificial neural networks, fuzzy logic, both of which belong to artificial intelligence, and autoregressive models.

Comparing with NWP-based method, the time-series approaches might be superior when doing shorter time scale prediction (less than 6 hours). Particularly, autoregressive processes are preferred because of their powerful time-series technique and easy implementation. Among all kinds of wind forecasting models, the AI techniques available, artificial neural networks (ANN) have been successfully applied for wind speed/power forecasting because of its noise tolerant ability and quick-learning ability. Instead of choosing proper parameters for specific statistical models, the data-driven ANN models 'let the data speak for themselves'. Svm, a brand new learning machine, has been commonly accepted as the substitute of ANN due to its superior performance in forecasting applications.

A wind forecasting model based on fuzzy logic has been built in [43], taking into account the spatial correlations, which have been proved that it could yield quite high forecasting accuracy. However, like other models, persistence approach, time-series analysis, artificial intelligence, and so on, spatial correlation models require quite long historical data. Besides, spatial correlation models need wind information of different sites and its correlations, which would not be available usually. Thus spatial correlation will not be considered in this chapter. The output variability smoothness when considering a large geographical spreading of wind power was not taken into account as well.

4.6 ACCURACY AND ERROR MEASUREMENTS

Accuracy is the main concern of any kind of forecasting. Forecasting wind speed/power is of no exception.

In order to be accurate, the performance of the forecasting tool must be stable. It should be noted that the performance of a wind power prediction tool may greatly vary depending on the site [105]. Forecasting wind power for wind farms located in a flat or complex terrain situation is different from that for wind farms located near shore or offshore. Offshore conditions affect the wind vertical profile, which may not be logarithmic as this is the usual assumption. Moreover, the current meteorological forecasts are of great influence on the forecasting skills. Most of the errors on wind speed forecasting stem from the NWP model. There are two types of error: level errors and phase errors, where level error is the wind speed difference without considering directions while phase difference does consider the wind direction changes. The level error is easy to get hold of by using standard time-series error measures, while the phase error is hard to quantify. However, the phase error has a determining impact on the traditional error scores.

Some method has been previously introduced to cope with these errors. In [48], the contribution of data from local and remote sites to forecast via neural network models were examined. Also, a feasible way to improve the forecasting accuracy was suggested.

The forecasting error, used for measuring the accuracy of wind forecasting results, could be quantified by different error functions.

In the field of statistics, a forecast error is the difference between the actual/real value and the prediction/forecasting value of a time series, to be more specific, a difference between a computed, estimated, or measured value and the true, specified, or theoretically correct value, which can be always decomposed into two parts, systematic error and random error [106]. Therefore, at time origin t,

the forecast error for the leading time *k* should be as follows:

$$Error(t + k) = Measured(t + k) – Forecast(t + k) \tag{4.1}$$

The errors are calculated to illustrate a forecasting model's performance. There are several criteria could be followed, among which, the Mean Absolute Percentage Error (MAPE) and the Root Mean Squared Error (RMSE) are both the most commonly used ones.

As the name suggests, the mean absolute percentage error is a weighted average of the absolute errors, with the relative frequencies as the weight factors, i.e. "an alternative but much less desirable name for the mean deviation". The Mean Absolute Error function is as follows::

$$MAPE = \frac{1}{n}\sum_{t=1}^{n}\left|\frac{A_t - F_t}{A_t}\right| \tag{4.2}$$

where the actual value is denoted as A_t, and the forecasting value is denoted as F_t. MAPE is a percentage error so one can compare the error of fitted time series that differ in level.

Mean square error (MSE) is the same as mean absolute error except using squared difference instead of absolute differences, and the root mean squared error (RMSE) is simply the square root of the MSE [28].

4.7 FORECASTING MODEL STRUCTURE

4.7.1 ENSEMBLE EMPIRICAL MODE DECOMPOSITION

The precursor of EEMD is EMD, which was firstly introduced in [107]. EMD has been commonly accepted to be an efficient tool to decompose nonlinear and non-stationary time series, e.g. a time series of wind speed/power. Thus, EMD will identify the intrinsic wind oscillatory modes by their characteristics time

scales in the time series empirically, and then decomposes the original time series accordingly into finite number of IMFs with fast and slow oscillation modes and the residue component. IMFs, ranging from high frequency to low frequency, are subjected to the following two conditions:

(1) Over the entire length of the time series, the number of extrema and that of zero crossing must either equal or differ at most by one;

(2) at any point, the mean value of the envelope determined by the local maxima and that defined by the local minima is zero.

The process of decomposing a time series into individual IMFs and the residue component via EMD can be summarized by the following steps:

Step 1. Given a time series $v(t)$, identify all the maxima and minima. Generate the upper and lower envelope of $v(t)$. Average the two envelopes to compute the local mean series ΔP_T, with $h = v(t) - m$.

Step 2. Treat h as a new $v(t)$. Repeat Step 1 until h can be treated as an IMF according to some iterating stopping criterion. Here, the iteration would stop once the standard deviation of the latest h and the previous one is below a threshold which typically lies between 0.2 and 0.3 [107]. Let $c_1 = h$, which is the first generated IMF, IMF_1.

Step 3. Let $r = v(t) - c_1$. r is taken as another new $v(t)$. Repeat the above process, and get $IMF_2, c_2, ..., IMF_n, c_n$.

Step 4. Check the properties of IMF_n and c_n, either of which satisfies the definition of a true IMF or residue function according to some iterating stopping criterion, e.g. the range of the residue is below a predetermined level or the residue r has a monotonic trend, the process ends.

Then, the original time series $v(t)$ is decomposed into several IMFs c_i and a residue r, which could be described as follows:

$$v(t) = \sum_{i=1}^{n} c_i + r \tag{4.3}$$

where n is the number of IMFs, c_i represents the *i*th generated IMF, which is nearly orthogonal to the others and with a mean close to zero, r is the final residue.

Although EMD has been commonly accepted as an intuitive, direct and adaptive decomposition tool, yet the usually companied mode mixing problem would compromise the decomposition results. To solve this problem, a new noise assisted method, EEMD, is proposed in [108]. The process of EEMD decomposition could be demonstrated by the following steps:

Step 1. Given a numerically generated white noise $n(t)$ with magnitude ε, let $v_n(t) = v(t) + \varepsilon n(t)$.

Step 2. Decompose $v_n(t)$ by EMD.

Step 3. Repeat the above process for L_d times with different white noises. Thus, B ensembles of IMFs are obtained: $c_i^1, c_i^2, ...c_i^b, ...c_i^B$.

Step 4. Calculate the ensemble means of the corresponding IMFs as the final result:

$$c_i = \frac{1}{B}\sum_{b=1}^{B} c_i^b \tag{4.4}$$

It has been pointed out in [109] that the white noise magnitude ε is not an issue as long as it is finite but not infinitesimal. This means that EEMD is also adaptive.

4.7.2 SUPPORT VECTOR MACHINE

Support vector machine (Svm) is a novel learning machine introduced in 1995 [110] and has now been commonly accepted as the substitute of ANN due to its superior performance in forecasting applications. Training Svm is similar to solving a linearly constrained quadratic programming problem. This feature hints a drawback of time-consuming, yet on the other side, also means that Svm usually

yields a unique and globally optimal solution. Furthermore, compared with traditional models, Svm is based on the structural risk minimization principle rather than empirical risk minimization, i.e. consider not only the training error but also the confidence interval. Support vector regression (SVR) can be applied for non-stationary time series forecasting. Given a set of training data $\{x_i, y_i\}(i = 1,2,...n) \in R^n \times R$, Svm approximates the function using the equation as follows:

$$f(x) = w^T \varphi(x) + b \tag{4.5}$$

where $x \in R^d$ is the input with a dimension of *d*. If Svm itself is used as a wind forecasting model, then $x \in R^d$ would be the history wind speed, other meteorological factors, and so on. If EMD or EEMD decomposition is performed in advance to assistant wind forecasting, then Svm would be applied to each IMF and the residue component in the same way, i.e. $x \in R^d$ would be the history decomposed IMF value, other meteorological factors, and so on. $f(x) \in R$ is the forecasting output, $\varphi(x)$ represents the high-dimensional feature spaces which is nonlinearly mapped from the input space *x*. *w* and *b* are model coefficients that are estimated by minimizing the regularized risk function as follows:

$$\begin{aligned} &\min \frac{1}{2}\|w\|^2 + \frac{1}{2}\gamma \sum_{i=1}^{n} e_i^2 \\ &\text{s.t.} \quad w^T \varphi(x_i) + b + e_i = y_i (i = 1,2,...,n) \end{aligned} \tag{4.6}$$

where $e_i \in R$ denotes the error, γ is the regularization parameter. The first term, $\frac{1}{2}\|w\|^2$ is the so-called regularized term, minimizing of which control the function capacity since it will force a function as flat as possible. While the second term, $\frac{1}{2}\gamma \sum_{i=1}^{n} e_i^2$ represents the empirical error.

In order to solve the above optimization problem, Lagrange multipliers, $\lambda \in R^{n\times 1}$, are introduced to exploit the constraints as follows:

$$\min J = \frac{1}{2}\|w\|^2 + \frac{1}{2}\gamma \sum_{i=1}^{n} e_i^2 - \sum_{i=1}^{n} \lambda_i [w^T \varphi(x_i) + b + e_i - y_i] \tag{4.7}$$

Based on the Karush–Kuhn–Tucker (KKT) conditions[111] and the Least Squares principle [112], the solution for the above equation is as follows:

$$\begin{bmatrix} b \\ \lambda \end{bmatrix} = \begin{bmatrix} 0 & E^T \\ E & \Omega + \dfrac{I}{\gamma} \end{bmatrix}^{-1} \begin{bmatrix} 0 \\ Y \end{bmatrix} \tag{4.8}$$

in which $\lambda = [\lambda_1, \lambda_2 ... \lambda_T]$, $E = [11...1]^T$, $\Omega \in R^{N \times N}$ with $\Omega_{ij} = \varphi(x_i)^T \varphi(x_j) = K(x_i, x_j)$, where K is the kernel function to satisfy Mercer conditions, $Y = [Y_1, Y_2 ... Y_n]^T$ is the set for all forecasting outputs' expectations. Thereafter, a kernel function $K(x_i, x_j)$ is introduced to replace the inner product in the estimating function to form the final forecasting expression as follows:

$$f(x) = \sum_{i=1}^{n} \lambda_i K(x_i, x) + b \tag{4.9}$$

Common examples of the kernel function are polynomial kernel $K(x_i, x_j) = (x_i \cdot x_j + 1)^d$, Sigmoid Kernel $K(x_i, x_j) = \tanh(\gamma(x_i, x_j) + C)$. In this chapter, Radial Basis Function (RBF) kernel $K(x_i, x_j) = \exp(-(\dfrac{1}{\sigma^2})(x_i - x_j)^2)$ would be used as the kernel function, where σ is the kernel parameter.

To get an estimate of how well the model newly built performs, the best approach is to compare the forecasting results with those of the reference models. As the most advanced learning machine, Svm model itself is chosen as one of the reference models for short-term wind forecasting as well. The results obtained from applying it will be compared with the results from utilizing the new proposed hybrid method.

4.7.3 MODEL DEVELOPMENT

This chapter deals with the application of using EEMD and Svm to build a novel wind forecasting model as illustrated in Fig. 4.3:

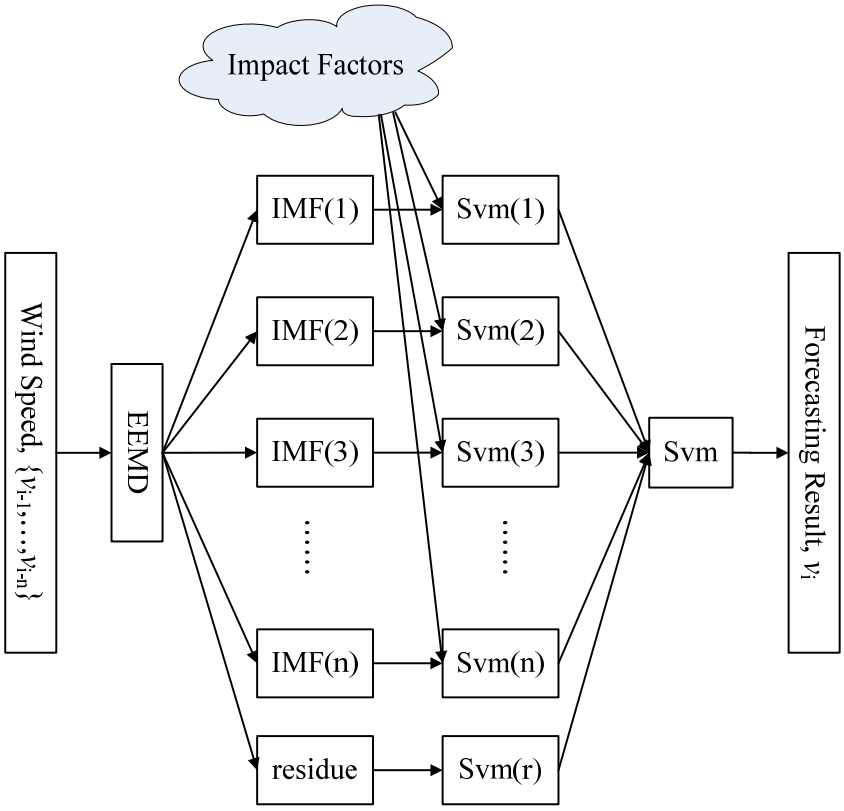

Fig. 4.3 EEMD-Svm based short-term wind forecasting model

As could be seen from Fig. 4.3, the forecasting procedure is as follows:

Step 1 Decompose the original wind speed data into a residue and a series of IMF components in different scale space via EEMD sifting procedure.

Step 2 Normalize all inputs, i.e. all IMF components, the residue, and the other meteorological factors would be normalized to the range of [-1,1] via linearization in order to form the training sets.

Step 3 Estimate parameters to determine each Svm model, which would be trained by using the previously formed training sets.

Step 4 Reconstruct and concord all results forecasted by Svm models to obtain the final forecasting value. Here, the input of Svm, $x \in R^d$, would be all the forecasting results from Svm(1) to Svm(n) and Svm(r) as shown in Fig. 4.3. The output of this Svm, $f(x) \in R$, would be the final wind forecasting result.

4.8 SIMULATION AND RESULTS

4.8.1 DECOMPOSITION TESTING

In order to test the decomposition effects of applying EEMD and EMD, a testing sample is introduced as follows:

$$y = x_1 + x_2 \tag{4.10}$$

where $x_1 = \sin(2\pi t)$ $x_2 = \sin(20\pi t)$. Add a white noise with a signal to noise ratio (SNR) of 20dB, the testing sample y_p is formed as could be seen in Fig. 4.4:

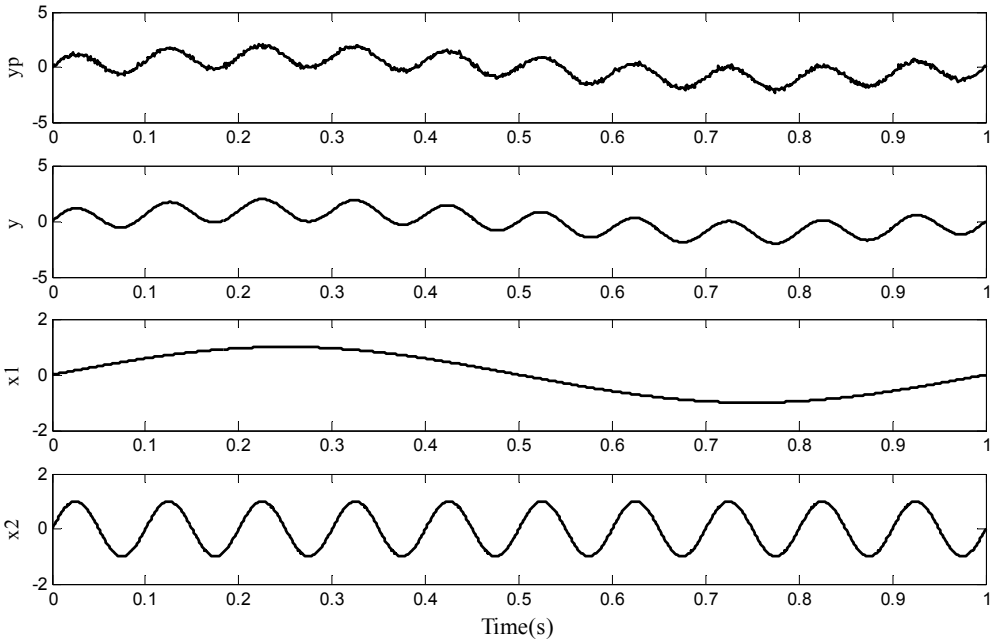

Fig. 4.4 Testing sample and its components

The testing sample y_p is decomposed by applying EEMD and EMD, respectively. Both of the decomposition results are shown in Fig. 4.5 and Fig. 4.6 as the following:

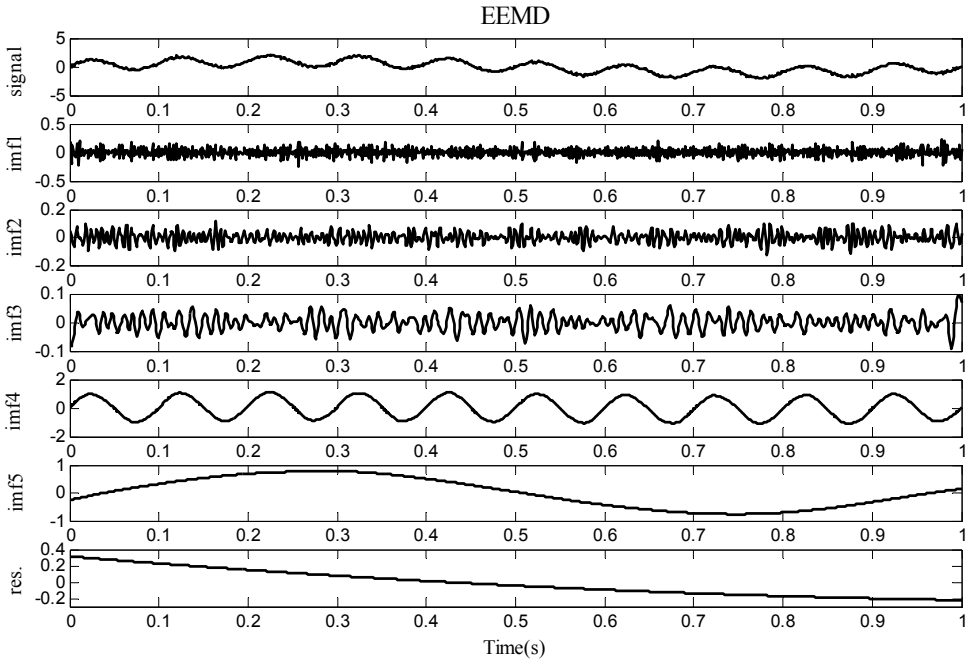

Fig. 4.5 Decomposition via EEMD

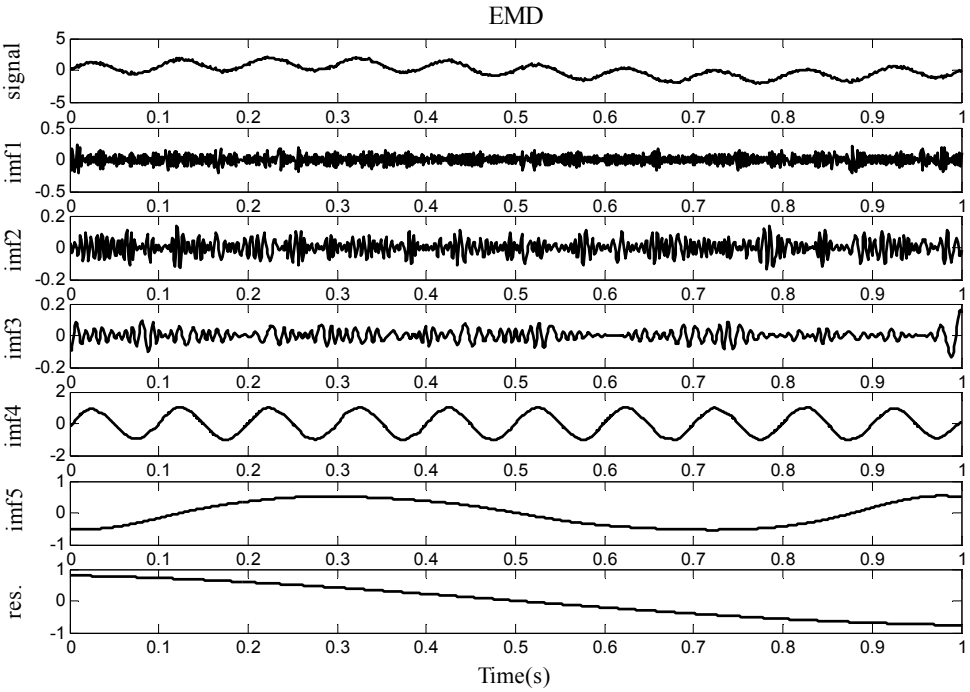

Fig. 4.6 Decomposition via EMD

It would be easy to tell from the Fig. 4.5 and Fig. 4.6 that the imf4 and imf5 components obtained from EEMD and EMD decompositions are both periodic

components of the original testing sample. Simply relying on the corresponding EMD and EEMD decomposition results, it would be quite difficult to tell whether EEMD decomposition could actually outperform EMD decomposition. Therefore, for comparison purpose, the corresponding instantaneous frequency curve of the imf4 and imf5 components obtained from EEMD and EMD decompositions are calculated and shown in Fig. 4.7.

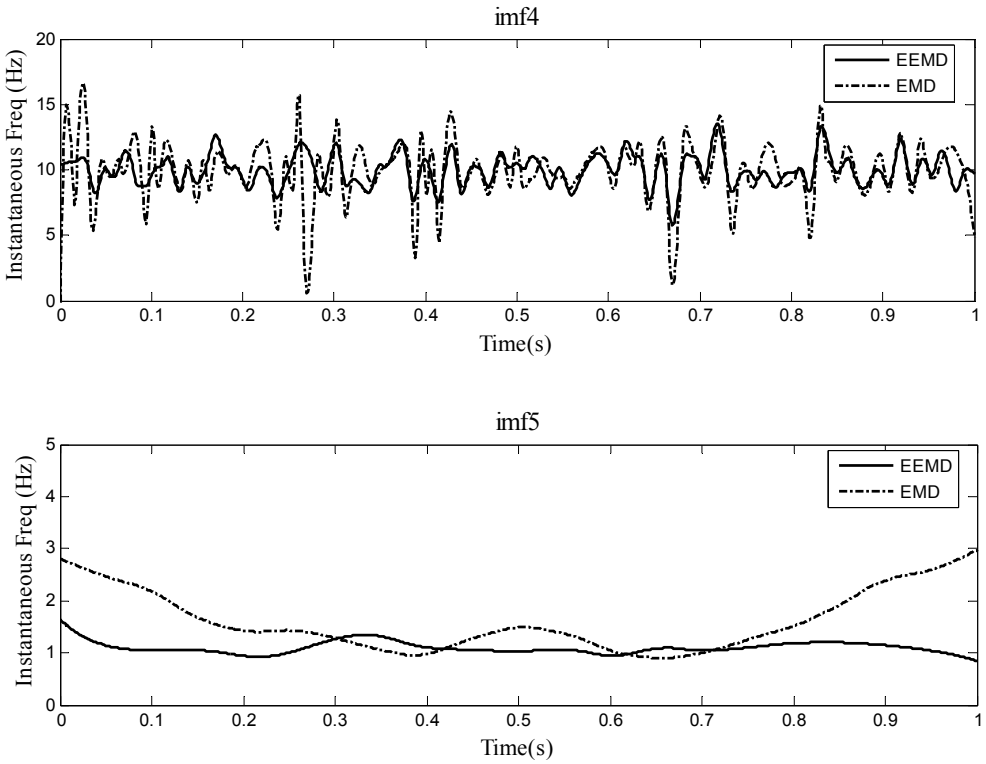

Fig. 4.7 Instantaneous frequency of the imf4 and imf5 components

As could be clearly seen from Fig. 4.7, the instantaneous frequency curve corresponding to EEMD decomposition is much smoother than the one obtained from EMD decomposition. This phenomenon provides strong evidence that EEMD would overcome the problem of mode mixed appearing in the process of EMD decomposition. Therefore, when being compared with EMD decomposition,

EEMD decomposition yields better results with components that show more obvious periodicity and smoother instantaneous frequency curve, which would contribute a lot to obtaining a more accurate wind forecasting result.

4.8.2 FORECASTING RESULTS

The prerequisite of building a forecasting model is to choose a set of appropriate time series, which, in this case, is a set of data that would be able to effectively represent the dynamic behaviors of wind. This means that the chosen wind data should cover a long enough period of time horizon with a reasonable time step and the whole time series should not contain any missing data ideally. Otherwise, the forecasting results would be comprised by the so-called sensor failures or data acquisition failures. One of the wind data used in this chapter is a time series obtained from a Hong Kong meteorological station. Another set of data obtained from a UK island meteorological station would be adopted as well to further verify the longer term performance of the proposed model. Both of the wind data contain two weeks of hourly measured wind speeds with no missing data, 336 points, as the training data. There would be always a compromise between efficiency and accuracy. Based on experience and tests, two weeks would be a long enough training period for the proposed forecasting model since it does not only yield quite high accuracy, but also involves reasonable computations. The implementation of the wind forecasting was realized using Matlab 2009a run on a computer with Intel Core 2 Duo 2.4 GHz CPU.

4.8.2.1 WIND SPEED FORECASTING IN HONG KONG

The original wind speed sequences at Hong Kong, as well as their EMD and EEMD decomposition results, were depicted in Fig. 4.8 and Fig. 4.9 respectively.

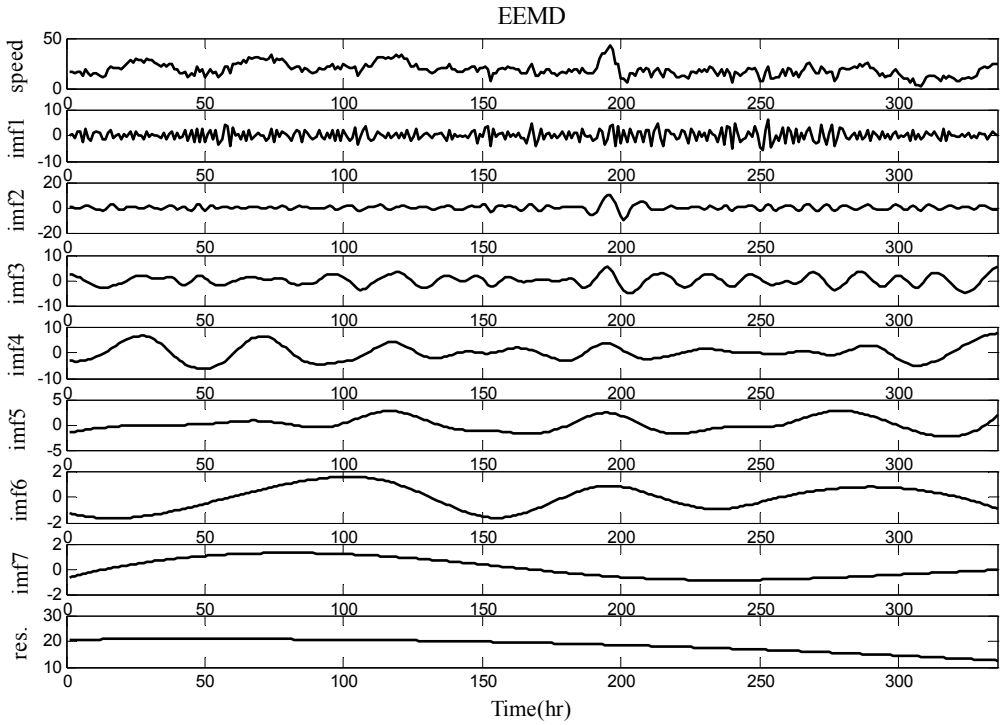

Fig. 4.8 Decomposition of wind speed via EEMD

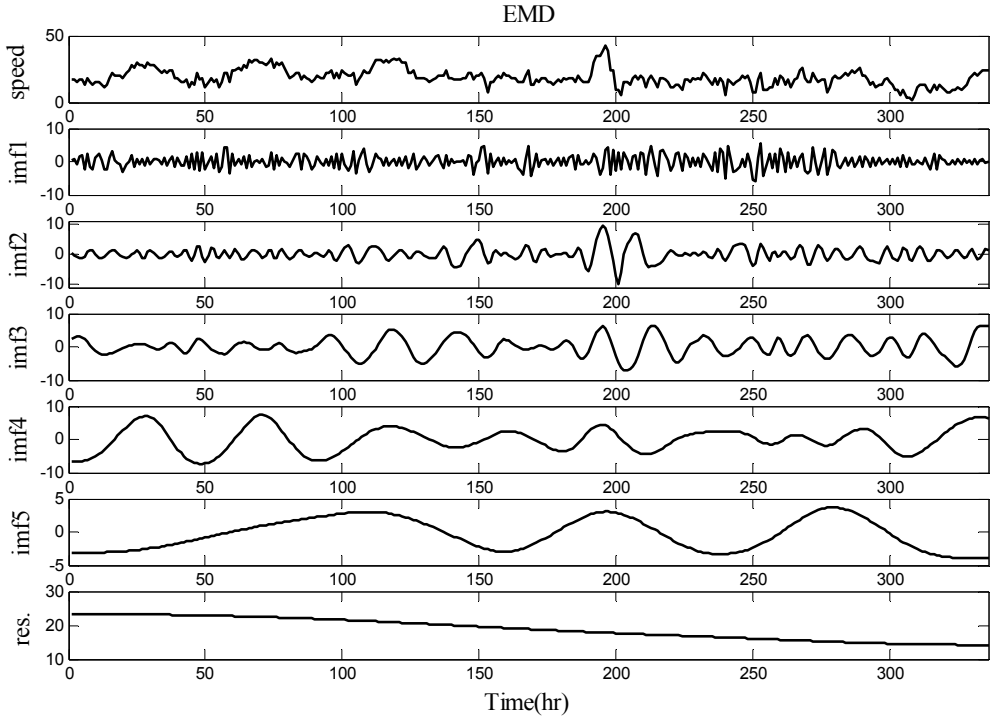

Fig. 4.9 Decomposition of wind speed via EMD

As could be seen from Fig. 4.8 and Fig. 4.9, it is clear that EEMD is better than EMD as it would yield more IMFs, which are more stable and smoother. This phenomenon verifies that EEMD would overcome the problem of mode mixed appearing in the process of EMD decomposition. Therefore, Svm would be applied to forecasting and superimpose seven IMF components and a residue obtained from EEMD decomposition, which would yield the final forecasting results in Fig. 4.10. The wind forecasting by Svm itself as a reference model is also included in Fig. 4.10. Forecasting results by the simplest persistence model and EMD-ARMA model, which were fully discussed and developed in [113], are stated as reference models in Fig. 4.10 as well.

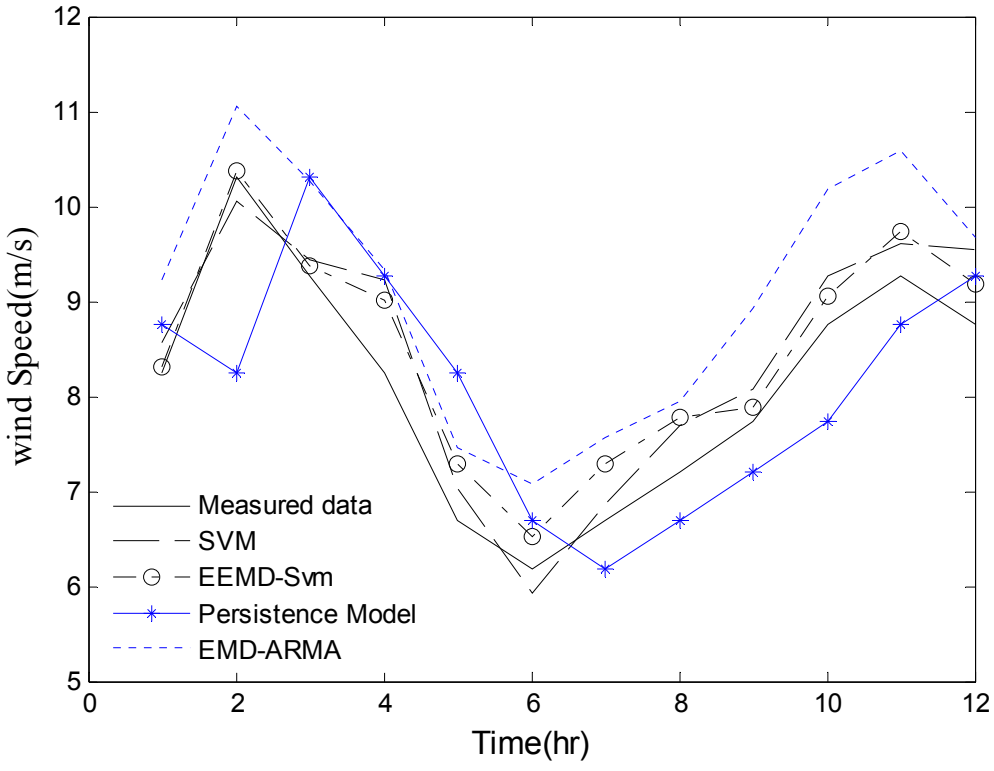

Fig. 4.10 Comparison of forecasting results (HK)

Each forecasting result was derived from the immediate pass two weeks' historical wind data referred as the training data. Since the training complexity

would vary with the training data, the required training time for each forecasting point in this particular study would vary from 0.8 to 2 seconds.

As illustrated by Fig. 4.10, the famous and simplest persistence model yields the worst forecasting results and the forecasting results from both Svm model and EMD-ARMA model are both reasonably better than the results from persistence model. To further distinguish the performance difference between the proposed and reference models, the absolute percent error (APE) statistics for each model was calculated and presented in Table 4.2 to measure quantitatively the accuracy of the wind forecasting. It is clear that the proposed EEMD-Svm wind forecasting model does outperform all the reference models in terms of forecasting accuracy.

Forecasting Model	Mean APE (%)	Maximum APE (%)	Minimum APE (%)	RMSE
EEMD-Svm	4.86	9.30	0.77	7.58
Svm	5.51	11.82	1.76	8.60
EMD-ARMA	7.74	10.12	4.63	12.07
Persistence	10.50	23.08	5.55	16.38

Table 4.2 Absolute forecasting error statistics over 12 hr period (HK)

To further verify the fact that the proposed EEMD-Svm model does give the most accurate wind forecasting results, Fig.4.11 compares the forecasting error between the proposed and reference models for each forecasting point. As could be seen from Fig.4.11, persistence model does not perform well at all comparing to the other forecasting models, especially when there is a large wind speed transition. Persistence and EMD-ARMA models have done a reasonable good job when the wind speed fluctuation is mild since both of them are pure statistical models. Actually, no forecasting models could beat persistence model when wind speed

remains the same all the time. On the other hand, both the proposed and Svm models yield much better forecasting results under all wind conditions. Especially, the proposed EEMD-Svm model is clearly the best performed model because it incorporates the advantages of both EEMD decomposition and Svm forecasting.

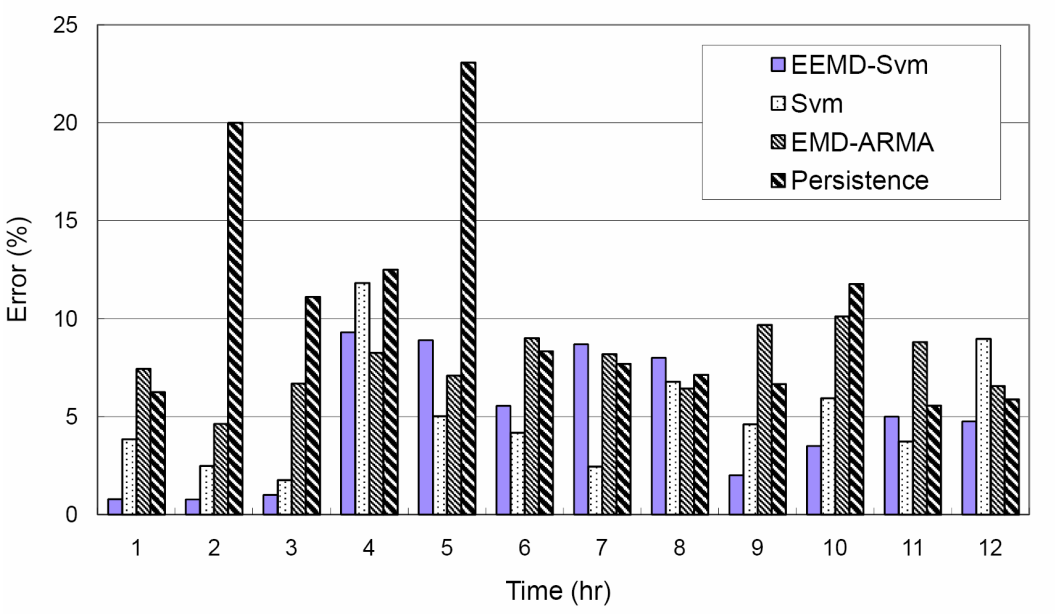

Fig. 4.11 Forecasting error comparison (HK)

4.8.2.2 WIND SPEED FORECASTING IN UK

In order to verify the reliability of the proposed model, the proposed and reference wind forecasting models were applied to forecast the hourly wind speed on a UK island over a two weeks period, 336 forecasting points in total, using historical wind data obtained from a UK island meteorological station. The first 24 forecasting points produced by the proposed EEMD-Svm and reference models were plotted in Fig.4.12.

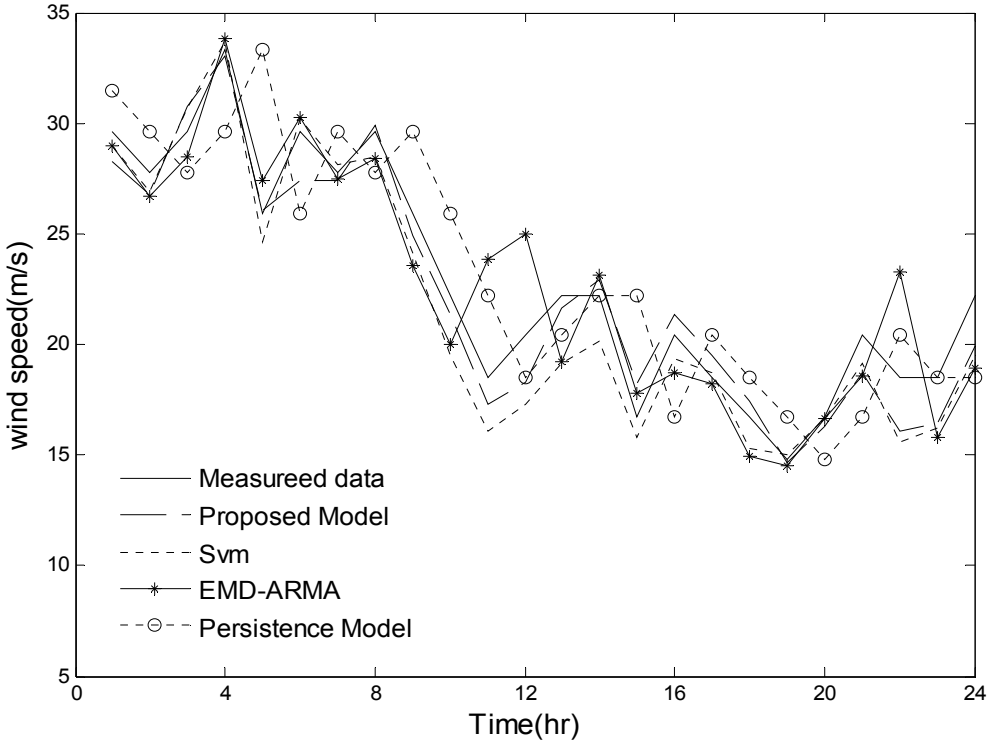

Fig. 4.12 Comparison of forecasting results (UK)

The absolute percentage error statistics of all the 336 forecasting points is calculated and shown in Table 4.3 to verify the superiority and reliability of the proposed model.

Forecasting Model	Mean APE (%)	Maximum APE (%)	Minimum APE (%)	RMSE
EEMD-Svm	6.99	20.62	0.75	10.9
Svm	9.70	25.61	0.46	15.13
EMD-ARMA	10.88	30.36	2.13	16.97
Persistence	16.56	44.96	0	25.83

Table 4.3 Absolute forecasting error statistics over 2 weeks period (UK)

Furthermore, the forecasting results and corresponding computation time (training time) with training data worth (training window) of 1 week, 2 weeks, and

3 weeks were collected to investigate the effects of training window to the computation efficiency and forecasting accuracy. Both the computation time and the absolute percentage error statistics with different training windows are summarized Table 4.4. Though the forecasting accuracy could be improved slightly with larger training window, the computation time would increase largely as a result. As a best compromise, a training window of 2 weeks was adopted in this chapter to generate all the forecasting results presented previously. In case the computation time is not a concern, larger training window would be recommended for better forecasting accuracy.

Training Window (week)	Training Time (s)			APE (%)		
	Mean	Max	Min	Mean	Max	Min
1	0.73	0.96	0.53	8.96	26.30	1.02
2	1.42	1.95	0.84	6.99	20.62	0.75
3	3.28	3.92	2.62	6.08	18.91	0.66

(a) Computation time

Training Window (week)	MAPE (%)	Max (%)	Minimum (%)
1	8.96	26.30	1.02
2	6.99	20.62	0.75
3	6.08	18.91	0.66

(b) Forecasting error

Table 4.4 Effects of training window size (UK)

4.9 PRELIMINARY APPLICATIONS

The results of the wind speed forecast presented above would provide an estimated mean speed v_s and an expected deviation of the forecast error σ_s. With these data, the power output from one wind power unit can be determined by using wind turbine speed and power curve, the mean $E(p_w)$ and standard deviation $\sigma(p_w)$ could be then obtained.

4.9.1 RESERVE CALCULATION

The quantity of reserve level is determined when the wind forecast errors are being considered. The increased reserves are not mainly due to the variability of wind power itself but rather its average predictability. Like the other forecasts, there is an error associated with wind power forecast, the difference between forecast and actual output of wind power. Therefore, in this chapter, reserve level is neither capacity reserve nor spinning reserve but a reserve level associated with the wind forecasting time frame. The wind forecast error could be modeled as a Gaussian stochastic variable with a mean of zero and a standard deviation of σ_w. In addition, the load forecast error could be modeled in a same way as a Gaussian stochastic variable with a mean of zero and a standard deviation of σ_l. Load forecast error should be less than the wind forecast error since it is far more predictable due to its repetitive nature.

The aggregation of variations in system load and wind generation will determine the total regulating power required by the system. This aggregation can be done by treating wind power as negative load. If wind generation and load consumption are assumed to be uncorrelated since little research has been done to the nature of forecast error correlation, the total forecast error of net load, load minus wind power production, can be given as follows:

$$\sigma_t = \sqrt{\sigma_w^2 + \sigma_l^2} \ . \tag{4.11}$$

In order to quantify the requirement of extra reserve, not only the forced outage rate, but also the load and wind power variations should be taken into account. The forced outage rate is not a rate but rather an estimator for a probability, which can be defined as follows:

$$FOR = \frac{FOH}{FOH + SH} \tag{4.12}$$

where Forced Outage Hours (FOH) is the number of hours a unit was in an unplanned outage state, and Service Hours (SH) is the number of hours a unit was in the in-service state. In this chapter, the impact of wind forecast uncertainty will be emphasized and the influence from FOR is assumed to be negligible.

The extra reserve requirement associated with wind power has not been directly modeled in existing analysis tools, so a proper reliability criterion should be brought in to take into account the impact of the forecast errors. Among all criterions, the Loss of Load Expectation (LOLE) is the most commonly used one, which is expressed as hours per year and is a measure of how long the available capacity is likely to fall short of the demand on average. In other words, LOLE represents the likelihood of failure statistically and would not measure to what extent that supply could not to meet demand. In this chapter, LOLE was adopted to introduce wind forecast uncertainty as in [114]. The calculation of the LOLE considering forecasting uncertainty is described in [115].

The required reserve need to be corresponding to the reliability criterion mentioned above. In this chapter, a load shedding incident is assumed to be an incident when there is not sufficient system reserve to satisfy a generation shortage and the probability of load shedding for hour *h* is as follows:

$$\mathrm{P}_{\mathrm{LoadShedding_h}} = \frac{\mathrm{LOLE}}{8760 \times \mathrm{MeanSheddingPeriod}} \tag{4.13}$$

in which it is assumed that the probability that a load shedding incident occurs in

each hour is the same during the whole year.

Thus, the reserve level could be corresponding to the probability of load shedding in any given hour as follows:

$$P_{LoadShedding_t} = 1 - \phi(\frac{P_{Reserve_h}}{\varphi_t}) \quad (4.14)$$

where $P_{Reserve_h}$ = Reserve Level, $\phi(x)$ = Normalized Gaussian distribution function

In this test system, the generating capacity is set to be 3405 MW, and the installed wind capacity is set to 340 MW, which provide a 10% wind power penetration. The forecast peak load is set to be 2840 MW with an approximate load-duration curve. The load forecast error was assumed to be with a mean of zero and a standard deviation of 39 MW. Similarly, the wind power forecast error is set based on the results from the above forecast model, with a mean of zero and a standard deviation of 56 MW. Results show that a power system with a forecast error as set above need an extra reserve of about 89 MW comparing with the case that wind power forecast uncertainty is not considered.

4.9.2 FORECASTING ERROR COST IN TRADING MARKET

Accurate forecasting also improves the wind energy trading price, i.e., the more accurate the wind speed forecasting, the higher income from selling the wind energy. Assume that wind energy trading is based on an electricity bid market in which the wind farm owner has to provide the forecasting wind energy and price an hour ahead, i.e. the gate closure time is one hour. Single-side bidding and a linear bid model is adopted here with a fixed system demand of 2840 MW.

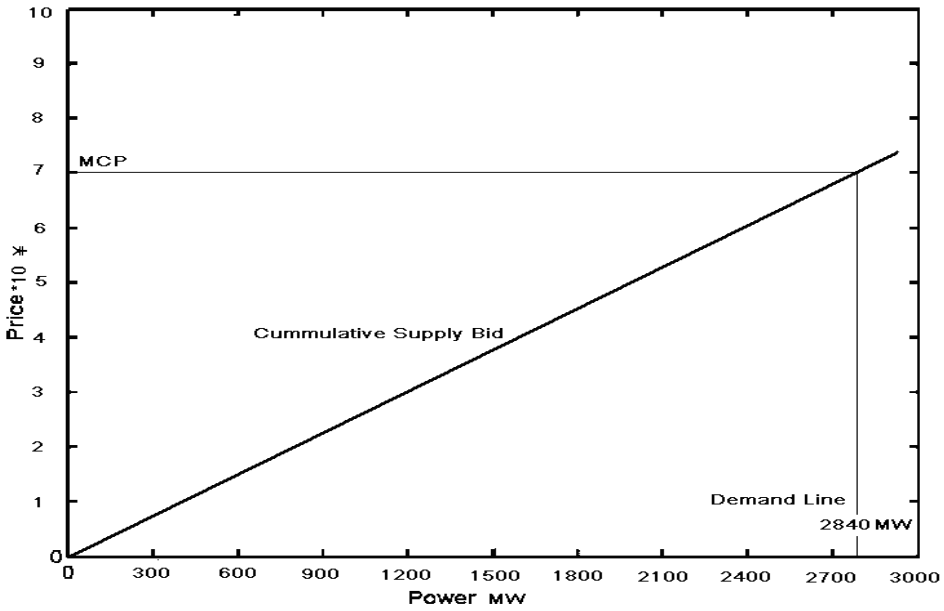

Fig. 4.12 Linear supply bid with fixed demand

As shown in Fig. 4.12, the cumulative supply curve could be expressed as follows:

$$Q = \sum_{i=1}^{N} \frac{p}{m_{si}} [u(q_{i,} q_i^{\min}) - u(q_{i,} q_i^{\max})] \tag{4.15}$$

$$u(q, q_0) = \begin{cases} 1, (q \geq q_0) \\ 0, (q \leq q_0) \end{cases} \tag{4.16}$$

where a cumulative supply curve Q is a function of the market price p of any bidder i with m_{si} as the slope of the supply curve. The ith generator has an output limit of $q_i^{\min} \leq q_i \leq q_i^{\max}$. Let equation 4.15 equal to the total demand 2840 MV, the market clearing price is calculated as ￥70/MW.

Suppose the capacity credit for the wind farm is 50% (much more efficient than the average, which is 20% usually) and, an average output of 170MW from wind farm is determined. If just this 170MW wind power is being taken into the competitive electricity market for the next hour, the scheduled output powers of the bidders will be reduced accordingly as follows:

$$\Delta q_i = \frac{p_w}{m_{si} \sum_{i=1}^{N} (\frac{1}{m_{si}})} \tag{4.17}$$

Meanwhile, there will be a reduced market clearing price (MCP). However, the MCP is determined without considering the wind power in order to benefit the wind farm owner.

In [116], some examples that wind generations participate into the day-ahead or hour-ahead energy market without imbalance penalties were provided, which would cause gaming problems. In this case, the wind farm owners have to perform wind speed forecasting and submit the output amount. Otherwise, a wind farm owner can overstate its output or gamble to gain extra profit in the market. The market penalty for the forecasted wind power would be as follows:

$$(\left|ForecastEnergy - ActualEnergy\right|) \times \sigma_d \tag{4.18}$$

where σ_d is the deviation penalty of the MCP.

Results show that, with a deviation penalty of 17% of the MCP, the penalty for the wind farm with a forecast error as set previously will be ￥654.5. Therefore, the wind farm income will be ￥11245.5, not ￥11900 when wind forecasting error is not considered.

4.10 SUMMARY

Financial crisis provides not only the challenges, but also opportunities to dealing with energy security and environment issues, which are the main reasons for developing renewable energy. Among all kinds of renewable energy sources, wind energy was introduced as the most promising one and a leading technology. A higher requirement for wind forecast accuracy is raised because of the dramatically increased wind power capacity all over the world. Wind forecasting can be categorized into long-term, medium-term, and short-term by different time scale. Some statistical and physical models have been applied for daily, weekly, or even monthly time series, which belong to long to medium term wind

forecast. Yet some other models can be applied for much shorter time scale, from a few seconds to a few hours, which are so called short-term wind forecasting. Different types of forecasting will bring benefits to generation dispatch in electricity market and system security in different aspects. Short-term forecasting wind power contributes significantly to cutting down the costs of the whole power system in terms of dealing with variable-output generation.

This chapter focused on short-term wind speed forecasting. A novel model for wind speed forecasting employing EEMD and Svm has been built and compared with a number of reference models. The essence of this proposed model is to decompose the wind data into residue and some IMF components via EEMD, which would make the corresponding forecasting time series more stationary. The decomposition results from a test function as well as real wind speed time series show that EEMD would do a good job to improve the forecasting accuracy. Furthermore, each individual component is forecasted by Svm analysis. Finally, all forecasting results would be reconstructed to give the forecasting result by Svm. Extensive tests with historical wind data obtained from meteorological stations in Hong Kong and UK verified that the newly proposed EEMD-Svm wind forecasting model indeed yields a more accurate forecasting result, and therefore would assist a large amount of wind power integration into the present power system. To be more specific, the preliminary simulations results also show that a more accurate wind power forecast would to some extend reduce the reserve requirement and increase the wind farm revenue, which should be realized in the nearly future since the improvement of wind power forecast technology is quite promising. In other words, a robust wind forecast with higher forecasting accuracy would assist a large amount of wind power integration into the present power system.

CHAPTER V WIND PENETRATION ESTIMATION BY SOC

5.1 INTRODUCTION

Energy security and environment concerns are currently the major concern, which propel us to move away from the high-carbon economy and look for alternative energy sources. In order to deal with energy security and environment issues, wind energy was introduced as the most promising and leading technology among all kinds of renewable resources. Thus, wind has been used for generating electricity on a large scale throughout the world. Not only such, there is a tendency to carry out a much greater integration of Wind Energy Conversion Systems (WECS) in many utilities' networks. As WECS being wildly and increasingly installed into the present power system, it is extremely desirable to determine the wind penetration limit given the existing electrical power system.

The amount of wind power that can be assimilated by the grid without major problems is highly dependent on the nature of the electrical power system itself [80]. Power systems with strong transmission network and robust interconnections to neighboring systems are expected to show a superior capability of absorbing large amount of wind power [81]. Denmark is an outstanding case with a wind power penetration limit of 50% or so, a wind energy penetration level of about 16.2%, and an installed wind capacity penetration level of around 29.0% [82]. For the enabling of a substantial amount of wind power integration, intensive researches have been done to assist the determination of the wind penetration limit. A method of quantifying wind penetration was applied based on the amount of fluctuating power that could be filtered by wind turbine generators and thermal plants [83]. The results yield a penetration level of 50%

when being estimated conservatively and a bold attempt of 90% when the smoothing capability was vastly improved. The transmission capacity of an existing transmission system considering a large amount of wind integration was estimated according to its thermal limitations [84]. Furthermore, the frequency response between fixed speed generator and doubly-fed induction generator was compared with frequency stability analysis as well. The assessment of penetration limit in isolated electricity grids were reported in [87, 88], which illustrated efficient methods for quantifying the maximum penetration level in autonomous systems, like the situation in an island [89]. However, the upper limit on wind power penetration will definitely rise when interconnectivity strategy is adopted.

From a system level viewpoint, the contribution of this chapter is to evaluate the wind power penetration level by analyzing the self-organized criticality of power system with increasing wind penetration. The power system self-organized criticality has been introduced in the literature review and would be discussed in length in the following sections. The proposed algorithm is implemented on the slightly modified IEEE 30-bus system and 118-bus system. Preliminary results illustrate that the instantaneous power penetration level can reach to nearly 50% in IEEE 30 and nearly 20% in IEEE 118.

5.2 SELF-ORGANIZED CRITICALITY

The philosophy of self-organized criticality and the current models available has been generally introduced in Chapter 1. It is based on the complexity theory, which could be described as that the complex behavior can develop spontaneously in certain many-body systems whose dynamics vary abruptly, i.e. the nonlinear dynamics of a complex system under disturbances organized the global system state near to the state; that is marginal to major disruptions, often appeared as

cascades .

The archetype of a self-organized critical system, one of the simplest models, is a sand pile model shown as in Fig. 5.1 [72]. Sand is slowly dropped onto the ground, forming a sand pile. At first, of course nothing much happens. The new grains just pile on top of the old ones. However, as the pile grows, piles are then forming, getting higher, and at some point the slope is going to get more and steeper. Finally, the weight of the grains at the top would overcome the friction, which means that avalanches would occur. At some point, the whole sand pile would be in a critical state, which means that the system (sand pile) is at the edge of an avalanche. Another drop of grain may cause the whole sand pile to collapse. Once a sand slide happens, the system would then end up in another critical state again. The slope of the pile that becomes independent of the rate, at which the system is driven by dropping sand, is the so-called self-organized critical slope.

Fig. 5.1 Sand pile model for SOC

There are several important characteristics to a system in an SOC state [73]:

(1) Power laws:

A power law is basically any relationship between two variables where one is a power of the other.

(2) Fractal geometry:

A fractal pattern is self-similar, i.e. similar things go on no matter what scale being looked at. Theoretically speaking, there is also an infinite amount of detail.

(3) Flicker noise:

The flicker noise is also called *1/f* noise since the frequency (*f*) is inversely proportional to the power. Flicker noise is a signal that consists of all sorts of frequencies, among which the low frequencies are strong, and the high frequencies are weak, i.e. lots of small but few big things going on.

For the modern electricity networks, researches into the failure data of North America illustrates that the scale of power system blackout has the power law characteristics shown as in Fig. 5.2 [71], where the *x*-axis is the power loss of blackout, and the *y*-axis denotes the probability of event whose power loss is larger than *x*. This instanced that the complex electric power transmission systems obey self-organized criticality like dynamics since, as being discussed above, power law distribution is a typical token of self-organized criticality.

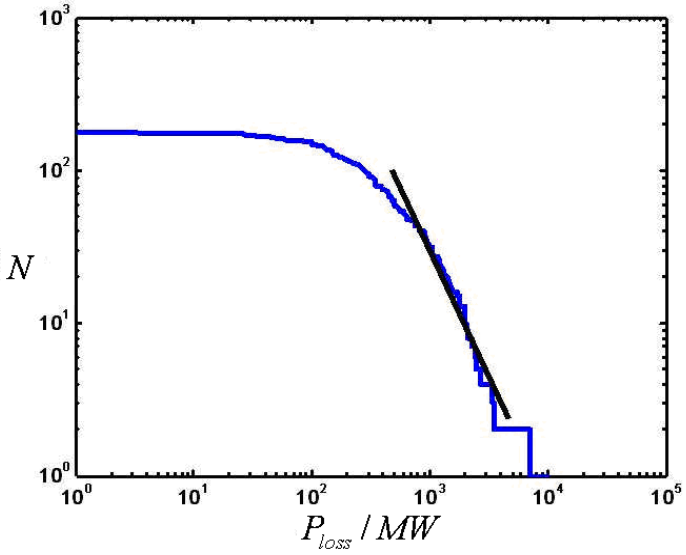

Fig. 5.2 Power law characteristics of the scale of power loss

The modern electricity network could be treated as a typical complex system because of its four specific features as below:

1. Extremely large-scale network;
2. Various and complex components;
3. Instantaneously power supply and demand balance;
4. Great amount of stochastic factors.

From the above four features, it would not be difficult to see that electricity network could be treated as an object of complexity theory study.

Although the modern electricity networks are very complex, yet it has been working quite well in the sense of robustness and reliability. However, this more and more complex system does not only bring enormous social and economic benefits, but also introduces increasingly higher risk of power system collapse, which means a bigger challenge for electrical engineers and researchers in power system planning and operation.

To prevent power system suffering from collapse, i.e. cascading failures and loss of loads, many conventional strategies and measures have been carried out. However, the recently occurred blackouts all over the world imply that conventional strategies would not be sufficient. Instead of focusing on some specific element or index, SOC tries to concentrate on the whole status of the system. As a general tendency, interconnections of power system do not only provide convenience, like enhance the capability of the electricity network to absorb wind power, but also cause problems. For example, cascading events are highly likely to occur in large and heavily stressed power systems. Modern electricity network is such a system since the transmission system are running more and more closely to their operating limits due to the increasing consumption and economical tradeoff. Therefore, as important as the state of individual

components, the global system state needs to be analyzed as well from a system level viewpoint. In this chapter, not only to simulate the power system SOC mechanism under a high wind penetration level, a new AC-based OPF blackout model with wind integration is proposed to quantify the wind penetration limits and give some good inspirations to power network optimization.

5.3 WIND FARM MODELING

The output of a fixed speed wind turbine based WECS is relating to many factors, such as wind speed distribution, wind turbine modeling, electric generator modeling, etc [117]. The wind turbine model as well as the power flow analysis would be illustrated here.

The mechanical output power of the wind turbine is modeled as in Chapter 3:

$$P_m = \frac{1}{2}\rho A v^3 C_p(\lambda, \beta) \tag{5.1}$$

The wind speed versus power curve of a typical wind turbine is shown in Fig. 3.4 in Chapter 3. The most commonly used electric generator coupled with a fixed speed wind turbine is a squirrel cage induction machine as shown in Fig. 5.3.

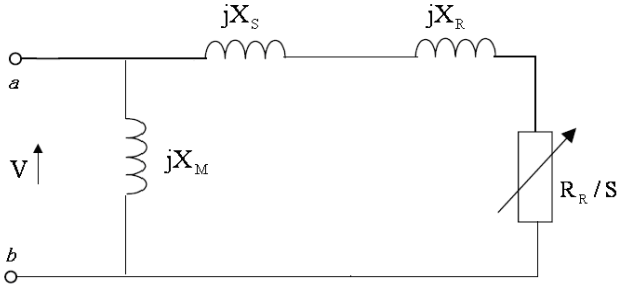

Fig. 5.3 Equivalent circuit of induction generator

Supposing wind speed is known, the active power output of a WECS could be assumed to be equal to the wind turbine mechanical power output as follows:

$$P_w \approx P_m \tag{5.2}$$

The equation for determining the active power output of an induction generator could be expressed as follows:

$$P_w = \frac{-V^2 R_R / S}{(R_R / S)^2 + (X_S + X_R)^2} \tag{5.3}$$

When the terminal voltage V is initially assumed, equation (5.3) could be rewritten to calculate the slip of the induction machine, S, as follows:

$$S = -\frac{V^2 R_R - \sqrt{V^4 R_R{}^2 - 4P_w{}^2 (X_S + X_R)^2 R_R{}^2}}{2P_w (X_S + X_R)^2} \tag{5.4}$$

Since $\frac{P_w}{Q_w} = \frac{R_{ab}}{X_{ab}}$, reactive power Q_w can be calculated as follows:

$$Q_w = \frac{R_R{}^2 + (X_S + X_R)(X_S + X_R + X_M)S^2}{R_R X_M S} P_w \tag{5.5}$$

where R_{ab} and X_{ab} are the total resistance and reactance from point *a* to point *b* respectively.

A wind farm bus is definitely not a PV bus in power flow analysis because the terminal voltage V is not easy to maintain at a specific value. Yet a wind farm bus cannot be treated as a normal PQ bus as well since the reactive power Q_w would not remain constant. Thus, an iteration method for determining V and Q_w would be applied. Obtaining P_w and Q_w from equation (5.2) and (5.5), the updated terminal voltage will be calculated in the power flow analysis. Q_w and V are then varying across iterations until convergence is reached.

5.4 AC-BASED OPF BLACKOUTS MODEL

Cascading failure is one of the main causes of power system blackouts. In modern electricity transmission systems, components employed are often highly stressed due to the economic compromise and heavy consumption. Especially when there are large amounts of wind generation in the power system network, once some malfunction or damage makes a specific component fail to transmit

power, the power flow would be redistributed. Thus, there would be an increase in the loading of other system components, which might cause another round of fail and overloading, i.e. propagation of failures.

Based on SOC, a complex system would be in danger if it comes to a critical state. In other words, the probability of major interruptions becomes large in a critical state, under which even a tiny disturbance could end up with an uncontrollable system collapse. Therefore, an AC-based OPF blackout model is proposed here to simulate the self-organized criticality of power system. The wind power generation output would be increased gradually to locate the critical point. The wind penetration level at this critical point could be treated as the penetration limit.

In this chapter, the wind farm is assumed to operate under a fixed schedule in order to facilitate the wind penetration level determination, i.e. the total active power output of the wind farm is controlled to a specified value irrespective to the wind speed variation by switching on/off some of the WECSs within the wind farm. Thus, the corresponding total reactive power required could then be calculated. The AC-based SOC model simulates power flow and cascading failure while considering the actions of dispatch, line outages and weak line updating. In this chapter, load shedding is adopted as the main control measure to cope with system collapse, i.e. OPF failed to coverage, and the amount of load shedding, i.e. average loss of load, is considered as an important index for assessing the wind penetration limit. The essence of this model is to depict the whole system status via the loss of load probability distribution curve and an index calculated from the average loss of load. Though tap changing and reactive power compensation could help to strengthen the system, they are not included in the current OPF model without loss of generality of the proposed AC-based OPF blackout model. A flow chart representing the mechanism of this model is shown in Fig. 5.4.

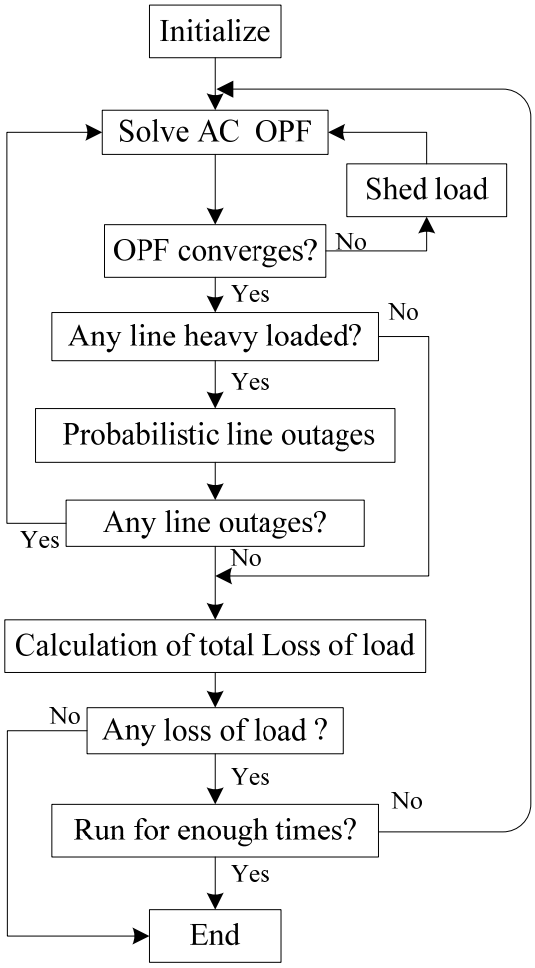

Fig. 5.4 The flow chart of the AC-based OPF blackout model

The AC-based OPF blackouts model with wind integration is implemented by the following process.

Step 1 Initialize the system with a specified wind generation.

Step 2 Solve the AC-based OPF. Go to step 3 if OPF converges; otherwise, shed the load connected to the most stressed line by 5% until OPF converges, then go to step 3.

Step 3 Check the line flows. If there is any lines with load level exceeding the threshold, i.e. $F_l / F_l^{\max} \geq \alpha$, go to step 4; otherwise go to step 5. Here, F_l is the apparent power of line l, and $F_l^{\max}$ is its power rating; α denotes a certain threshold value of the load level of the corresponding line.

Step 4 Test the outage of each stressed line with probability β, where $1-\beta$ is the probability of relay protection failure, i.e. fail to trip an overloaded line. If there is any line outages, go to step 2; otherwise, go to step 5.

Step 5 Compute the total loss of load and stop the process if there is no loss of load or sufficient number of trials has been done.

In the above process, the AC-based OPF has the objective of achieving the minimum power loss as follows:

$$\min f(P,Q) = \sum_{i \in G} P_{gi} - \sum_{j \in L} P_{lj} \tag{5.6}$$

where G and L are the generator and load, respectively, P_{gi} is the active power output of generator i, and P_{lj} is the active load of load j. The two controllable variables here, P and Q are the active and reactive power generation.

Given a system with n buses and m transmission lines, the major equality and inequality constraints being faced are as follows:

(1) Equality constraints:

$$P_i = V_i \sum_{i=1}^{n} V_j (G_{ij} \cos\theta_{ij} + B_{ij} \sin\theta_{ij}) \tag{5.7}$$

$$Q_i = V_i \sum_{i=1}^{n} V_j (G_{ij} \sin\theta_{ij} - B_{ij} \cos\theta_{ij}) \tag{5.8}$$

In the above active and reactive power flow balance equations, P_i and Q_i are the active and reactive power injected in bus *i*; V_i and θ_i are the voltage magnitude and its phase angle at bus *i*; with $\theta_{ij} = \theta_i - \theta_j$; G_{ij} and B_{ij} are the transfer admittance between bus *i* and *j*.

(2) Inequality constraints:

$$P_{gi}^{\min} \le P_{gi} \le P_{gi}^{\max} \tag{5.9}$$

$$Q_{gi}^{\min} \le Q_{gi} \le Q_{gi}^{\max} \tag{5.10}$$

$$V_i^{\min} \le V_i \le V_i^{\max} \tag{5.11}$$

$$-F_l^{\max} \le F_l \le F_l^{\max} \tag{5.12}$$

The steady-state operation constraints of the system include the upper and lower limits of the generator outputs, bus voltage magnitude constraints, and the transmission capacity constraints. P_{gi} and Q_{gi} are active power and reactive power of the generator *i*, respectively, with $P_{gi}^{\max}$ and $Q_{gi}^{\min}$ as the upper limits and $P_{gi}^{\min}$ and $Q_{gi}^{\min}$ as the lower limits. Likewise, $V_i^{\max}$ and $V_i^{\min}$ are the upper and lower limit of the voltage V_i at bus i. For the line capacity, F_l and $F_l^{\max}$ are the power flow and capacity of line *l*, respectively.

Since some lines and loads on the initial state might be shed, the scale of the power system accident and failure could be represented by total loss of load.

Because of the randomicity in this model, the model needs to be run for numerous times so as to obtain the probability distribution of loss of load. In this chapter, the model would be run for 1000 times for each wind generation output.

5.5 RESULTS ASSESSMENT

Though the wind power penetration limit could be assessed subjectively by comparing the probability distribution curves of loss of load or the average loss of load when the wind power output levels are around the wind penetration limit, it could be further evaluated quantitatively by the risk of loss of load using the concept of Value-at-Risk (VaR) and Conditional Value-at-Risk (CVaR) [118-121].

VaR was firstly introduced by the J.P.Morgan Company for investment risk evaluation to indicate the risk level in the Riskmetrics System [119]. VAR is a term used for assessing risk via applying traditional statistical techniques that are routinely incorporated in some specific field. VaR is often computed to estimate the maximum loss over a defined decision-making horizon such that there is a low/pre-specified probability that the actual loss would not be larger. Here, VaR is adopted to measure the largest loss of load with the confidence level σ in a

certain period. The mathematical definition of VaR is as follows:

$$\text{Prob}(x > VaR_{\sigma}) = 1 - \sigma \tag{5.13}$$

where σ is the confidence level, x is the loss of load, and VaR_{σ} is the VaR under σ. Given the probability density function $p(x)$, VaR can be calculated as follows.

$$\sigma = \int_{-\infty}^{VaR_{\sigma}} p(x)dx \tag{5.14}$$

Taking Fig. 5.5 below for instance, for a given confidence level of σ = 95%, VaR is the largest possible loss of load.

For a given confidence level σ, two values $VaR_{\sigma 1}$ and $VaR_{\sigma 2}$ are assigned such that $\sigma_1 < \sigma < \sigma_2$; and VaR_{σ} can then be determined using a bisection search method.

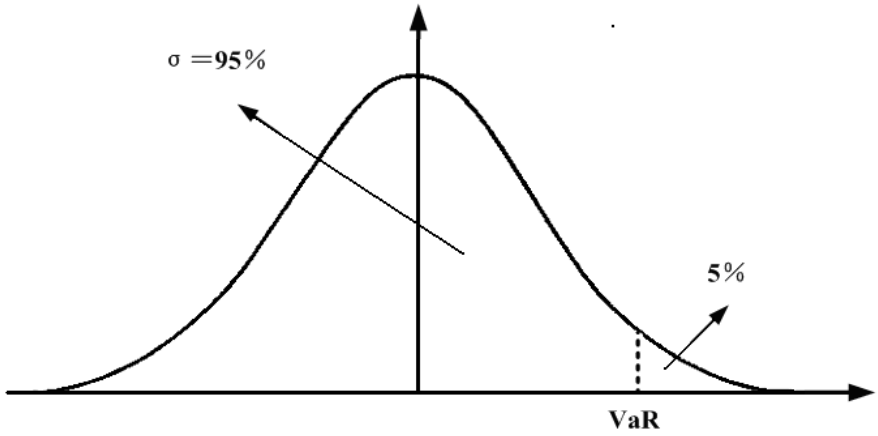

Fig. 5.5 Loss of load distribution

VaR perfectly measures not only the scale of loss, but also the probability of it. The loss level with a specific σ could be calculated easily as well. But applying VaR also has some drawbacks. VaR does have the tendency to assume normal distributions, and thus low probability of 'extremes'. In this sense, conditions that are more skewed than normality are simply ignored. Therefore, it suffers from instability and difficulty when losses are not normally distributed,

which in fact is quite often the case in reality since loss distributions tend to exhibit 'fat tails' or empirical discreteness. It could be easily told from Fig. 5.6 that, the VaR value is the same. In addition, the areas on the right of the VaR value, both in dot line and in solid line, are the same. However, Fig. 5.6 also illustrates that, under some extreme cases, the loss of load in dot line is much bigger than the one in solid line.

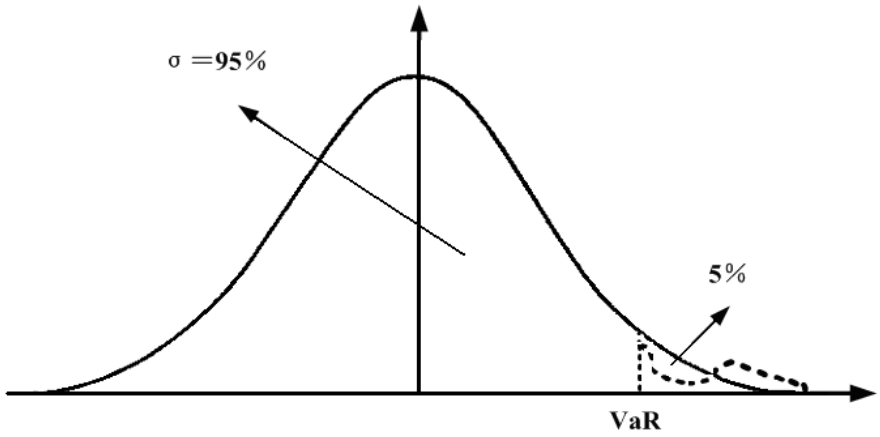

Fig. 5.6 Different tail-losses under the same VaR

Since VaR neither sufficiently measures the tail-loss nor satisfies the Coherent Axiom [120], CVaR was subsequently proposed by Rockafeller and Uryasey to overcome these two shortcomings [121]. CVaR is defined as follows:

$$CVaR = \int_{VaR_\sigma}^{\infty} xp(x)dx \tag{5.15}$$

where x is the loss of load and $p(x)$ is probability density function of a given loss of load x. Complementary to the VaR, those extremely large loss of loads for a given confidence level could be perfectly measured by CVaR complementary to VaR.

Together with the average loss of load, VaR and CVaR could be used to depict the system status at different angles and consolidate the wind power penetration limit assessment.

5.6 SIMULATIONS AND RESULTS

5.6.1 SYSTEM UNDER STUDY

Two IEEE test systems were slightly modified for demonstrating and verifying the proposed approach, namely the IEEE 30-bus and 118-bus systems. For the blackout model and the wind power penetration limit assessment in both test systems, the parameters α, β and σ are set to be 0.95, 0.7 and 0.95, respectively. The implementation of the blackout model and the self-organized criticality mechanism of power system were realized using Matlab 2009a.

For the modified IEEE 30-bus system as shown in Fig. 5.7, a wind farm is connected to Bus 30. Three transmission lines (29→30, 27→30, 27→29) were strengthened to increase their transfer capacity for transmitting the power generated by WECS at Bus 30. Similarly, for the modified IEEE 118-bus system as shown in Fig. 5.8, a wind farm is connected to Bus 35. Three transmission lines (35→36, 35→37, 34→36) were strengthened as well to transmit the power generated by WECS at Bus 35. Data for transmission line constraints of the IEEE 118-bus system were obtained from [122] and listed in Appendix I.

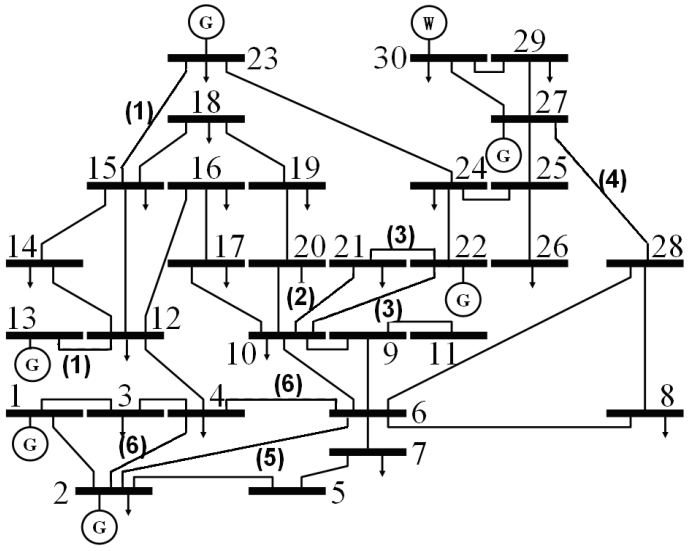

Fig. 5.7 Modified IEEE 30-bus system

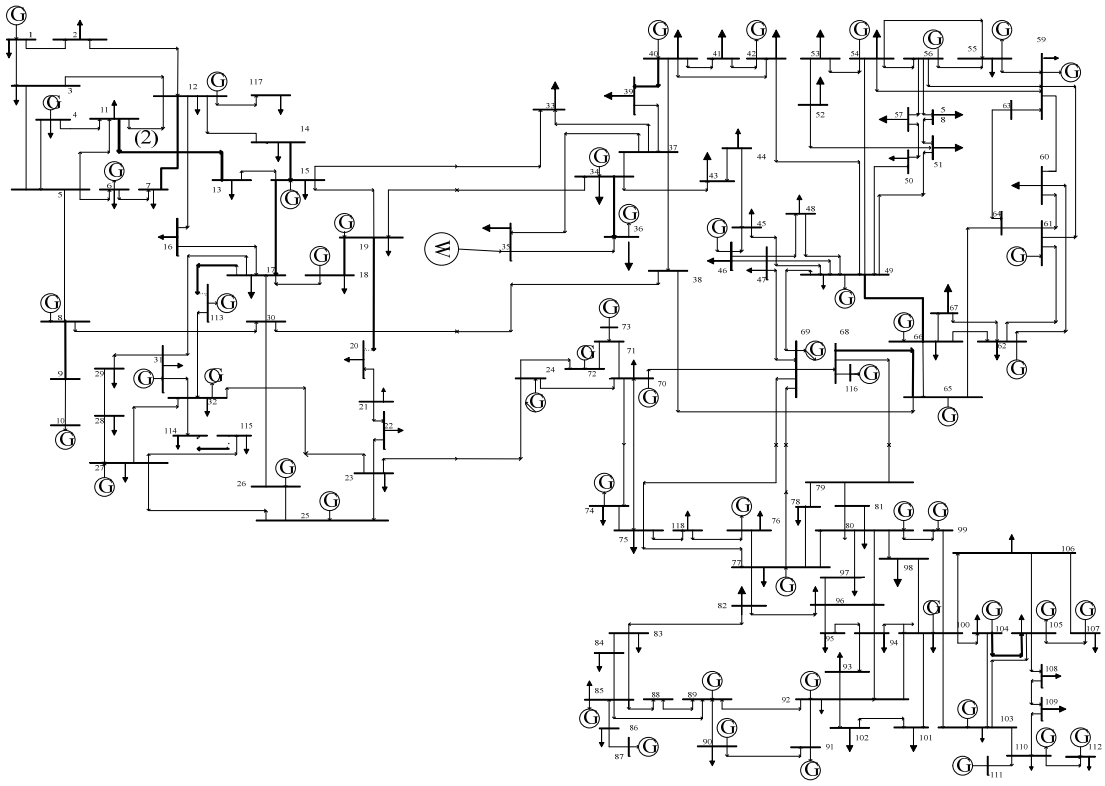

Fig. 5.8 Topology of the IEEE 118-bus system

5.6.2 SIMULATION RESULTS

In order to simulate the behavior of the self-organized criticality of power system with a gradually increased wind penetration level, the wind generation output is increased gradually from 0MW to 100MW with a step of 5MW for the modified IEEE 30-bus system. Fig. 5.9 shows the probability distribution curve of loss of load when the wind generation is 90MW, 95MW and 100MW, respectively.

It could be seen that the curve with wind generation of 95MW shows a power law tail characteristics. But the curve with wind generation of 90MW does not have any power law tail characteristic at all yet companied with only small scale accidents. However, when the wind generation increases to 100MW, there would be a suddenly increase in the probability of the occurrence of large-scale incidents, which is of course an undesired situation. Thus, the system is considered to be in non-critical status when the wind power output is below 90MW, under which the

effects of minor disturbances in the system are quite limited. On the other hand, the probability of large loss of load increases greatly with wind power output at 95MW, i.e. the system reaches to a critical status since a tiny incident would highly possibly cause a cascading failure. Therefore, as a conservative estimation, 90MW of wind generation could be treated as the wind penetration level limit. Since the total load of the modified IEEE 30-bus system is 189.2MW, the penetration limit is nearly 50%.

For the modified IEEE 118-bus system, the wind generation output is again increased gradually from 0MW to 830MW with a step of 10MW. Fig. 5.10 shows the probability distribution curve of loss of load when the wind power is 800MW, 810MW, 820MW and 830MW, respectively.

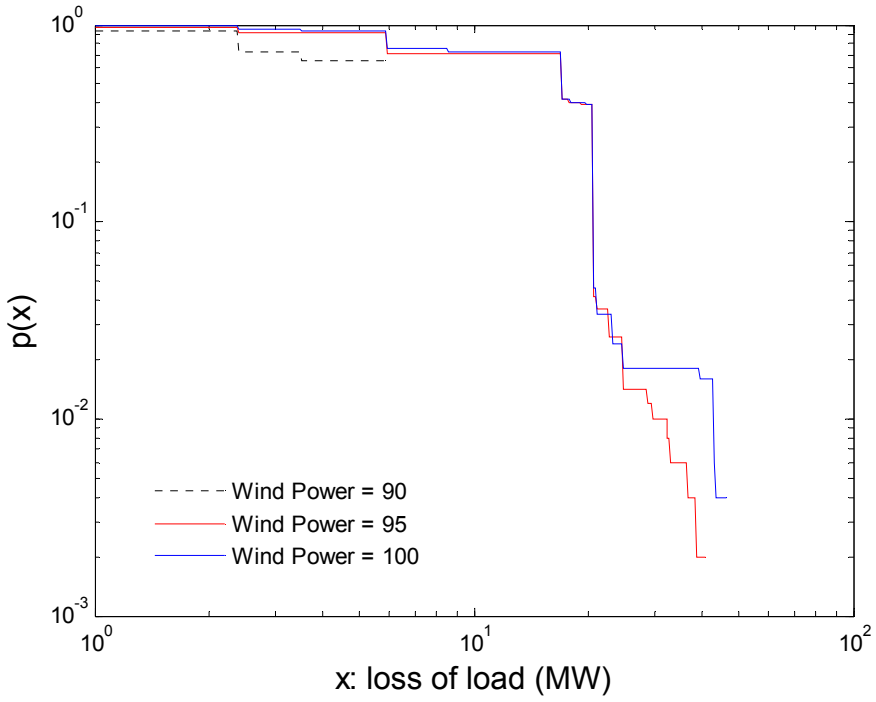

Fig. 5.9 Probability distribution curve of loss of load when the wind power is 90MW 95MW and 100MW (IEEE 30)

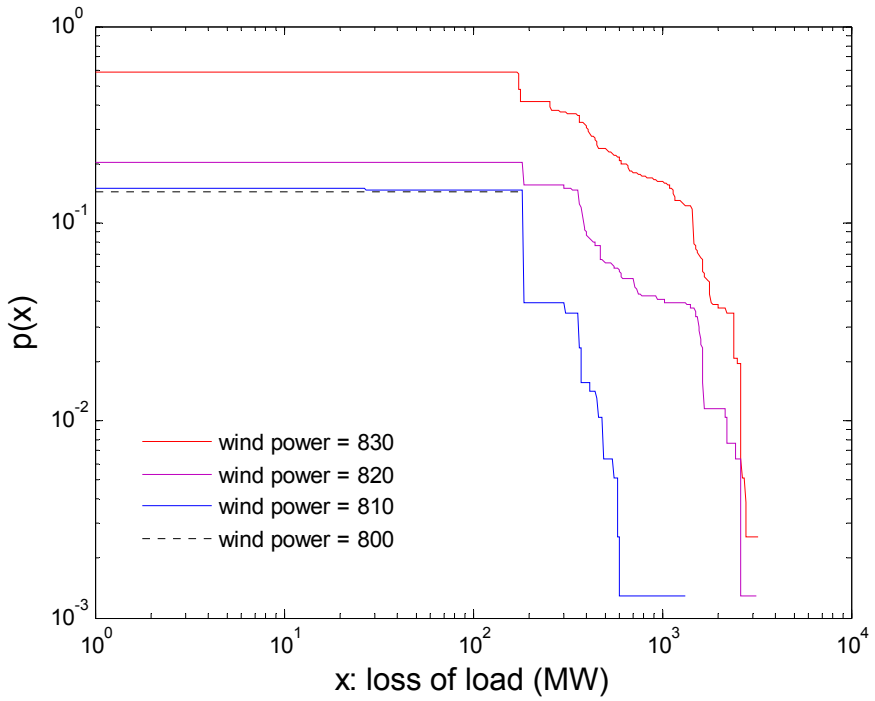

Fig. 5.10 Probability distribution curve of loss of load when the wind power is 800MW, 810MW, 820MWand 830MW (IEEE 118)

Fig. 5.10 shows that the curve with wind generation of 800MW is only in company with some tiny scale incidents, which means that it is not likely to have a large scale of loss of load. As the wind penetration level increases, the curve with a wind generation of 810MW starts to show some medium scale incidents, which is still not considered to lead to a system crisis. But when the wind generation output rises to 820MW, a power law tail characteristics shows up. There would be a much greater probability that large-scale loss of load would occur, which would be considered as a critical status under the concept of SOC. If the wind generation had continued to increase, say 830MW, there would be a further greater possibility to have a larger scale of incidents, i.e. the system would totally collapse if running under such condition.

The above phenomena show that the system remains in non-critical status if the wind power output is under 800MW. Once the wind power output exceeds

810MW, system would reach to a critical status, i.e. the probability of large loss of load would increase greatly. Thus, a wind generation of 800MW could be taken as a conservative wind penetration level limit. Since the total load of the modified IEEE 118-bus system is 4,242MW, the penetration limit would be nearly 20%.

The wind power penetration limit assessments of the above two test systems could further be verified by the average loss of load as shown in Table 5.1 and 5.2 for IEEE 30-bus and 118-bus systems, respectively.

Wind power (MW)	Average loss of load (MW)	VaR (MW)	CVaR (MW)
0~60	0	0	0
65	1.0032	2.4	0.12
70	1.5216	5.9	2.950
75	3.3460	5.9	2.950
80	3.4644	5.9	2.950
85	4.2754	5.9	2.950
90	4.6098	5.9	2.950
95	15.2408	20.5647	1.2801
100	15.7871	20.5647	1.4760

Table 5.1 Average loss of load, VaR and CVaR for IEEE 30-Bus System with increasing wind generation

Wind power (MW)	Average loss of load (MW)	VaR (MW)	CVaR (MW)
0~760	0	0	0
770	26.523	184	9.2
780	27.233	184	9.2
790	22.26	184	9.2
800	26.523	184	9.2
810	37.501	184	19.105
820	134.77	708.45	80.574
830	418.33	1764.3	117.52

Table 5.2 Average loss of load, VaR and CVaR for IEEE 118-Bus System with increasing wind generation

Fig. 5.11 shows the average system loss of load curves for the IEEE 30-bus and 118-bus systems with increasing wind generation output. Fig. 5.11(a) illustrates that, for the modified IEEE 30-bus system, there would be practically zero average loss of load if the wind power output is lower than 60MW. Yet the average loss of load would gradually rise as the increase of wind generation output after the load level exceeding 60MW and suddenly increase dramatically once the wind power exceeds 90MW. This implies that the critical point of wind power output may be 90MW. Likewisely, Fig. 5.11(b) illustrates that, for the modified IEEE 118-bus system, the average loss of load remains 0MW until the wind power output is higher than 760MW and rises dramatically when the load level exceeds 810MW after a steady increase. Another sharper increase shows up when the load level exceeds 820MW.

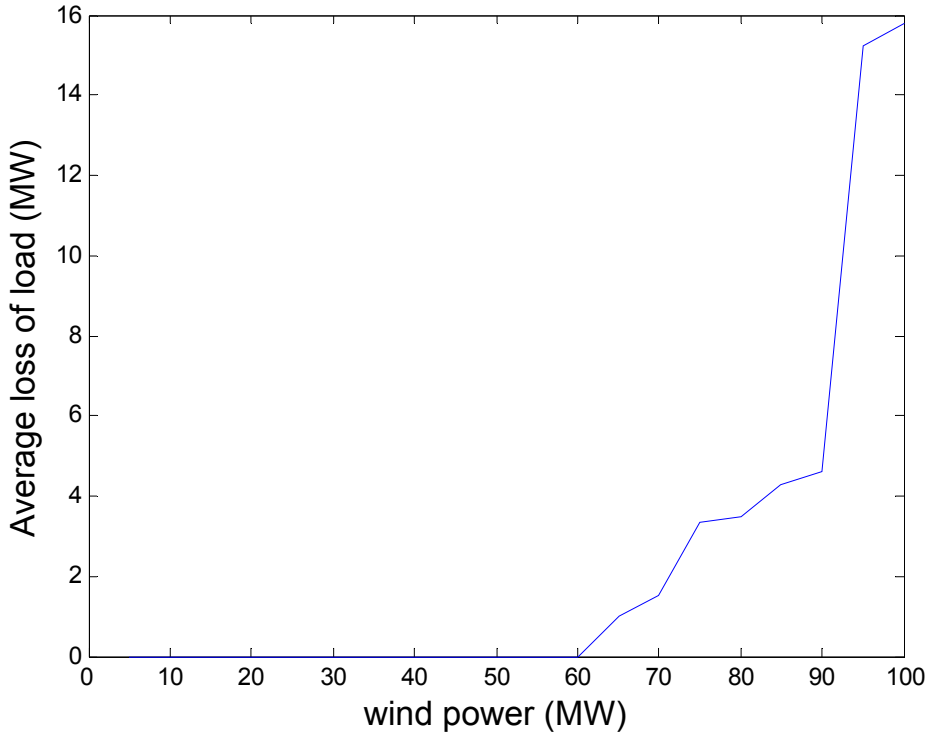

(a) IEEE 30-bus system

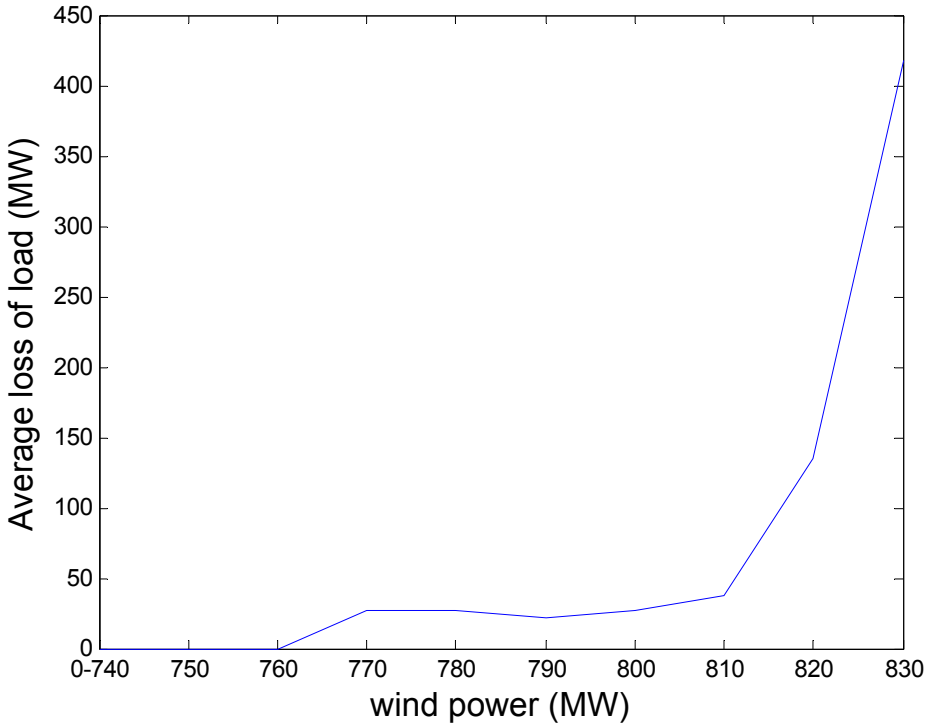

(b) IEEE 118-bus system

Fig. 5.11 Plots of average system loss of load curves against wind power output

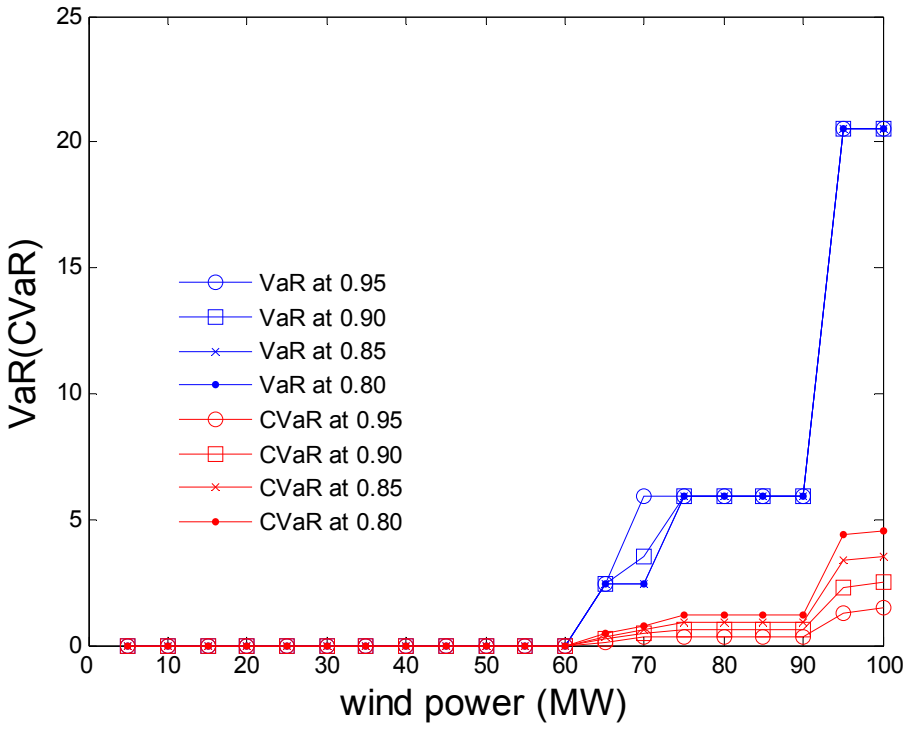

(a) IEEE 30-bus system

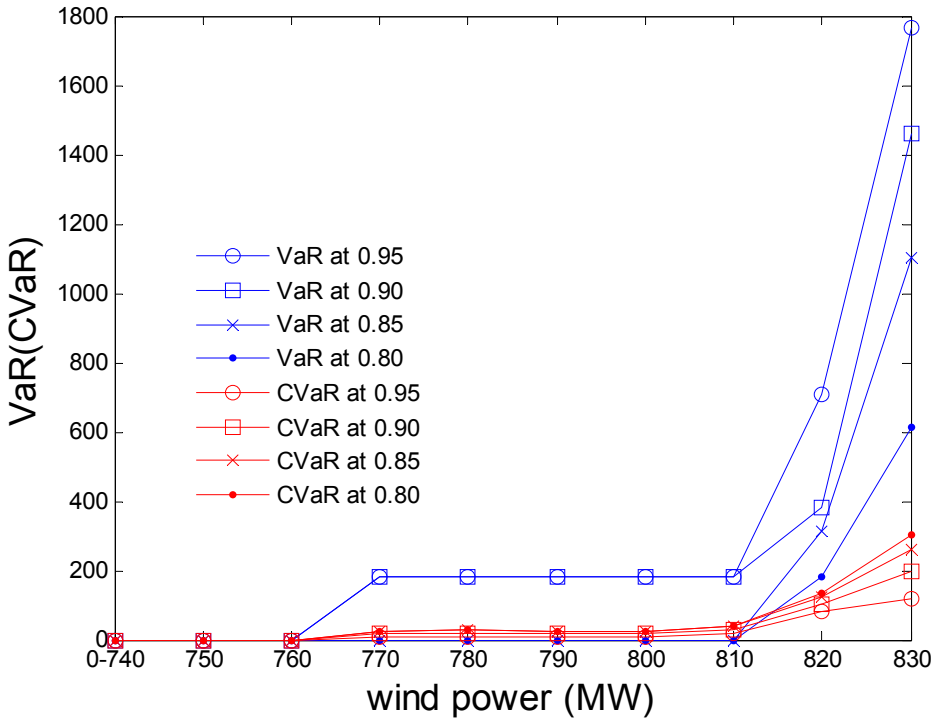

(b) IEEE 118-bus system

Fig. 5.12 Plots of VaR and CVaR curves against wind power output

Fig. 5.12 shows the plots of VaR and CVaR for the IEEE 30-bus and 118-bus systems. It shows not only the VaR and CVaR curves under the confidence level of 0.95 as calculated in Table 5.1 and 5.2, but also curves under confidence level of 0.90, 0.85, and 0.80 for comparison.

Both VaR and CVaR curves support that 90 MW wind generation output is the critical point for the modified IEEE 30-bus system and range 810-820 MW wind generation output is the critical range for the modified IEEE 118-bus system. It could also be seen that VaR and CVaR curves tend to have the same trends under different confidence level.

5.7 SUMMARY

Many technical and economical problems rise with increasing wind penetration level, which could be limited under various concepts. Lessons from recently occurred blackouts have drawn attention to studying the whole power system state rather than only evaluating individual components. Instantaneous wind power penetration is the ratio of the wind power output to the total load demand at some specific moment. This chapter focused on quantifying the instantaneous wind power penetration limit for a given power system under a relatively new concept, self-organized criticality, which focuses on evaluating the global state of the electricity system rather than some single elements. Under disturbances, the nonlinear dynamics of a system with SOC characteristics would vary abruptly to major disruptions spontaneously with a power law tail characteristic.

In reality, not all sites are suitable for wind farm. It would be constrained by terrain, local wind characteristics, population, land expenses, and so on. Therefore, it is highly possible that only a few (sometimes one) specific sites would be chosen

as the potential wind farm locations. Knowing the locations, the specific point of common coupling buses would then be decided for carrying out the wind penetration limit assessment. This thesis raised a novel methodology assessing the wind penetration level based on an existing power system and a hypothetical wind farm location. This methodology could be further developed to quantify wind penetration limit with multiple wind farm locations. The effects of not only different site locations but also the proportional allocation of wind generation in each predetermined locations could be analyzed and assessed. Case studies on two test systems verified that the probability distribution curve of loss of load did show a power law tail characteristics when the wind generation output was increased to near the maximum instantaneous penetration level since the global system state is approaching a collapse point due to the continuous increase of wind generation. This chapter further applies a new AC-based OPF blackout model and the concept of Value-at-Risk (VaR) and Conditional Value-at-Risk (CVaR) to quantitatively assess this penetration level limit by evaluating the risk of loss of load. VaR measures the largest loss of load for a given confidence level. CVaR efficiently measures those extremely large losses of load for a given confidence level. Together with the average loss of load, VaR and CVaR would fully describe the change of the global system state when the wind generation output was increased to near the penetration level limit. Case studies show that the wind penetration level could be as high as about 50% for the modified IEEE 30-bus system and about 20% for the modified IEEE 118-bus system.

CHAPTER VI ESTIMATION OF WIND PENETRATION AS LIMITED BY NERC'S CONTROL PERFORMANCE STANDARDS

6.1 INTRODUCTION

Although Copenhagen Accord seems to be a daunting task for all 192 countries to sign up, yet the continually deteriorated environment is definitely the biggest concerns for humanity at the moment. Besides, every country is trying its best to develop smarter energy security strategies and policies to achieve a greener economy, which would lead to an energy independent nation that free from foreign energy supply. Among all renewable resources, wind power is definitely the most promising and booming technology. However, many problems would rise if large amounts of wind are integrated into the existing power system. Therefore, how to fit a large amount of wind generation into the existing grid is getting more and more attention. As the installed wind power generation capacities increase, power system planners and operators are facing many new economic and technical challenges because of wind's variability and average predictability. The power generation characteristics are directly determined by conditions like weather, location, and so on. When companied with a high wind penetration level, the system definitely needs some novel and better services.

Although variability is nothing new in a modern electrical power system, yet comparing with the predictable load variations, it is much more difficult to obtain an accurate wind forecasting results. With the recent rapid development in power electronics and increasing demand pressure for generation with low-carbon emission, more and larger capacity grid-connected wind farms would contribute significantly to the system operation and security. For instance, a high level wind

penetration level would exert great influence on the frequency control of the power system.

From the viewpoint of utilities, these wind power fluctuations could be considered as ‘a negative stochastic load disturbance sources’, which would result in more complicated and uncertain load variations, i.e. lead to a great influence on the frequency control of power systems. Automatic Generation Control (AGC) is one of the key control systems required for a successful operation of interconnected power systems. The primary objective of AGC is to maintain the frequency of each control area and to keep the tie-line power close to the scheduled values by regulating the power outputs of AGC generators to accommodate fluctuating load demands. AGC performances in the normal interconnected power system operation are usually monitored and assessed by interchange power flow, system frequency and other guideline standards all the time.

The contribution of this chapter is to propose a novel methodology to estimate the installed capacity penetration limit, i.e. the maximum ratio of the installed wind generation capacity to the total generation capacity on the system [59]. The impacts of wind penetration on the AGC system are investigated via simulations based on the representative and historical system data from the China Southern Power Grid power system. The proposed algorithm has been implemented and tested on the detailed China Southern Power Grid power system model. Simulation results illustrate that the installed wind capacity penetration level as limited by NERC's new Control Performance Standards (CPS), CPS1 and CPS2, could reach to about 14.85% with an installed wind generation capacity of around 8975.4MW in Guangdong power grid.

6.2 NERC'S NEW CONTROL PERFORMANCE STANDARDS

The evolution and development of NERC's control performance standards has been generally introduced in Chapter 1. The control area's AGC performance in normal interconnected grid operation has been monitored and assessed by Control Performance Criteria (CPC), A1 and A2 criteria since the 1960's. Both criteria are based on the quantity called Area Control Error (ACE), which is defined as 'the difference between scheduled interchange and metered control area boundary flow, plus a factor proportional to the difference between prevailing and scheduled interconnection frequency.' For a long time, it was highly believed that there was not much connection between satisfactory interconnected grid operation and high quality A1 and A2 control area performance. Fortunately, the new control performance standards, CPS1 and CPS2, with whose solid technical foundation, was established. The new standard is supposed to be designed in such a way that it would evaluate the control performance without prescribing how control is to be implemented, which would:

(1) allow control areas to tailor their own algorithms to maintain the necessary control of area interchange flows and interconnection frequency;

(2) minimize the non-productive adjustments of generation.

The resultant reduced operation of generation units would realize more efficiently operations and less maintenance due to reduced wear and tear. These brand new standards also provide a strategy to control the frequency characteristic. Therefore, if the frequency characteristic could be relaxed without threatening the system reliability, it might be even possible to allow the control performance alter to the point where the desired frequency characteristic is achieved.

Electric power systems consist of a number of interconnected control areas,

which are mainly responsible for two tasks [123]:

(1) supplying power to their native load,

(2) maintaining interchange power with their neighbors to its scheduled value.

The control areas of power systems must maintain an energy balance since the power demand is constantly changing. The area control error would be used to assess the energy balance for area *i*, which would be given as follows:

$$ACE = \Delta P_T - 10B\Delta F = (P_a - P_s) - 10B(F_a - F_s) \tag{6.1}$$

where ΔF is the interconnection frequency error, which is the difference of the net actual and scheduled system frequency, $F_a - F_s$; ΔP_T is the tie-line power error, which is the difference of the net actual and scheduled tie flows, $P_a - P_s$; B represents a control area's frequency bias expressed with a unit of -MW/0.1 Hz.

Control area needs to be in compliance with the NERC's new control performance standards, CPS1 and CPS2, to obtain a fair operation of an interconnected system. The purposes of this new standard are to enhance the frequency supporting efforts from power control areas and to relax the pressure of regulating *ACE* to zero. CPS1 is acting as a limit on the average of a function combining *ACE* and interconnection frequency error ΔF from schedule, i.e. for frequency control. The role that CPS2 plays is to restrict the unacceptable and unpredictable tie-line power flow. The control performance of each control area needs to be monitored and reported compliance with CPS1 and CPS2 to NERC at the end of each specific period, which could be a month or a year [60].

6.2.1 CPS1 STANDARD

A1 criterion was replaced by the CPS1 standard. For A1 criterion, ACE is required to cross zero one time at least every ten minutes. However, CPS1 adopts a much more reasonable methodology based on statistical theory. A control area has

to contribute to the reliability of its own interconnected system. To what extent this contribution make would be quantitatively represented by an expression called, the Compliance Factor CF. This expression consists of two components, the ΔF components and the *ACE* components. Whenever a nonzero *ACE* shows up in a control area, which at the same time is companied by ΔF , a nonzero CF would be formed. This CF could be either positive or negative depending upon the signs of *ACE* and ΔF at that moment. A positive CF means that, for that specific moment, the corresponding area would act as a burden to the regulation requirements of interconnections. On the other hand, a CF with negative sign shows that the area contributes to the regulation requirements of interconnections. One CF value would be calculated every clock-minute based on two items, the clock-minute average of frequency error and the clock-minute average of *ACE* divided by their bias. CF requires the control area *i* to satisfy the following constraints in a certain assessment period (such as one minute) as follows:

$$\alpha_{\mathrm{CF1}} = \frac{\sum (E_{\mathrm{AVE-min}} \cdot \Delta F_{\mathrm{AVE}})}{(-10B_i) \cdot n} \le \varepsilon_1^2 \tag{6.2}$$

where α_{CF1} is the CF, $E_{AVE-\mathrm{min}}$ is the one minute average of ACE values, ΔF_{AVE} is the one minute average of frequency error, B_i represents the frequency bias of the *i*th control area, ε_i represents a target bound for the 12 month root-mean-squares (RMS) of one minute average interconnection frequency error, *n* is the number of minutes in the assessment period. CPS1 for this assessment period is then obtained as follows:

$$CPS1 = (2 - \alpha_{\mathrm{CF1}} / \varepsilon_1^2) \times 100\% \tag{6.3}$$

6.2.2 CPS2 STANDARD

The second performance standard, CPS2, which is very similar to the A2 criterion, would limit the magnitude of short-term *ACE* values. The difference is

that CPS2 uses a statistically derived ten-minute average ACE limit, referred as L_{10}, instead of the A2's empirical L_d, which is only based upon a control area's load characteristic [60]. L_{10} depends upon the interconnection's targeted RMS of ten-minute average frequency error from schedule, a control area's frequency bias, and the interconnection's total frequency bias [124, 125]. Hence, a control area connected to stronger interconnections tends to have a larger L_{10} due to the larger total frequency bias of the interconnection [125]. The CPS2 standard requires the 10-min averages of a control area's ACE to be no more than the constant (L_{10}) given as follows:

$$\left|\sum E_{\text{AVE-min}}\right| / 10 \le L_{10} \tag{6.4}$$

$$L_{10} = 1.65 \cdot \varepsilon_{10} \cdot \sqrt{(-10B_i) \cdot (-10B_s)} \tag{6.5}$$

where B_s is the summation of the frequency bias of all control areas, and ε_{10} is a target bound for the 12 month RMS of 10 minute average interconnection frequency error. A CPS2 compliance percentage could be calculated as follows:

$$CPS2 = \left[1 - \frac{\text{violations}_{\text{month}}}{\text{total periods} - \text{unavailable periods}}\right] \times 100\% \tag{6.6}$$

where $\text{violations}_{\text{month}}$ are a count of the number of periods that the 10-min averages of ACE are greater than L_{10} in one month. In order to follow NERC, CPS1 compliance should not be any more than 100% while each control area has to make its CPS2 compliance as much as 90%. More details about NERC's CPS can be obtained from [68].

More details on NERC's CPS are available from [64, 66, 68]. In the Chinese electricity industry, the logical flow chart for determining the NERC's CPS compliance is shown in Fig. 6.1 [126].

According to the Grid Code of the China Southern Power Grid, the determination of CPS compliance for a certain assessment period (typically 10 minutes) is assessed as follows:

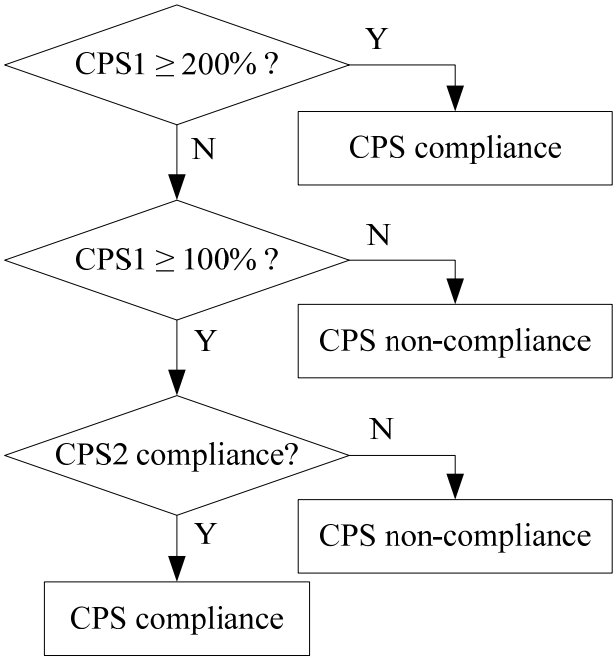

Fig. 6.1 Flow chart for the determination of CPS compliance

i. If CPS1 ≥ 200%, then there is no need to consider CPS2 standard and CPS control performance rating is Pass. This is to encourage the frequency supporting efforts from other interconnected control areas during emergency and to fully explore the benefits of large-scale interconnected power grids. The AGC control behaviors of the control area in this case are considered advantageous to the improvement of overall interconnection frequency quality during this assessment period.

ii. If 100% ≤ CPS1 < 200% and CPS2 compliance is satisfied, then CPS control performance rating is Pass.

If 100% ≤ CPS1 < 200% and CPS2 standard is in violation, then CPS control performance rating is Fail.

iii. If CPS1 ≤ 100%, then CPS control performance rating is Fail.

Therefore, the CPS compliance percentage on a daily, monthly or yearly basis could be calculated as follows:

$$CPS(\%) = \left[1 - \frac{\text{violation periods}}{\text{total periods - unavailable periods}}\right] \times 100\% \qquad (6.7)$$

An analytical framework for the formulation and evaluation of control performance criteria in LFC, taking account into the uncertainty in the measured variables in LFC, was reported in [127]. Detailed statistical and dynamic analyses of CPS were illustrated in [128, 129]. The state-of-the-art in AGC strategies designed to work under CPS criteria were comprehensively reported in [62] and further investigated in [123, 130, 131]. One of the most significant advantages of the new CPS is the elimination of the ACE zero-crossing requirement. As reported in [132], 'one control area reported that over 75% of its control actions were required by the Al criteria to cross zero, and almost one-half of those actions were identified to be in a direction to adversely impact the system frequency.' Therefore, by controlling units according to new CPS requirements, in which the ACE zero crossing is eliminated, unit fuel efficiency improvements and unit wear-and-tear reductions would be expected. Additionally, the ten-minute average ACE limit, L_{10}, required by the CPS2 standard would be significantly larger than L_d as required by the A2 criterion [66]. A larger average ACE limit indicates looser control, which would lead to relatively low control costs.

6.3 AGC CONTROL STRATEGY BASED ON CPS STANDARDS

The CPS Standards has been widely adopted by utilities over the world, including the East China Power Grid and China Southern Power Grid (CSG) in 2001 and 2005 respectively. CSG has been implementing a hierarchical AGC system developed by Nanjing Automation Research Institute (NARI). The AGC strategy under NERC's CPS adopted in the Energy Management System (EMS) is an improved proportional-integral (PI) control methodology [133, 134]. This control scheme has been proved to be very efficient in maintaining frequency

quality and providing power support to interconnected control area during emergency. The AGC control strategy based on CPS standards could be described geometrically using the 2-dimensional CPS phase control space as shown in Fig. 6.2.

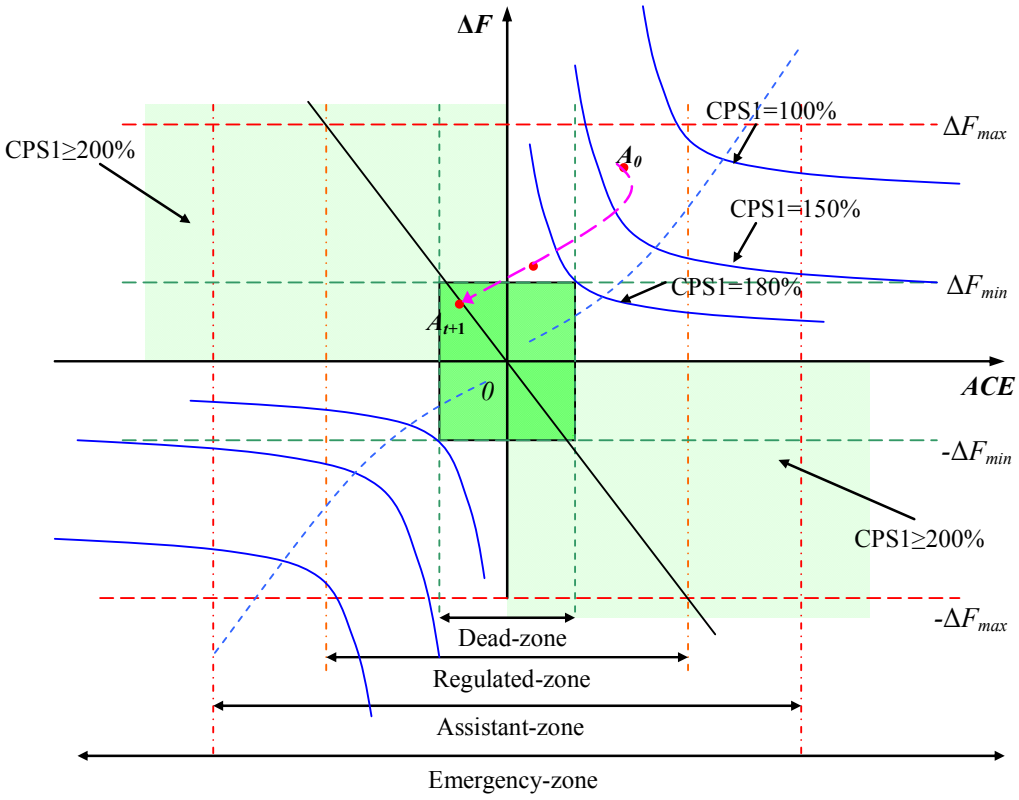

Fig. 6.2 Schematic diagram of 2-dimensional AGC control space under CPS

The NARI's AGC control strategy, which is based on the classical PI control methodology, has been further developed. The AGC total regulating power command could be expressed as follows:

$$\Delta \mathbf{P}_{\sum AGC} = \Delta P_P + \Delta P_{CPS} + \Delta P_I \tag{6.8}$$

where $\Delta \mathbf{P}_{\sum AGC}$ is the total AGC regulation power command within the control area; ΔP_P is the proportional component of the regulation command; ΔP_I is the integral component of the regulation command; ΔP_{CPS} is the CPS component in the regulation command.

6.3.1 CPS1 CONTROL ALGORITHM

As could be seen from equation (6.8), ΔP_P and ΔP_{CPS} mainly contribute to maintaining the CPS1 compliance target. The detailed control algorithm could be depicted as follows:

(1) Control Algorithm of ΔP_P:

When ACE lies in the dead-zone, $\Delta P_P = 0$;

When ACE lies in the normal regulated-zone:

$$\begin{cases} \Delta P_P = -G_P E_{ACE} & CPS1 < 200\% \\ \Delta P_P = 0 & CPS1 \geq 200\% \end{cases} \tag{6.9}$$

When ACE lies in the assistant-zone or emergency-zone:

$$\begin{cases} \Delta P_P = -G_P E_{ACE} & CPS1 < 200\% \ or \ CPS1 \geq 200\% \ \& \ |\Delta F| < \Delta F_{CPS} \\ \Delta P_P = 0 & CPS1 \geq 200\% \ \& \ |\Delta F| \geq \Delta F_{CPS} \end{cases} \tag{6.10}$$

where the filtered frequency deviation in the control area is defined as $\Delta F = f - f_N$; ΔF_{CPS} is the CPS threshold value of frequency deviation that is normally between 0.03Hz and 0.05Hz; E_{ACE} is the filtered instantaneous ACE value; G_P is the proportional gain, which is normally 1 or slightly more than 1. ΔF_{CPS} is set to be 0.03Hz in the case study. It should be pointed out that the CPS1 control is required in equation (6.10) when $CPS1 \geq 200\% \ \& \ |\Delta F| < \Delta F_{CPS}$ in order to avoid the deterioration of CPS1 index due to the sudden sign reversal of frequency deviation ΔF.

(2) Control Algorithm of ΔP_{CPS}:

$$\begin{cases} \Delta P_{CPS} = -G_{CPS}\Delta F & \Delta F_{\min} \leq |\Delta F| \leq \Delta F_{\max} \\ \Delta P_{CPS} = 0 & |\Delta F| < \Delta F_{\min} \\ \Delta P_{CPS} = \dfrac{-G_{CPS}\Delta F_{\max}\Delta F}{|\Delta F|} & |\Delta F| > \Delta F_{\max} \end{cases} \tag{6.11}$$

where G_{CPS} is the frequency gain factor, whose value is determined by how

much power support could be provided temporarily by the control area. For instance, when the frequency deviation is 0.1Hz, if the desired ACE is -50MW, then G_{CPS}=500MW/Hz. The maximum frequency deviation $\Delta F_{\max}$ could be as much as 0.2Hz, and the minimum frequency deviation ΔF_{CPS} would be set to be 0.03 in this case study.

6.3.2 CPS2 CONTROL ALGORITHM

As could be seen from equation 6.8, ΔP_I mainly focus on making sure that the average ACE is limited to a specific boundary given an assessment period, i.e. guarantee the CPS2 compliance. This could be achieved by regulating the integral component. The control algorithm could be expressed as follows:

$$\begin{cases} \Delta P_I = 0 & |I_{ACE}| < I_{\min} \\ \Delta P_I = -G_I I_{ACE} & |I_{\min}| \le |I_{ACE}| \le |I_{\max}| \\ \Delta P_I = \dfrac{-G_I I_{\max} I_{ACE}}{|I_{ACE}|} & |I_{ACE}| > I_{\max} \end{cases} \tag{6.12}$$

where G_I is the integral gain; I_{ACE} is the integration of the ACE, which would be reset to zero at every beginning of the evaluation period and be limited by $I_{\min}$ and $I_{\max}$. The integration component I_{ACE} could be actually treated as the exchange power during the evaluation period, thus the value of $I_{\min}$ and $I_{\max}$ .could be determined by the limits of exchange power.

NARI further modified the control algorithm to obtain the total regulating power $\Delta \mathbf{P}_{\sum AGC}$, which is expressed by equation 6.8. The schematic diagram of CPS control space could be seen in Fig. 6.2. It is not necessary for AGC to give any command and instruction in the second or the fourth quadrant (CPS1>200%). However, if it accompanied with the sign-alternation of ΔF and a large $|ACE|$, CPS1 would be dramatically deteriorated. In order to measure the absolute value of the sigh-alternated $|ACE|$ under some frequency deviation ΔF, $|ACE|$ is usually compared with its threshold value Eth, which could be expressed as

follows:

$$E_{th} = -K_{CPS}\Delta F \tag{6.13}$$

If $|ACE|$ lies between Eth and ΔP_{CPS}, then $\Delta P_{CPS} = -\Delta P_P$. If $|ACE|$ is greater than Eth, then $\Delta P_{CPS} = E_{th}$.

Therefore, a one-to-one correspondence between the actual range of the total regulating power command $\Delta P_{\sum AGC}$ and the control range of the ACE have been formed: $\Delta P_{\sum D}$ is the regulating threshold value of the static dead-zone (a value of 50MW is selected); $\Delta P_{\sum A}$ is the threshold value of the assistant-zone (a value of 190MW is selected); $\Delta P_{\sum E}$ is the power threshold value of emergency-zone (a value of 398MW is selected).

6.4 WIND POWER VARIATION SIMULATION

Since Guangdong power grid would be treated as the detailed study control area, it is assumed that all hypothetical wind power generation are from Guangdong area.

6.4.1 WEATHER RESEARCH AND FORECASTING MODEL

Due to the fact that the direct observation wind data for the off-shore wind farm is unavailable, the Weather Research and Forecasting (WRF) model would be adopted to simulate the wind data. WRF is a next-generation mesoscale numerical weather prediction (NWP) system designed to serve both operational forecasting and atmospheric research needs [135]. It accepts the WRF terrestrial data and gridded meteorology data, using meteorology model to process and produce the forecasting data of a given geographical site. In this chapter, such data was used as the substitution for the unavailable historical data.

Running on a PC cluster, the advanced research WRF (ARW) system was

configured with 5-layer nested grids to simulate the wind resource data of the hypothetical Huilai Offshore Wind Farm. The sizes of the increasingly fine grids are 81.0km, 27.0km. 9.0km, 3.0km and 1.0km, respectively. Huilai wind farm is one of the largest offshore wind farms currently planned in China. The geographical coordinates of this long-term simulation are set to be latitude 23.02 and longitude 116.18 with a height of 80 meters. The Thermal diffusion scheme and the NCEP FNL Operational Model Global Tropospheric Analysis data [136] are used as the land surface scheme and the input meteorology data, respectively. The detailed configuration of this NWP model is shown in Table 6.1.

Parameter	Value
Mesoscale NWP model	ARW
Sizes of nested grids	91km, 27km, 9km, 3km, 1km
Vertical Layers	28
Integration time step	300
Geographical data resolution of nested grids	10m, 5m, 2m, 30s, 30s
Elevation database	3 second SRTM
Soil classification	30 second USGS
Surface parameterization	30 second USGS
Map projection	Lambert
Microphysics option	WSM 6-class graupel scheme
Longwave radiation option	Rrtm scheme
Shortware radiation option	Dudhia scheme
Surface Layer option	Monin-Obukhov scheme
Land Surface scheme	Thermal diffusion scheme
Boundary Layer option	YSU model

Table 6.1 The detailed parameter configuration of NWP model

Since the minimum time step of NWP is 60 seconds, Hermite interpolation would be applied to generate a time series of wind speed values with a time step of 8s [137]. Fig. 6.3 below plots the Huilai wind data simulated for a month from 1 to 30 September 2009.

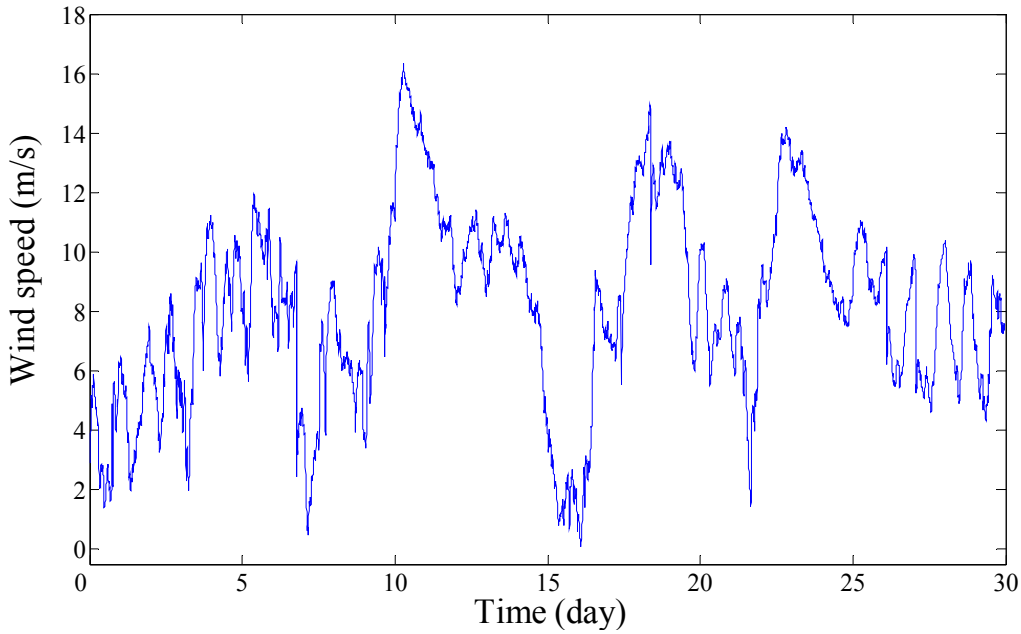

Fig. 6.3 Simulated Huilai wind data (1-30 September 2009)

6.4.2 WIND TURBINE

The mechanical output power of the wind turbine is modeled as in Chapter 3. Also, the wind speed versus power curve of a typical wind turbine is shown in Chapter 3 as well.

In this chapter, a fixed speed wind turbine based wind energy conversion system would be adopted. With the simulated wind speed historical as described previously, the active power output of a wind turbine based generator could be calculated according to the wind turbine power curve. For simplicity, an aggregated model, which would provide an enough approximation of the wind farm performance for applications in interconnection studies, would be adopted

in this chapter.

The total wind power generation in a system, $P_W(t)$, could be decomposed into three components: (1) a slow moving average, $P_a(t)$; (2) a fast fluctuating part, $P_t(t)$; and (3) a ramp event, $P_r(t)$, as follows [55]:

$$P_W(t) = P_a(t) + P_t(t) + P_r(t) \tag{6.14}$$

It was generally accepted that the slow moving average part, the trend/moving average, would be handled by the load-following devices so as not to have influence on CPS1 and CPS2 [55]. The moving average of the wind generation was calculated and presented in Fig.6.4. Therefore, the non-conforming load caused by wind generation fluctuations could be modeled as the sum of the fast and the ramp components, i.e. the difference between the total wind power generation and the slow moving average part. Considering the time frame of interest, the rolling or trending window would be set to be 10-min in this chapter. The non-conforming load caused by wind generation fluctuations was calculated and presented in Fig.6.5.

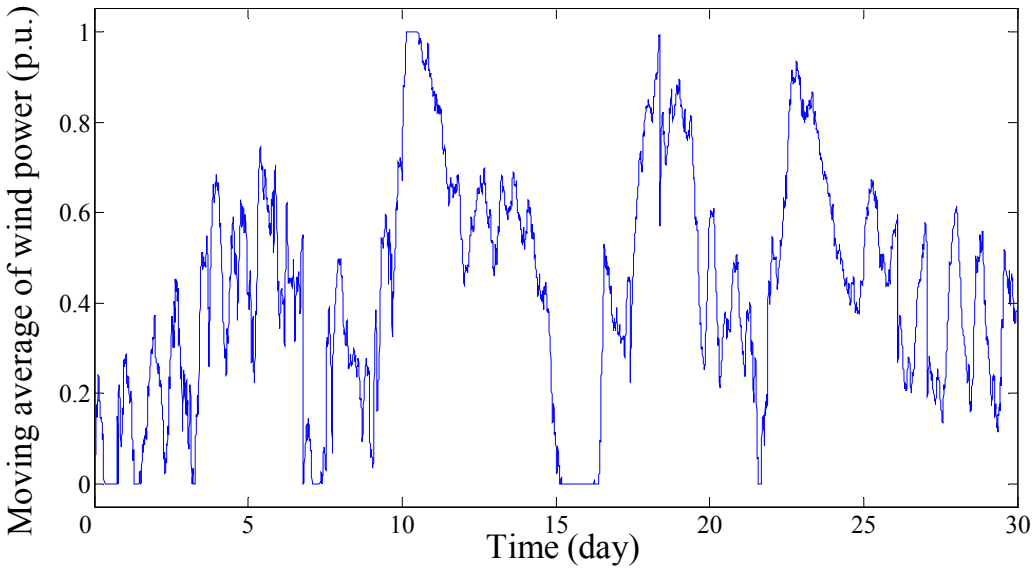

Fig. 6.4 The plot of the moving average part of wind generation

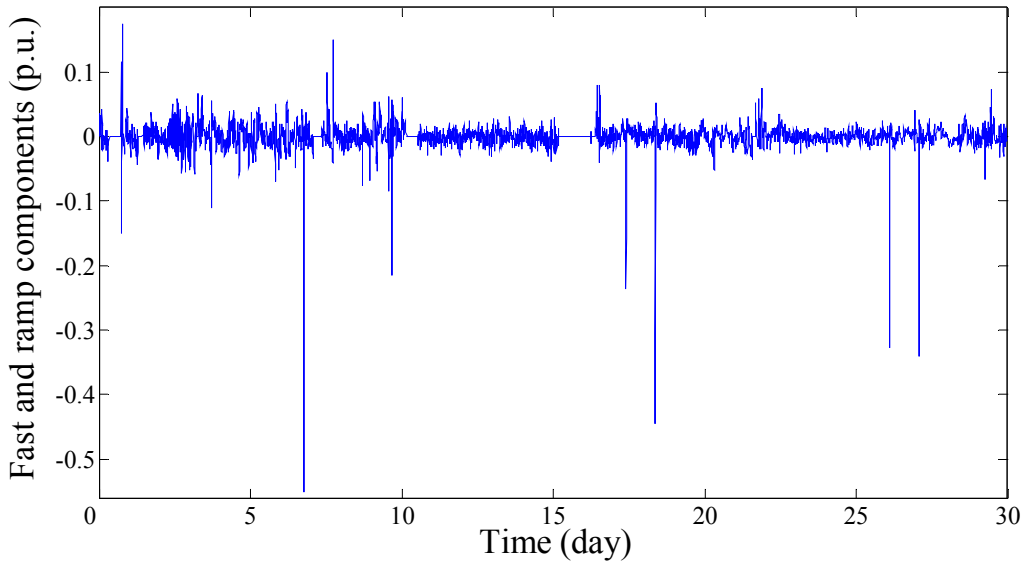

Fig 6.5 The plot of non-conforming load curve caused by wind

6.5 CASE STUDY

6.5.1 SIMULATION ENVIRONMENT

(1) Overview

The impacts of high penetration level of wind power generation on the China Southern Power Grid (CSG) power system would be fully studied via simulations based on the representative and historical system data. The detailed CSG power system models previously developed for the Guangdong power dispatching center projects was adopted as the study system [138].

In this simulation environment, the AGC simulator, which implements the NARI's AGC control strategy, would model the individual power plant dynamics and the system frequency dynamic. The AGC decision cycle is simulated every 8 seconds, and the AGC performance would be assessed with NERC's CPS.

The CSG system is uniquely characterized by parallel HVDC-HVAC transmission systems, multi-infeed HVDC transmission, high rates of load growth, and major generation resources that are remote from load centers. The benchmark

CSG power systems has four interconnected control areas as illustrated in Fig.6.6 with Guangdong power grid as the detailed study area. In the simulation, HVDC system is modeled as a first-order constant-power control model, and power plant models for fossil-fuel-fired, liquefied natural gas (LNG) and hydro generators are included. Each plant output is determined by the governor and the setpoint of AGC pulse from economic dispatch (ED) according to their participation factors.

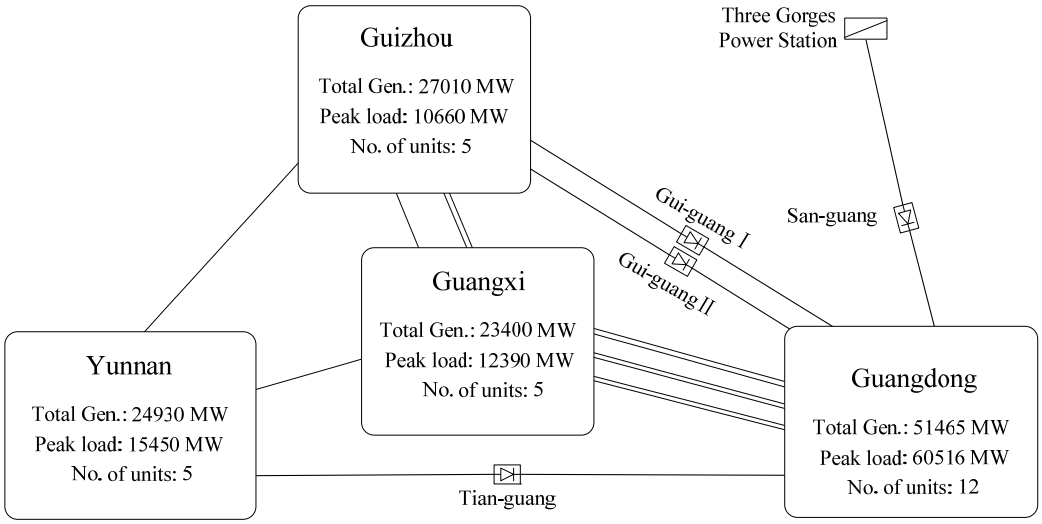

Fig. 6.6 The interconnected network of China Southern Power Grid

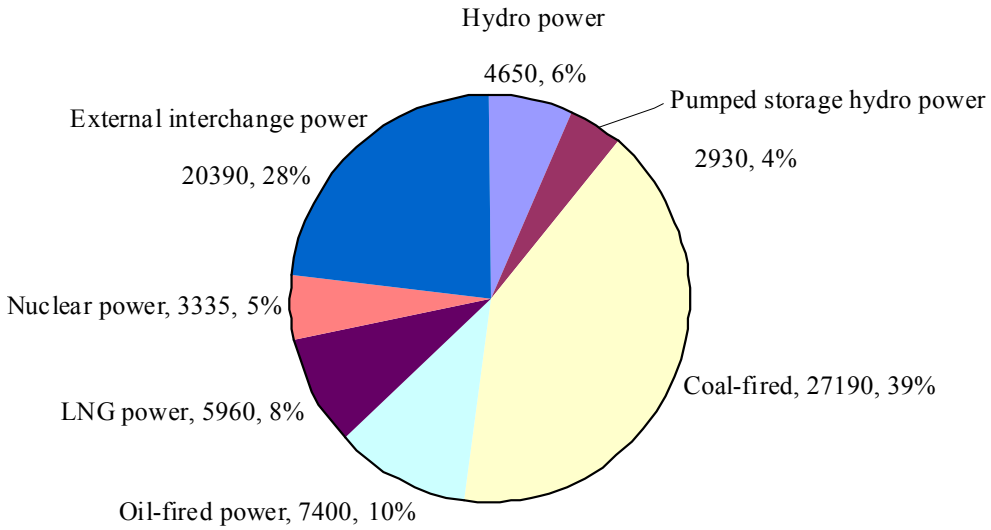

Fig. 6.7 Energy structure of Guangdong Power Grid in 2009 (MW)

(2) Unit Model

The following unit models are included in the simulation. The fossil-fuel unit models, such as coal-fired units, oil-fired units and liquefied natural gas (LNG) units, would imitate the behavior of the super-critical and sub-critical once-through units, boiler-following drum units, and coordinated-control drum units [139]. The other unit models include single-lag, combustion turbine, nuclear, and hydro [139]. In this chapter, Guangdong power grid is regarded as the detailed study control area, which includes twelve units of different types and generation capacities. Fig. 6.7 shows the energy structure of Guangdong Grid in 2009 with total installed capacity of 51,465MW [140].

(3) Operating Mode

The following four unit operational modes were implemented in the CSG power system model. The units would receive a settled setpoint in base loaded mode, which means that it would not take part in any frequency regulation and power dispatch. Yet in manual dispatch mode, the units would receive a generation setpoint every 5 minutes from economic dispatch center. However, these units are forbidden to contribute to the frequency regulation. The third mode, automatic mode, allows the units to participate in either regulation or economic dispatch. Finally, a proportional mode, in which the regulation participation factor for each AGC unit is proportional to the adjustable reserve capacity of the unit, is employed to tackle the generation allocation with various types of AGC generators.

(4) Unit Commitment

The simulator incorporates a simplified Unit Commitment scheme to commit units in the study area according to the load condition changes. When the reserve of the study area falls below some minimum value, the highest available off-line unit will be turned on. Similarly, the lowest on-line unit would be turned off whenever the reserve rises in excess of a maximum limit.

(5) Economic Dispatch

Dispatch module would also be incorporated to distribute the system load demand amongst all the generating sources so that the system operating costs are minimized. Every unit would have an economic participation factor, and Economic Dispatch would be carried out every five minutes to provide the base load setpoints for AGC in base loaded mode. AGC regulating command could be allocated to those Automatic units and Manual Dispatched units according to their participation factors.

(6) Load Data and Non-Conforming Load Data

In order to evaluate the efficiency of the primary and secondary frequency control, it is important to understand the load fluctuation of power system and to provide both realistic and representative load data. One month of continuous load data for the Guangdong power grid recorded by the Guangdong power dispatching center, including coincident nonconforming load (NCL) data [141], was shown in Fig.6.8 and used in the simulation test.

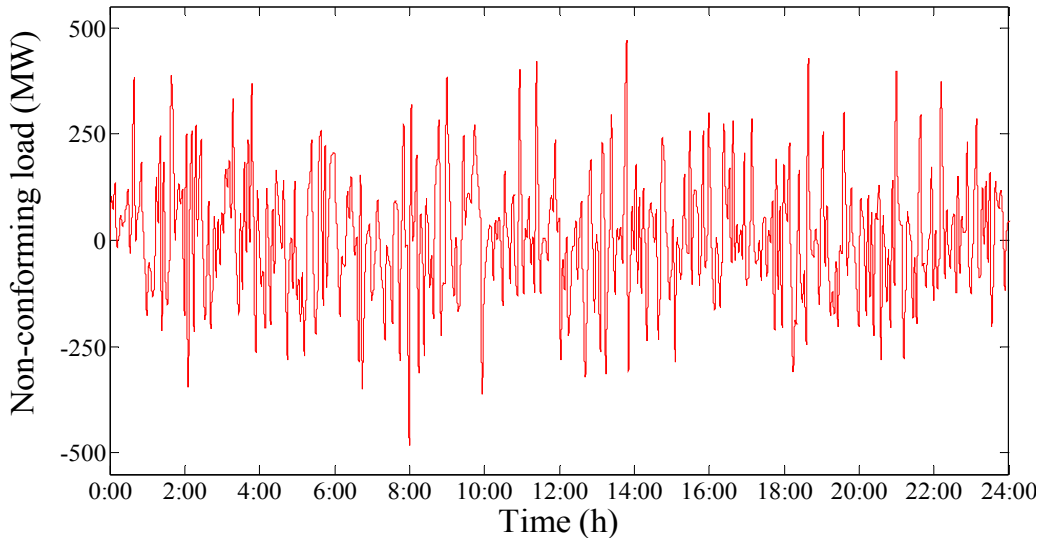

Fig. 6.8. The plot of non-conforming load curve on 7th September 2009

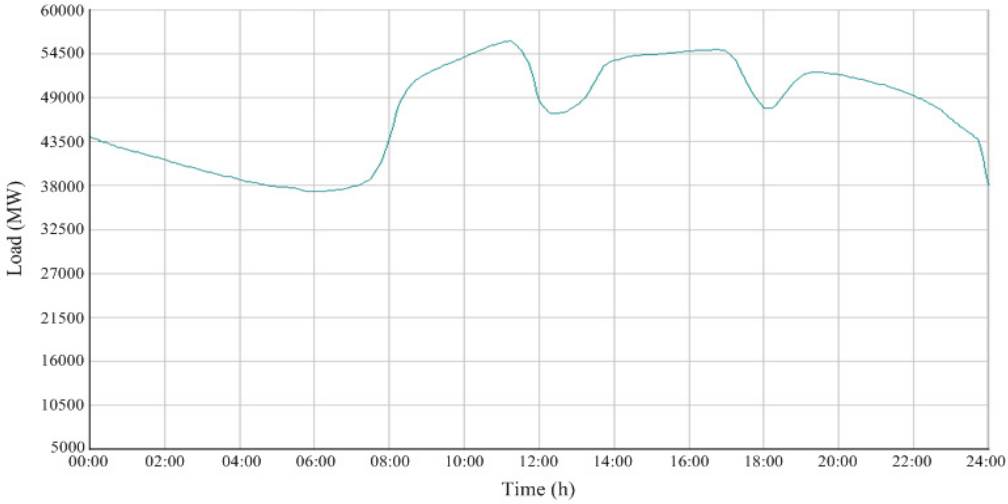

Fig. 6.9. The plot of daily load curve in 7th September 2009

Fig.6.9 plots the daily load curve on 7th September 2009. The set of load data with NCL for each provincial power grid was used as the forcing function for the AGC simulator. The integration of wind farms into the power system is treated as a load frequency control problem here in the sense that the wind generation would act as a negative load disturbance source. The system historical load data is combined with the wind power output as the synthesized load disturbances.

6.5.2 SIMULATION COMPARATIVE EXPERIMENT

The following parameters used in the simulation are predetermined by the utility. The frequency bias coefficients B_i used in equation (6.1) are -225 MW/Hz in Guangdong, -35 MW/Hz in Guangxi, -37.5 MW/Hz in Yunnan, and -40 MW/Hz in Guizhou. The threshold limit for the CPS2 assessment (L_{10}) is set to 288MW in Guangdong, 75MW in Guangxi, 78MW in Yunnan, and 81MW in Guizhou. In addition, the ε_{10} and ε_1 are 0.042 and 0.052, respectively.

The simulation comparative experiment presented here was implemented using the recorded load data on 7th September 2009 and the simulated wind power data outlined previously. Fig.6.10 and Fig.6.11 show the AGC performance results for CPS1 and CPS2 in the study area with 10 minutes assessment period.

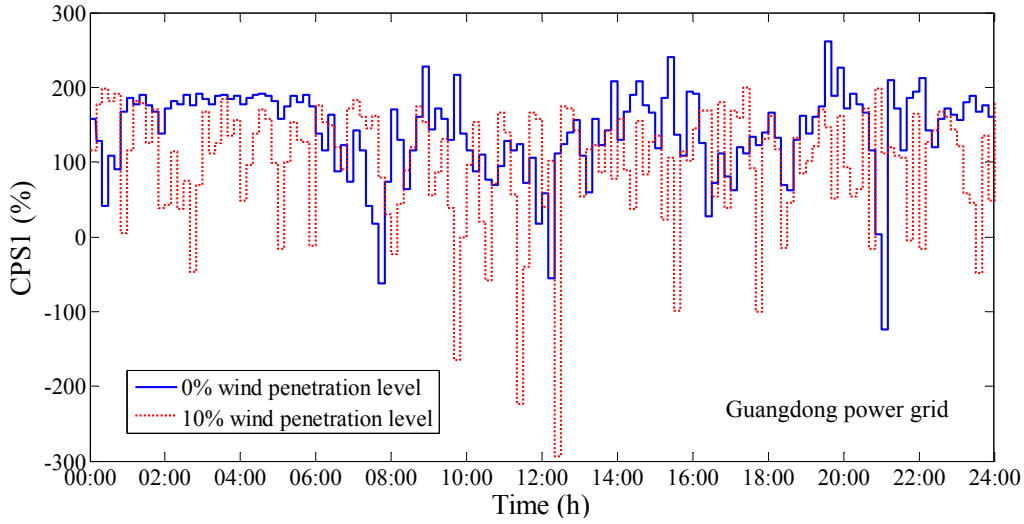

Fig. 6.10. CPS1 comparison curves with and without wind power generation

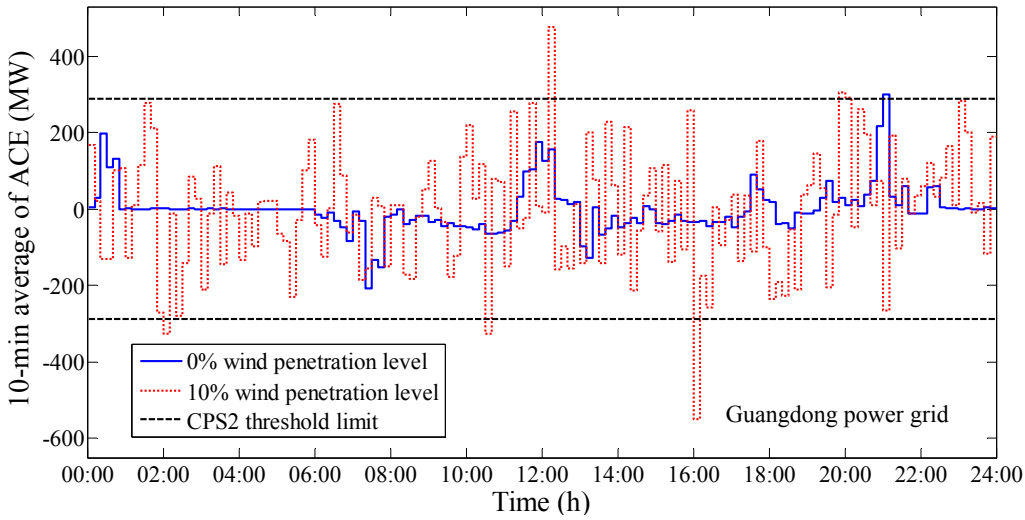

Fig. 6.11. ACE comparison curves with and without wind power generation

It is clear that in the event of high level of wind penetration, both CPS1 and CPS2 indices would be significantly affected. For instance, the number of CPS1 non-compliance points was increased from 26 with no wind power generation to 58 when the wind penetration level was increased to 10%. The corresponding CPS1 compliance declined from 140.2% to 97.1%. Likewisely, the number that CPS2 indices exceed the threshold was also increased from 1 to 6, with a corresponding declined CPS2 compliance from 99.31% to 95.83%. Following the CSG Grid Code [142], the number of CPS non-compliance points as determined

with the logic depicted in Fig.6.1 were increased from 25 with no wind power generation to 60 when the wind penetration level was increased to 10%, with a corresponding CPS compliance declining from 82.64% to 58.33%.

6.5.3 STATISTICAL EXPERIMENTS ON CSG SYSTEM

The long-term AGC performance could be assessed with data statistical comparative experiments being implemented on the detailed China Southern Power Grid power system. In the experiments, the AGC simulator of CSG system is started in a quiescent state with system frequency and tie-line flow at scheduled mode. The simulations are then carried out with the preset disturbance conditions over a 30-days period. The realistic simulations based on the representative and historical system data recorded from the CSG power system have revealed the impacts of wind penetration on the AGC system. Clearly, both the CPS1 and CPS2 indices are deteriorated with the increase of the installed wind generation capacity penetration level.

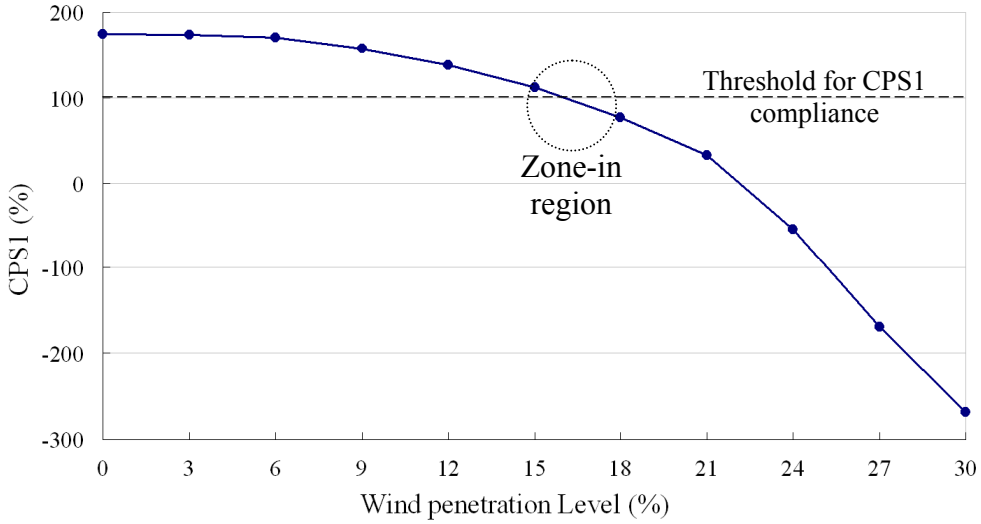

Fig. 6.12. Correlation between CPS1 compliance and wind penetration level

To investigate the impacts of wind penetration on the AGC system, the base value of the wind generation installed capacity was increased from 0MW to

22,056MW, which corresponds to a wind penetration from 0% to 30% in the CSG power systems. The specific AGC performance results in the Guangdong power grid are shown in Fig.6.12 and Fig.6.13 As could be seen from the simulation test, CPS1 and CPS2 compliance both decrease as the installed wind power capacity penetration level increases. It could also be found that the value of wind penetration level limited by CPS1 standard is between 15% and 18%, and between 12% and 15% by CPS2.

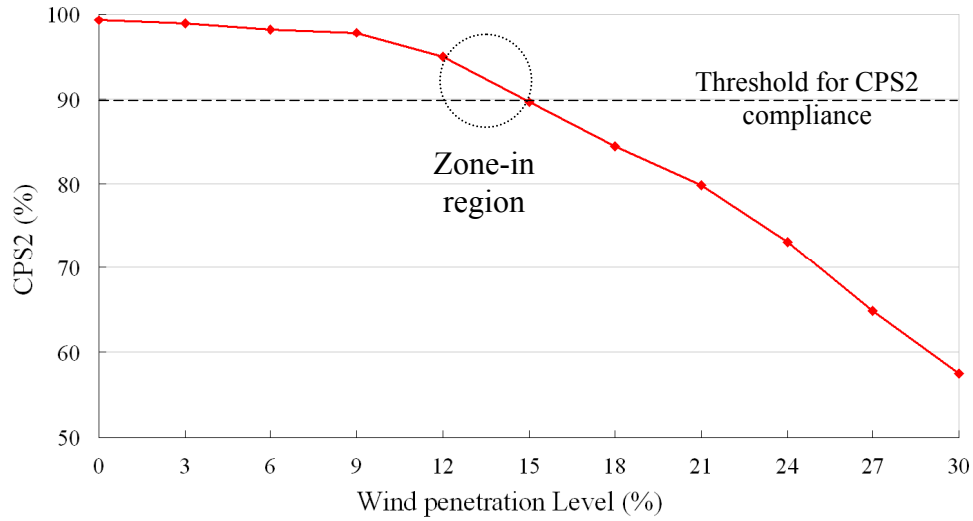

Fig. 6.13. Correlation between CPS2 compliance and wind penetration level

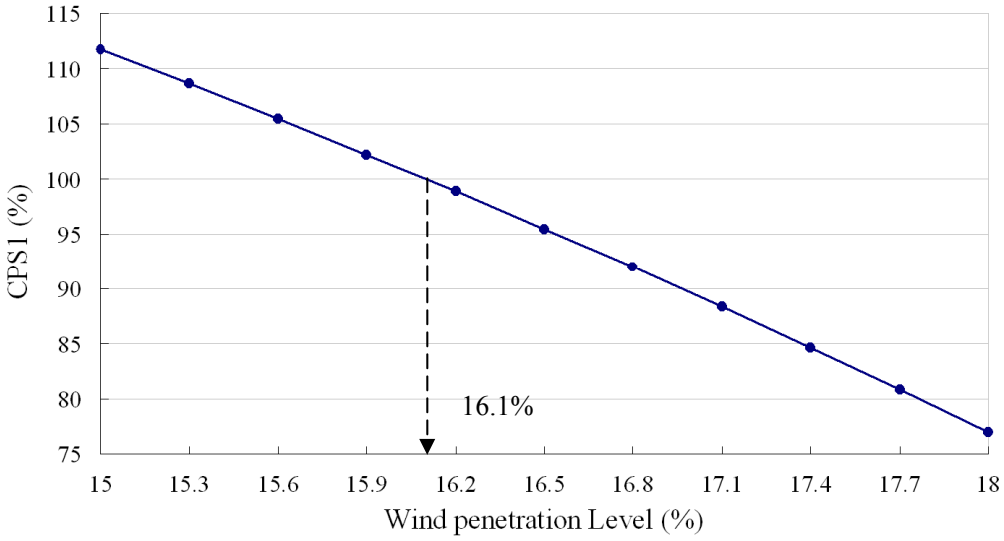

Fig. 6.14. Estimation of wind penetration level as limited by CPS1 index

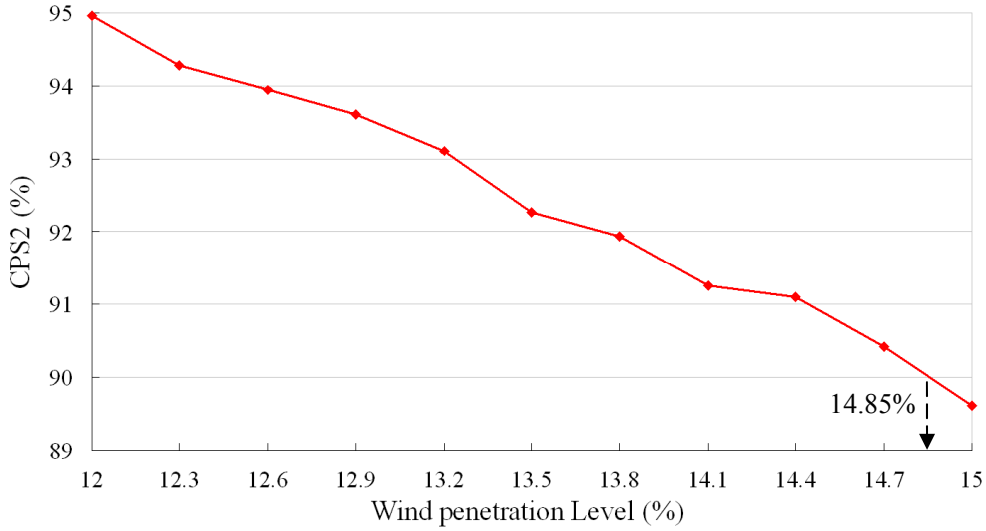

Fig. 6.15. Estimation of wind penetration level as limited by CPS2 index

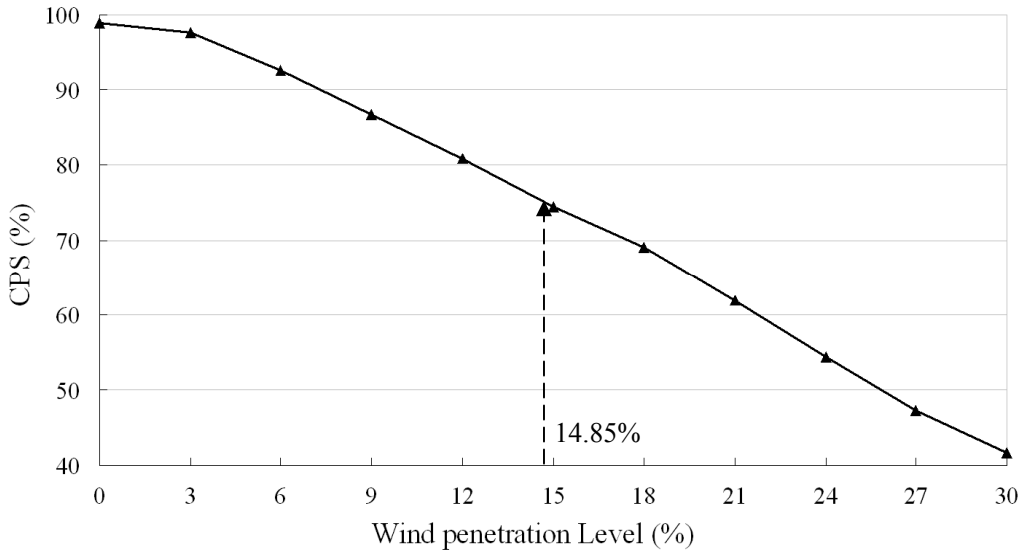

Fig. 6.16. Correlation between CPS compliance and wind penetration level

For more accurate estimation of the wind penetration limit by NERC's CPS standards for the Guangdong power grid, more simulations with a smaller incremental change (0.3%) to the wind penetration level were preformed. The results shown in Fig.6.14 and Fig.6.15 indicated that the wind penetration level as limited by CPS1 and CPS2 could reach approximately 16.1% and 14.85%, respectively. This concludes that, by following the analytical framework and CPS standards as presented here, the wind penetration level as limited by NERC's

CPS standards could reach to about 14.85% with an installed wind generation capacity of around 8975.4MW in the Guangdong power grid.

Fig.6.16 plots the CPS value, as determined with the criterion shown in Fig.6.1, against the installed capacity wind power penetration level. It clearly shows a downward trend and indicates that CPS would be deteriorated with the increasing wind penetration level. Taking 14.85% as the maximum wind power penetration level determined as suggested above using the CPS1 and CPS2 compliance criterion, the corresponding CPS would reduce to about 75%.

6.6 SUMMARY

Among all kinds of renewable energy sources, wind energy was introduced as the most promising one and a leading technology. Many technical and economical problems would rise when large amounts of wind generation are integrated into the existing power system. The estimation of maximum wind penetration level, which could be limited under various concepts, is becoming a pressing need.

This chapter focused on the estimation of maximum installed capacity penetration level. A novel framework has been built based on NERC's new AGC performance standards, CPS1 and CPS2, to quantify the wind penetration limit. In this chapter, CPS1 and CPS2 are not only adopted as the AGC performance standards, but also a criterion for assessing the wind penetration level limit. Simulation study on the China Southern Power Grid (CSG) power systems using recorded historical load and generation data and simulated wind data for a hypothetical wind farm revealed that a large amount of grid-connected wind farm would exert great influence on the AGC control of power systems. Both CPS1 and CPS2 indices would deteriorate with the increase in wind power penetration level, and the CPS1 and CPS2 compliance could hence be used as a criterion for

determining the installed capacity wind power penetration limit. Simulation results on the CSG power systems indicated that the wind power penetration limit could reach 14.85% with an installed wind generation capacity of around 8975.4MW in the Guangdong power grid.

CHAPTER VII CONCLUSIONS AND FUTURE WORK

7.1 CONCLUSIONS

Although Copenhagen Accord seems to be a daunting task for all 192 countries to sign up, yet the continually deteriorated environment is definitely the greatest concerns for humanity currently. Besides, every country is trying their best to develop smarter energy security strategies and policies to achieve a greener economy. Among all renewable resources, wind power is definitely the most promising and booming one because of its relatively low cost and relatively mature technology. However, various problems would rise if there were large amounts of wind integration into the existing power system. As the installed wind power generation capacities increase, power system planners and operators would face many new economic and technical challenges because of wind's variability and average predictability. Therefore, how to fit a large amount of wind generation into the existing grid is becoming a hot topic and also is the primary focus of this research work, which could be summarized as follows.

a) *Wind forecasting could be the key for solving wind generation output variation.*

With the increasing wind power capacities, power system planners and operators would face many new challenges because of wind's unique characteristics. The performance of a Wind Energy Conversion System would be constrained by many conditions, such as weather, location, and so on. In a modern electrical power system, variability is nothing new. However, wind is much harder to forecast comparing with the predictable load variations. A high-level wind penetration would exert great influence on power system planning and operation. Therefore, wind forecasting is extremely needed to

ensure power system reliability and reduce the cost of the whole power system operation in light of dealing with the variable outputs.

In terms of different forecasting time scales, there are three types of forecasting applications, long-term, medium-term, and short-term. Short-term forecasting seems to be more attractive and deeply explored since it could help to cutting down the costs of the whole power system in terms of dealing with variable-output generations. Other applications include the sale of wind energy in spot market, the optimization of wind power and other energy resources, the programming of short period maintenances, and so on.

The first contribution of this thesis is to propose a novel short-term wind forecasting model based on Ensemble Empirical Mode Decomposition (EEMD) and Support vector machine (Svm). The forecasting results were compared with a number of reference models. The proposed model has a key advantage over the others since it would decompose the wind data into residue and some IMF components via EEMD, which would make the corresponding forecasting time series stationary. The methodology developed would use EEMD to identify the intrinsic wind oscillatory modes by their characteristics time scales in the data empirically, and then decompose the wind speed time-series accordingly into different IMFs with corresponding frequencies and the residue component. The decomposition results from EMD and EEMD were compared with each other as well. Decomposition results from both a test function and real wind speed time series indicated that EEMD would indeed outperform EMD, i.e. more number of IMFs or smoother and more stationary IMFs were obtained via EEMD, which would lead to an improved forecasting accuracy. Afterwards, Svm would be adopted to forecast each individual component. In the end, Svm reconstructed all forecasting results to generate the final forecasting result. Moreover, the expected impacts of wind speed forecasting with improved accuracy were also specified

and analyzed. Experimental results obtained from the wind speed data recorded in Hong Kong and UK both verified that the new proposed model yields a more accurate forecasting result. The preliminary results also showed that a more accurate wind forecasting could reduce the system reserve requirement and increase the wind farm revenue. In other words, a robust wind forecast with higher forecasting accuracy would assist a large amount of wind power integration into the present grids in both technical and economic way.

b) *Wind penetration level could be estimated by analyzing the self-organized criticality of power system based on the complexity theory. The self-organized criticality of the power system would be companied by an increasing instantaneous wind power penetration level.*

From a system level viewpoint, the second contribution of this thesis is to assess the maximum wind penetration level by analyzing the self-organized criticality of power system with increasing wind penetration level. Instantaneous wind power penetration is the ratio of the wind power output to the total load demand at that specific moment. Lessons learnt from recently occurred blackouts suggested that studying the whole power system state is as crucial as evaluating individual components. This thesis focused on evaluating the maximum instantaneous wind power penetration level for a given power system limited by the self-organized criticality (SOC) of power system. SOC theory focuses on evaluating the global state of electricity system rather than just some single elements. Furthermore, this research works built a novel AC-based OPF blackout model and use the concept of Value-at-Risk (VaR) and Conditional Value-at-Risk (CVaR) to quantitatively assess this penetration level limit by evaluating the risk of loss of load. VaR measures the largest loss of load for a given confidence level. CVaR efficiently measures those extremely large losses of load for a given

confidence level. Under disturbances, the nonlinear dynamics of a system with SOC characteristics would vary abruptly to major disruptions spontaneously and show a power law tail characteristic. Extensive simulation studies on a modified IEEE 30-bus system and a modified IEEE 118-bus system verified that the probability distribution curve of loss of load indeed posed a power law tail characteristic when the power system is operating close to the maximum instantaneous penetration level. From different angles, the average loss of load, VaR, and CVaR fully described the change of the global system state when the wind generation output was increased to near the penetration level limit. Case studies show that the wind penetration level could be as high as about 50% for the modified IEEE 30-bus system and about 20% for the modified IEEE 118-bus system.

c) *NERC's new AGC performance standards would be deteriorated as being companied by an increasing installed wind generation capacity penetration.*

When large amounts of wind generation are integrated into the existing power system, the variability of wind would become a major concern. Assuming that wind generation could be treated as a negative load, the total load variations would be caused by both load variations and wind variations. Although variability is nothing new in a modern electrical power system, yet compared with the predictable load variations itself, it would be much more difficult to forecast the total load variations because of wind's average predictability. With the recent rapid development in power electronics and increasing demand pressure for generation with low-carbon emission, more and larger capacity grid-connected wind farms would contribute significantly to the grid security and operation.

Wind power fluctuations could be considered as a negative stochastic load

disturbance sources from the viewpoint of utilities. The corresponding more complicated and uncertain load variations would lead to a great influence on the frequency control of power systems. Automatic Generation Control (AGC) is one of the key control systems required for a satisfactory operation of interconnected power systems. AGC is aiming at maintaining the frequency of each control area and keeping the tie-line power close to the scheduled values by regulating the power generated from AGC generators to accommodate load demands variations. AGC performances in the normal interconnected power system operation are usually 'monitored and assessed by interchange power flow, system frequency and other guideline standards all the time'.

The third contribution of this thesis is to propose a novel methodology to estimate the maximum installed wind capacity penetration of power system, i.e. the ratio of the installed wind generation capacity to the total generation capacity on the system. Realistic simulations based on the representative and historical load and generation data from the China Southern Power Grid (CSG) power system and simulated wind data for a hypothetical wind farm have been carried out to study the impacts of high wind penetration on the AGC system. A novel framework was built based on NERC's new AGC performance standards, CPS1 and CPS2, to assess the maximum installed wind penetration level. Since both CPS1 and CPS2 indices would deteriorate with the increase in wind power penetration level, the CPS1 and CPS2 compliance were not only adopted as the AGC performance standards, but also a criterion for determining the installed capacity wind power penetration limit. Simulation results on the CSG power systems indicated that the maximum wind power penetration level could reach 14.85% with an installed wind generation capacity of around 8975.4MW in the Guangdong power grid.

7.2 FUTURE WORK

In this thesis, a novel wind forecasting model has been built. It has been proved that the power system reliability could be improved with more accurate wind forecasting. Yet in the future, practical applications of wind forecasting could be further explored. For example, another two crucial issues, the impact of wind forecasting on power system operation and power trading market [143], could be studied and analyzed in details.

In this thesis, the impacts of high wind penetration level on NERC's new AGC control standards and the SOC characteristics of power system have been presented. Further study shall be continued to investigate and analyze the impacts of wind power on power system stability including but not limited to voltage and frequency stability [144,145] and power quality [146]. By means of better voltage and reactive power supports, larger amount of wind energy on the grid and optimized integration of wind power could be achieved. The frequency response characteristic of different types of wind turbines shall be further studied and compared to establish a new frequency control loop to provide fast respond to the frequency drops, release kinetic energy stored in the rotating masses, and increase active power output of wind turbines to support the grid frequency and lower the rate of frequency change. The future work could also focus on the modeling of voltage fluctuation and flicker caused by integrated wind power, and methods of the voltage fluctuation evaluation and flicker measurement.

Last but not least, with the rapid development of distributed generation system, especially the worldwide application of renewable energy, the work later could also be extended with the consideration of economic cost to give the optimal suggestion for large wind farm installation, control, and other issues.

APPENDICES

APPENDIX I IEEE 30-BUS SYSTEM

- *One-line diagram*

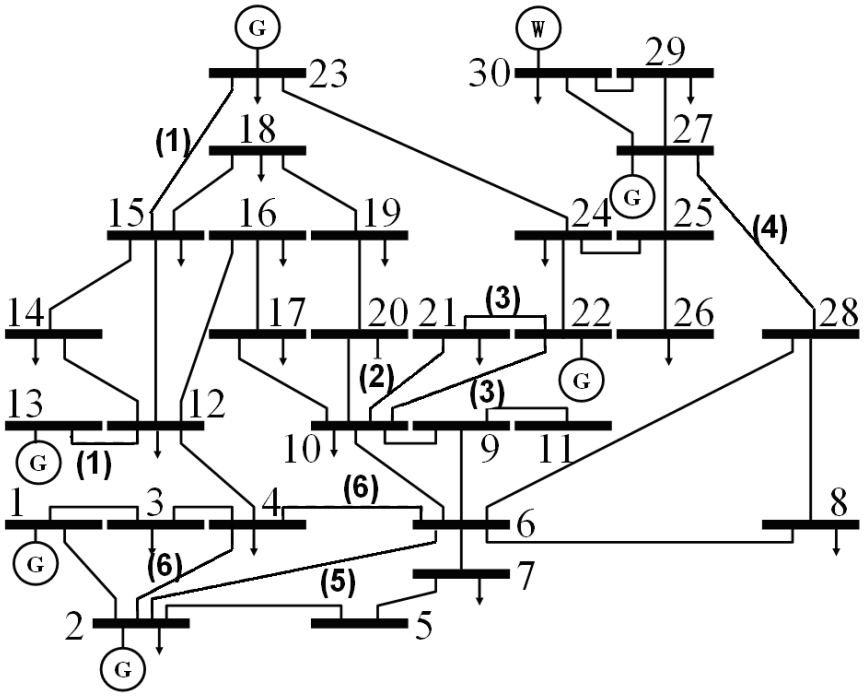

- *Bus and Demand Data*

Bus	P_L	Q_L	V	θ	Vmax	Vmin
1	0.00	0.00	1.0500	0.00000	1.05	0.95
2	21.70	12.70	1.0338	-2.7374	1.05	0.95
3	2.40	1.20	1.0309	-4.6722	1.05	0.95
4	7.60	1.60	1.0258	-5.5963	1.05	0.95
5	94.20	19.00	1.0058	-9.0005	1.05	0.95
6	0.00	0.00	1.0214	-6.4821	1.05	0.95
7	22.80	10.90	1.0073	-8.0435	1.05	0.95
8	30.00	30.00	1.0230	-6.4864	1.05	0.95
9	0.00	0.00	1.0583	-8.1508	1.05	0.95
10	5.80	2.00	1.0527	-10.0086	1.05	0.95
11	0.00	0.00	1.0913	-6.3003	1.05	0.95
12	11.20	7.50	1.0564	-9.2015	1.05	0.95

13	0.00	0.00	1.0883	-8.0216	1.05	0.95
14	6.20	1.60	1.0428	-10.0986	1.05	0.95
15	8.20	2.50	1.0393	-10.2212	1.05	0.95
16	3.50	1.80	1.0476	-9.8207	1.05	0.95
17	9.00	5.80	1.0459	-10.1598	1.05	0.95
18	3.20	0.90	1.0319	-10.8362	1.05	0.95
19	9.50	3.40	1.0307	-11.0109	1.05	0.95
20	2.20	0.70	1.0354	-10.8178	1.05	0.95
21	17.50	11.20	1.0404	-10.4668	1.05	0.95
22	0.00	0.00	1.0409	-10.4598	1.05	0.95
23	3.20	1.60	1.0314	-10.6662	1.05	0.95
24	8. 70	6.70	1.0292	-10.9159	1.05	0.95
25	0.00	0.00	1.0298	-10.8036	1.05	0.95
26	3.50	2.30	1.0124	-11.2117	1.05	0.95
27	0.00	0.00	1.0388	-10.4761	1.05	0.95
28	0.00	0.00	l.0177	-6.8955	1.05	0.95
29	2.40	0.90	1.0192	-11.6689	1.05	0.95
30	10.60	1.90	1.0080	-12.5242	1.05	0.95

- *Generation data*

Bus	P_G	Q_G	$Q_{G,max}$	$Q_{G,min}$	V	$P_{G,max}$	$P_{G,min}$
1	23.54	0	150	-20	1	80	0
2	60.97	0	60	-20	1	80	0
22	21.59	0	62.5	-15	1	50	0
27	26.91	0	48.7	-15	1	55	0
23	19.2	0	40	-10	1	30	0
13	37	0	44.7	-15	1	40	0

- *Branch data*

From	To	R	X	B	RateA	RateB	RateC
1	2	0.0192	0.0575	0.0264	130	130	130
1	3	0.0452	0.1852	0.0204	130	130	130
2	4	0.0570	0.1737	0.0184	65	65	65
3	4	0.0132	0.0379	0.0042	130	130	130

2	5	0.0472	0.1983	0.0209	130	130	130
2	6	0.0581	0.1763	0.0187	65	65	65
4	6	0.0119	0.0414	0.0045	90	90	90
5	7	0.0460	0.1160	0.0102	70	70	70
6	7	0.0267	0.0820	0.0085	130	130	130
6	8	0.0120	0.0420	0.0045	32	32	32
9	6	0.0000	0.2080	0.0000	65	65	65
6	10	0.0000	0.5560	0.0000	32	32	32
9	11	0.0000	0.2080	0.0000	65	65	65
9	10	0.0000	0.1100	0.0000	65	65	65
12	4	0.0000	0.2560	0.0000	65	65	65
12	13	0.0000	0.1400	0.0000	65	65	65
12	14	0.1231	0.2559	0.0000	32	32	32
12	15	0.0662	0.1304	0.0000	32	32	32
12	16	0.0945	0.1987	0.0000	32	32	32
14	15	0.2210	0.1997	0.0000	16	16	16
16	17	0.0824	0.1932	0.0000	16	16	16
15	18	0.1070	0.2185	0.0000	16	16	16
18	19	0.0639	0.1292	0.0000	16	16	16
19	20	0.0340	0.0680	0.0000	32	32	32
10	20	0.0936	0.2090	0.0000	32	32	32
10	17	0.0324	0.0845	0.0000	32	32	32
10	21	0.0348	0.0749	0.0000	32	32	32
10	22	0.0727	0.1499	0.0000	32	32	32
21	22	0.0116	0.0236	0.0000	32	32	32
15	23	0.1000	0.2020	0.0000	16	16	16
22	24	0.1150	0.1790	0.0000	16	16	16
23	24	0.1320	0.2700	0.0000	16	16	16
24	25	0.1885	0.3292	0.0000	16	16	16
25	26	0.2554	0.3800	0.0000	16	16	16
25	27	0.1093	0.2087	0.0000	16	16	16
28	27	0.0000	0.3960	0.0000	65	65	65

27	29	0.2198	0.4153	0.0000	16	16	16
27	30	0.3202	0.6027	0.0000	16	16	16
29	30	0.2399	0.4533	0.0000	16	16	16
8	28	0.0636	0.2000	0.0214	32	32	32
6	28	0.0169	0.0599	0.0065	32	32	32

APPENDIX II IEEE 118-BUS SYSTEM

- *One-line diagram*

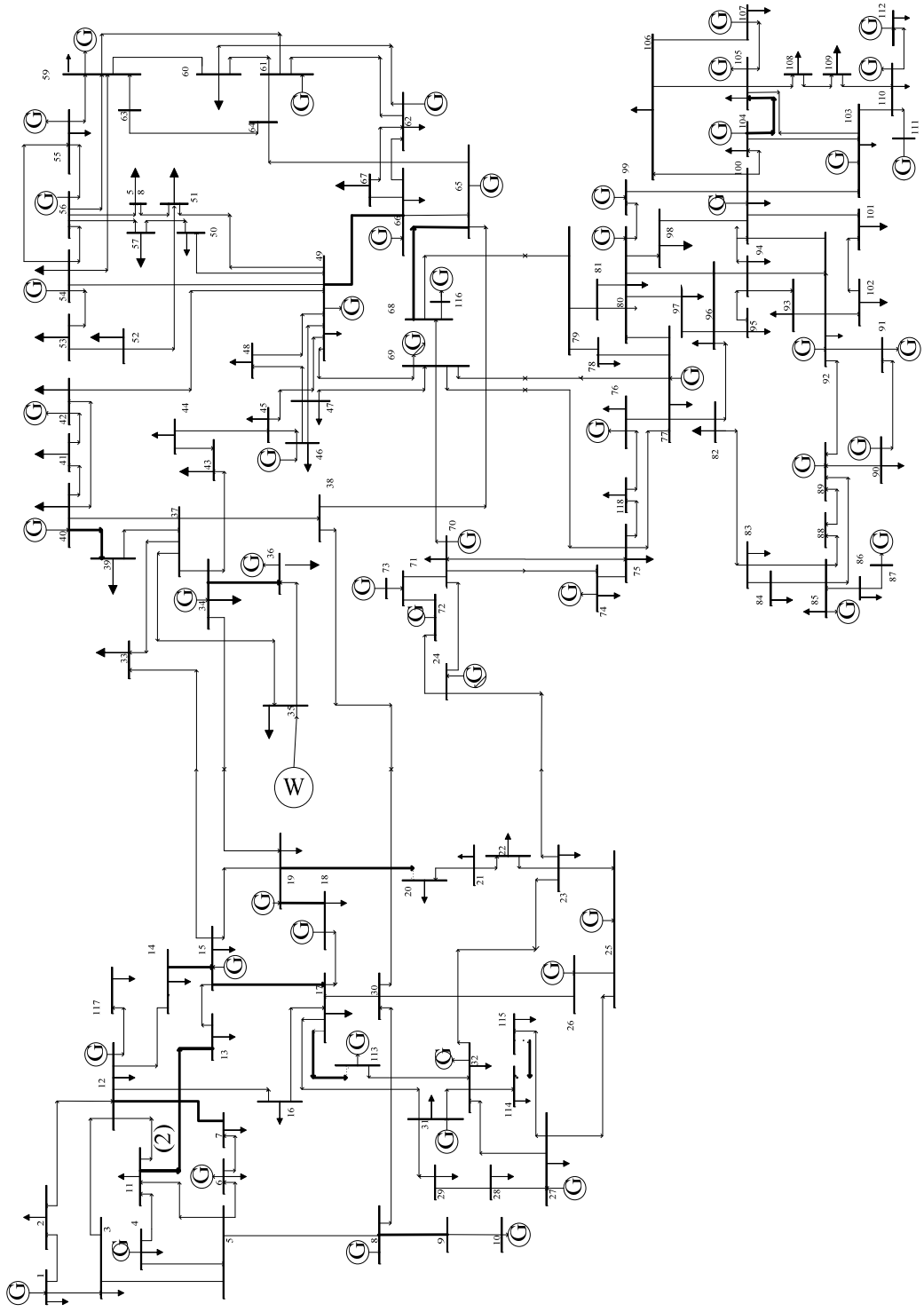

- *Bus and Demand Data*

Bus	P_L	Q_L	V	θ	Vmax	Vmin
1	51	27	0.955	10.983	1.06	0.94
2	20	9	0.97139	11.523	1.06	0.94
3	39	10	0.96769	11.866	1.06	0.94
4	39	12	0.998	15.583	1.06	0.94
5	0	0	1.00198	16.028	1.06	0.94
6	52	22	0.99	13.302	1.06	0.94
7	19	2	0.98933	12.857	1.06	0.94
8	28	0	1.015	21.049	1.06	0.94
9	0	0	1.04292	28.303	1.06	0.94
10	0	0	1.05	35.884	1.06	0.94
11	70	23	0.98509	13.016	1.06	0.94
12	47	10	0.99	12.499	1.06	0.94
13	34	16	0.9683	11.641	1.06	0.94
14	14	1	0.98359	11.783	1.06	0.94
15	90	30	0.97	11.489	1.06	0.94
16	25	10	0.98391	12.198	1.06	0.94
17	11	3	0.99513	14.006	1.06	0.94
18	60	34	0.973	11.793	1.06	0.94
19	45	25	0.963	11.314	1.06	0.94
20	18	3	0.95776	12.192	1.06	0.94
21	14	8	0.95841	13.779	1.06	0.94
22	10	5	0.96954	16.332	1.06	0.94
23	7	3	0.99972	21.249	1.06	0.94
24	13	0	0.992	21.118	1.06	0.94
25	0	0	1.05	28.184	1.06	0.94
26	0	0	1.015	29.965	1.06	0.94
27	71	13	0.968	15.613	1.06	0.94
28	17	7	0.96157	13.889	1.06	0.94
29	24	4	0.96322	12.897	1.06	0.94
30	0	0	0.98553	19.04	1.06	0.94

31	43	27	0.967	13.014	1.06	0.94
32	59	23	0.964	15.054	1.06	0.94
33	23	9	0.97161	10.864	1.06	0.94
34	59	26	0.986	11.505	1.06	0.94
35	33	9	0.9807	11.08	1.06	0.94
36	31	17	0.98	11.085	1.06	0.94
37	0	0	0.99208	11.969	1.06	0.94
38	0	0	0.96204	17.106	1.06	0.94
39	27	11	0.97049	8.598	1.06	0.94
40	66	23	0.97	7.525	1.06	0.94
41	37	10	0.96683	7.079	1.06	0.94
42	96	23	0.985	8.674	1.06	0.94
43	18	7	0.97858	11.459	1.06	0.94
44	16	8	0.98505	13.945	1.06	0.94
45	53	22	0.98667	15.776	1.06	0.94
46	28	10	1.005	18.582	1.06	0.94
47	34	0	1.01705	20.805	1.06	0.94
48	20	11	1.02063	20.025	1.06	0.94
49	87	30	1.025	21.028	1.06	0.94
50	17	4	1.00108	18.989	1.06	0.94
51	17	8	0.96688	16.37	1.06	0.94
52	18	5	0.95682	15.417	1.06	0.94
53	23	11	0.94598	14.442	1.06	0.94
54	113	32	0.955	15.353	1.06	0.94
55	63	22	0.952	15.063	1.06	0.94
56	84	18	0.954	15.25	1.06	0.94
57	12	3	0.97058	16.455	1.06	0.94
58	12	3	0.95904	15.598	1.06	0.94
59	277	113	0.985	19.452	1.06	0.94
60	78	3	0.99316	23.234	1.06	0.94
61	0	0	0.995	24.125	1.06	0.94
62	77	14	0.998	23.509	1.06	0.94

63	0	0	0.96874	22.831	1.06	0.94
64	0	0	0.98374	24.597	1.06	0.94
65	0	0	1.005	27.722	1.06	0.94
66	39	18	1.05	27.563	1.06	0.94
67	28	7	1.01968	24.923	1.06	0.94
68	0	0	1.00325	27.601	1.06	0.94
69	0	0	1.035	30	1.06	0.94
70	66	20	0.984	22.62	1.06	0.94
71	0	0	0.98684	22.209	1.06	0.94
72	12	0	0.98	21.112	1.06	0.94
73	6	0	0.991	21.998	1.06	0.94
74	68	27	0.958	21.671	1.06	0.94
75	47	11	0.96733	22.933	1.06	0.94
76	68	36	0.943	21.803	1.06	0.94
77	61	28	1.006	26.757	1.06	0.94
78	71	26	1.00342	26.453	1.06	0.94
79	39	32	1.00922	26.752	1.06	0.94
80	130	26	1.04	28.998	1.06	0.94
81	0	0	0.99681	28.149	1.06	0.94
82	54	27	0.98881	27.276	1.06	0.94
83	20	10	0.98457	28.465	1.06	0.94
84	11	7	0.97977	30.997	1.06	0.94
85	24	15	0.985	32.55	1.06	0.94
86	21	10	0.98669	31.181	1.06	0.94
87	0	0	1.015	31.44	1.06	0.94
88	48	10	0.98746	35.68	1.06	0.94
89	0	0	1.005	39.734	1.06	0.94
90	440	42	0.985	33.331	1.06	0.94
91	10	0	0.98	33.352	1.06	0.94
92	65	10	0.993	33.841	1.06	0.94
93	12	7	0.98737	30.837	1.06	0.94
94	30	16	0.99081	28.687	1.06	0.94

95	42	31	0.98111	27.716	1.06	0.94
96	38	15	0.9928	27.549	1.06	0.94
97	15	9	1.01143	27.923	1.06	0.94
98	34	8	1.02351	27.446	1.06	0.94
99	42	0	1.01	27.085	1.06	0.94
100	37	18	1.017	28.081	1.06	0.94
101	22	15	0.99276	29.649	1.06	0.94
102	5	3	0.99159	32.341	1.06	0.94
103	23	16	1.001	24.48	1.06	0.94
104	38	25	0.971	21.742	1.06	0.94
105	31	26	0.965	20.634	1.06	0.94
106	43	16	0.96114	20.379	1.06	0.94
107	50	12	0.952	17.576	1.06	0.94
108	2	1	0.96621	19.434	1.06	0.94
109	8	3	0.96703	18.982	1.06	0.94
110	39	30	0.973	18.135	1.06	0.94
111	0	0	0.98	19.78	1.06	0.94
112	68	13	0.975	15.036	1.06	0.94
113	6	0	0.993	14.004	1.06	0.94
114	8	3	0.96068	14.727	1.06	0.94
115	22	7	0.96053	14.72	1.06	0.94
116	184	0	1.005	27.166	1.06	0.94
117	20	8	0.97382	10.958	1.06	0.94
118	33	15	0.94944	21.945	1.06	0.94

- *Generation data*

Bus	P_G	Q_G	$Q_{G,max}$	$Q_{G,min}$	V	$P_{G,max}$	$P_{G,min}$
10	450	-51.04	200	-147	1.05	550	0
12	85	91.27	120	-35	0.99	185	0
25	220	49.72	140	-47	1.05	320	0
26	314	9.89	1000	-1000	1.015	414	0
31	7	31.57	300	-300	0.967	107	0
46	19	-5.25	100	-100	1.005	119	0

49	204	115.63	210	-85	1.025	304	0
54	48	3.9	300	-300	0.955	148	0
59	155	76.83	180	-60	0.985	255	0
61	160	-40.39	300	-100	0.995	260	0
65	391	80.76	200	-67	1.005	491	0
66	392	-1.95	200	-67	1.05	492	0
69	513.48	-82.39	300	-300	1.035	805.2	0
80	477	104.9	280	-165	1.04	577	0
87	4	11.02	1000	-100	1.015	104	0
92	607	0.49	9	-3	0.99	100	0
100	252	108.87	155	-50	1.017	352	0
103	40	41.69	40	-15	1.01	140	0
111	36	-1.84	1000	-100	0.98	136	0

- *Branch data*

From	To	R	X	B	RateA	RateB	RateC
1	2	0.0303	0.0999	0.0254	220	230	250
1	3	0.0129	0.0424	0.01082	220	230	250
2	12	0.0187	0.0616	0.01572	220	230	250
3	5	0.0241	0.108	0.0284	220	230	250
3	12	0.0484	0.16	0.0406	220	230	250
4	5	0.00176	0.00798	0.0021	440	460	500
4	11	0.0209	0.0688	0.01748	220	230	250
5	6	0.0119	0.054	0.01426	220	230	250
5	11	0.0203	0.0682	0.01738	220	230	250
6	7	0.00459	0.0208	0.0055	220	230	250
7	12	0.00862	0.034	0.00874	220	230	250
8	9	0.00244	0.0305	1.162	1100	1150	1250
8	5	0	0.0267	0	880	920	1000
8	30	0.00431	0.0504	0.514	220	230	250
9	10	0.00258	0.0322	1.23	1100	1150	1250
11	12	0.00595	0.0196	0.00502	220	230	250
11	13	0.02225	0.0731	0.01876	220	230	250
12	15	0.0215	0.0707	0.01816	220	230	250

12	17	0.0212	0.0834	0.0214	220	230	250
12	117	0.0329	0.14	0.0358	220	230	250
13	15	0.0744	0.2444	0.06268	220	230	250
14	15	0.0595	0.195	0.0502	220	230	250
15	17	0.0132	0.0437	0.0444	440	460	500
15	19	0.012	0.0394	0.0101	220	230	250
15	33	0.038	0.1244	0.03194	220	230	250
16	17	0.0454	0.1801	0.0466	220	230	250
17	19	0.0123	0.0505	0.01298	220	230	250
17	31	0.0474	0.1563	0.0399	220	230	250
17	113	0.00913	0.0301	0.00768	220	230	250
18	19	0.01119	0.0493	0.01142	220	230	250
19	20	0.0252	0.117	0.0298	220	230	250
19	34	0.0752	0.247	0.0632	220	230	250
20	21	0.0183	0.0849	0.0216	220	230	250
21	22	0.0209	0.097	0.0246	220	230	250
22	23	0.0342	0.159	0.0404	220	230	250
23	24	0.0135	0.0492	0.0498	220	230	250
23	25	0.0156	0.08	0.0864	440	460	500
23	32	0.0317	0.1153	0.1173	220	230	250
24	70	0.00221	0.4115	0.10198	220	230	250
24	72	0.0488	0.196	0.0488	220	230	250
25	27	0.0318	0.163	0.1764	440	460	500
26	25	0	0.0382	0	220	230	250
26	30	0.00799	0.086	0.908	660	690	750
27	28	0.01913	0.0855	0.0216	220	230	250
27	32	0.0229	0.0755	0.01926	220	230	250
27	115	0.0164	0.0741	0.01972	220	230	250
28	31	0.0237	0.0943	0.0238	220	230	250
29	31	0.0108	0.0331	0.0083	220	230	250
30	17	0	0.0388	0	660	690	750
30	38	0.00464	0.054	0.422	220	230	250
31	32	0.0298	0.0985	0.0251	220	230	250

32	113	0.0615	0.203	0.0518	220	230	250
32	114	0.0135	0.0612	0.01628	220	230	250
33	37	0.0415	0.142	0.0366	220	230	250
34	36	0.00871	0.0268	0.00568	220	230	250
34	37	0.00256	0.0094	0.00984	440	460	500
34	43	0.0413	0.1681	0.04226	220	230	250
35	36	0.00224	0.0102	0.00268	220	230	250
35	37	0.011	0.0497	0.01318	220	230	250
37	39	0.0321	0.106	0.027	220	230	250
37	40	0.0593	0.168	0.042	220	230	250
38	37	0	0.0375	0	660	690	750
38	65	0.00901	0.0986	1.046	440	460	500
39	40	0.0184	0.0605	0.01552	220	230	250
40	41	0.0145	0.0487	0.01222	220	230	250
40	42	0.0555	0.183	0.0466	220	230	250
41	42	0.041	0.135	0.0344	220	230	250
42	49	0.0715	0.323	0.086	220	230	250
42	49	0.0715	0.323	0.086	220	230	250
43	44	0.0608	0.2454	0.06068	220	230	250
44	45	0.0224	0.0901	0.0224	220	230	250
45	46	0.04	0.1356	0.0332	220	230	250
45	49	0.0684	0.186	0.0444	220	230	250
46	47	0.038	0.127	0.0316	220	230	250
46	48	0.0601	0.189	0.0472	220	230	250
47	49	0.0191	0.0625	0.01604	220	230	250
47	69	0.0844	0.2778	0.07092	220	230	250
48	49	0.0179	0.0505	0.01258	220	230	250
49	50	0.0267	0.0752	0.01874	220	230	250
49	51	0.0486	0.137	0.0342	220	230	250
49	54	0.073	0.289	0.0738	220	230	250
49	54	0.0869	0.291	0.073	220	230	250
49	66	0.018	0.0919	0.0248	440	460	500
49	66	0.018	0.0919	0.0248	440	460	500

49	69	0.0985	0.324	0.0828	220	230	250
50	57	0.0474	0.134	0.0332	220	230	250
51	52	0.0203	0.0588	0.01396	220	230	250
51	58	0.0255	0.0719	0.01788	220	230	250
52	53	0.0405	0.1635	0.04058	220	230	250
53	54	0.0263	0.122	0.031	220	230	250
54	55	0.0169	0.0707	0.0202	220	230	250
54	56	0.00275	0.00955	0.00732	220	230	250
54	59	0.0503	0.2293	0.0598	220	230	250
55	56	0.00488	0.0151	0.00374	220	230	250
55	59	0.04739	0.2158	0.05646	220	230	250
56	57	0.0343	0.0966	0.0242	220	230	250
56	58	0.0343	0.0966	0.0242	220	230	250
56	59	0.0825	0.251	0.0569	220	230	250
56	59	0.0803	0.239	0.0536	220	230	250
59	60	0.0317	0.145	0.0376	220	230	250
59	61	0.0328	0.15	0.0388	220	230	250
60	61	0.00264	0.0135	0.01456	440	460	500
60	62	0.0123	0.0561	0.01468	220	230	250
61	62	0.00824	0.0376	0.0098	220	230	250
62	66	0.0482	0.218	0.0578	220	230	250
62	67	0.0258	0.117	0.031	220	230	250
63	59	0	0.0386	0	440	460	500
63	64	0.00172	0.02	0.216	440	460	500
64	61	0	0.0268	0	220	230	250
64	65	0.00269	0.0302	0.38	440	460	500
65	66	0	0.037	0	220	230	250
65	68	0.00138	0.016	0.638	220	230	250
66	67	0.0224	0.1015	0.02682	220	230	250
68	69	0	0.037	0	440	460	500
68	81	0.00175	0.0202	0.808	220	230	250
68	116	0.00034	0.00405	0.164	440	460	500
69	70	0.03	0.127	0.122	440	460	500

69	75	0.0405	0.122	0.124	440	460	500
69	77	0.0309	0.101	0.1038	220	230	250
70	71	0.00882	0.0355	0.00878	220	230	250
70	74	0.0401	0.1323	0.03368	220	230	250
70	75	0.0428	0.141	0.036	220	230	250
71	72	0.0446	0.18	0.04444	220	230	250
71	73	0.00866	0.0454	0.01178	220	230	250
74	75	0.0123	0.0406	0.01034	220	230	250
75	77	0.0601	0.1999	0.04978	220	230	250
75	118	0.0145	0.0481	0.01198	220	230	250
76	77	0.0444	0.148	0.0368	220	230	250
76	118	0.0164	0.0544	0.01356	220	230	250
77	78	0.00376	0.0124	0.01264	220	230	250
77	80	0.017	0.0485	0.0472	440	460	500
77	80	0.0294	0.105	0.0228	220	230	250
77	82	0.0298	0.0853	0.08174	220	230	250
78	79	0.00546	0.0244	0.00648	220	230	250
79	80	0.0156	0.0704	0.0187	220	230	250
80	96	0.0356	0.182	0.0494	220	230	250
80	97	0.0183	0.0934	0.0254	220	230	250
80	98	0.0238	0.108	0.0286	220	230	250
80	99	0.0454	0.206	0.0546	220	230	250
81	80	0	0.037	0	220	230	250
82	83	0.0112	0.03665	0.03796	220	230	250
82	96	0.0162	0.053	0.0544	220	230	250
83	84	0.0625	0.132	0.0258	220	230	250
83	85	0.043	0.148	0.0348	220	230	250
84	85	0.0302	0.0641	0.01234	220	230	250
85	86	0.035	0.123	0.0276	220	230	250
85	88	0.02	0.102	0.0276	220	230	250
85	89	0.0239	0.173	0.047	220	230	250
86	87	0.02828	0.2074	0.0445	220	230	250
88	89	0.0139	0.0712	0.01934	440	460	500

89	90	0.0518	0.032	0.032	660	230	250
89	91	0.0099	0.032	0.065	220	220	220
89	92	0.0099	0.0505	0.065	220	690	750
90	91	0.0254	0.0505	0.065	660	230	250
91	92	0.0387	0.1272	0.032	220	230	250
92	93	0.0258	0.032	0.0218	220	230	250
92	94	0.0481	0.158	0.0406	220	230	250
92	100	0.0648	0.295	0.0472	220	230	250
92	102	0.0123	0.0559	0.01464	220	230	250
93	94	0.0223	0.0732	0.01876	220	230	250
94	95	0.0132	0.0434	0.0111	220	230	250
94	96	0.0269	0.0869	0.023	220	230	250
94	100	0.0178	0.058	0.0604	220	230	250
95	96	0.0171	0.0547	0.01474	220	230	250
96	97	0.0173	0.0885	0.024	220	230	250
98	100	0.0397	0.179	0.0476	220	230	250
99	100	0.018	0.0813	0.0216	220	230	250
100	101	0.0277	0.1262	0.0328	220	230	250
100	103	0.016	0.0525	0.0536	440	460	500
100	104	0.0451	0.204	0.0541	220	230	250
100	106	0.0605	0.229	0.062	220	230	250
101	102	0.0246	0.112	0.0294	220	230	250
103	104	0.0466	0.1584	0.0407	220	230	250
103	105	0.0535	0.1625	0.0408	220	230	250
103	110	0.03906	0.1813	0.0461	220	230	250
104	105	0.00994	0.0378	0.00986	220	230	250
105	106	0.014	0.0547	0.01434	220	230	250
105	107	0.053	0.183	0.0472	220	230	250
105	108	0.0261	0.0703	0.01844	220	230	250
106	107	0.053	0.183	0.0472	220	230	250
108	109	0.0105	0.0288	0.0076	220	230	250
109	110	0.0278	0.0762	0.0202	220	230	250
110	111	0.022	0.0755	0.02	220	230	250

110	112	0.0247	0.064	0.062	220	230	250
114	115	0.0023	0.0104	0.00276	220	230	250

REFERENCES

[1] "Green energy's future dims as economy slides," *CLIMATE,* from page 1, 2009.

[2] J. F. Li, P. F. Shi, J. L. Shi, L. J. Ma, H. Y. Qin, and Y. Q. Song, "China wind power report 2007," Beijing, November 01, 2007

[3] F. S. Wen, and Q. Wang, "Wind power generation in China: present status and future prospects," *Int. J. Energy Technology and Policy,* vol. 6, pp. 254 – 276, 2008.

[4] T. G. Barbounis*, et al.*, "Long-term wind speed and power forecasting using local recurrent neural network models," *IEEE Transactions on Energy Conversion,* vol. 21, pp. 273-284, Mar 2006.

[5] E. Muljadi*, et al.*, "Effect of variable speed wind turbine generator on stability of a weak grid," *IEEE Transactions on Energy Conversion,* vol. 22, pp. 29-36, Mar 2007.

[6] C. Abbey and G. Joos, "Effect of low voltage ride through (LVRT) characteristic on voltage stability," in *2005 IEEE Power Engineering Society General Meeting, Vols, 1-3*, pp. 1901-1907, 2005.

[7] R. D. Fernandez*, et al.*, "Contribution of wind farms to the network stability," in *2006 Power Engineering Society General Meeting, Vols 1-9*, pp. 704-709, 2006.

[8] F. M. Hughes*, et al.*, "Control of DFIG-based wind generation for power network support," *IEEE Transactions on Power Systems,* vol. 20, pp. 1958-1966, Nov 2005.

[9] Y. Wang and L. Xu, "Control of DFIG-Based wind generation systems under unbalanced network supply," in *IEEE IEMDC 2007: Proceedings*

of the International Electric Machines and Drives Conference, Vols 1 and 2, pp. 430-435, 2007.

[10] J. Morren*, et al.*, "Wind turbines emulating inertia and supporting primary frequency control," *IEEE Transactions on Power Systems,* vol. 21, pp. 433-434, Feb 2006.

[11] O. Anaya-Lara*, et al.*, "Contribution of DFIG-based wind farms to power system short-term frequency regulation," *IEE Proceedings-Generation Transmission and Distribution,* vol. 153, pp. 164-170, Mar 2006.

[12] G. Lalor*, et al.*, "Frequency control and wind turbine technologies," *IEEE Transactions on Power Systems,* vol. 20, pp. 1905-1913, Nov 2005.

[13] G. Fujita*, et al.*, "Dynamic characteristic of frequency control by rotary frequency converter to link wind farm and power system," in *Power Tech Conference Proceedings, 2003 IEEE Bologna*, Vol.2, 2003.

[14] F. W. Koch*, et al.*, "Dynamic simulation of large wind farms integrated in a multimachine network," in *Power Engineering Society General Meeting, 2003, IEEE*, Vol. 4, 2003.

[15] A. Larson, "Flicker Emission of Wind Turbines Caused by Switching Operations," *Power Engineering Review, IEEE,* vol. 22, pp. 59-59, 2002.

[16] T. Thiringer, "Power quality measurements performed on a low-voltage grid equipped with two wind turbines," *IEEE Transactions on Energy Conversion,* vol. 11, pp. 601-606, Sep 1996.

[17] G. Harding*, et al.*, "Wind turbines, flicker, and photosensitive epilepsy: Characterizing the flashing that may precipitate seizures and optimizing guidelines to prevent them," *Epilepsia,* vol. 49, pp. 1095-1098, Jun 2008.

[18] A. Larsson, "Flicker emission of wind turbines during continuous operation," *IEEE Transactions on Energy Conversion,* vol. 17, pp. 114-118, 2002.

[19] H. Sharma, S. Islam, and T. Pryor, "Power quality issues in a wind turbine driven induction generator and diesel hybrid autonomous grid," *Journal of Electrical and Electronics Engineering,* vol. 21, pp. 19-25, 2001.

[20] T. Thiringer*, et al.*, "Power quality impact of a sea located hybrid wind park," *IEEE Transactions on Energy Conversion,* vol. 16, pp. 123-127, Jun 2001.

[21] J. O. G. Tande, "Impact of wind turbines on voltage quality," in *Harmonics And Quality of Power, 1998. Proceedings. 8th International Conference on* 1998, vol.2, pp. 1158-1161.

[22] P. S. Dokopoulos, A. X. Patralexis, and I. M. Manousaridis, "Improvement of power quality distribution in a grid caused by wind turbines," in *the 8th international conference on harmonics and quality of power ICHQP'98, jointly organized by IEEE/PES and NTUA*, Athens, Greece, 1998.

[23] W. Z. Gandhare and G. R. Bhagwatikar, "Power pollution due to grid connected wind electric converter," in *Control Applications, 2000. Proceedings of the 2000 IEEE International Conference on* 2000, pp. 892-895.

[24] A. J. Covarrubias, "Expansion planning for electric power systems," *IAEA Bulletin,* vol. 21, pp. 55-64, 1979.

[25] H. Brannlund*, et al.*, "Optimal Short Term Operation Planning of a Large Hydrothermal Power System Based on a Nonlinear Network Flow Concept," *IEEE Transactions on Power Systems,* vol. 1, pp. 75-81, 1986.

[26] R. A. Smith and R. D. Shultz, "Operation Analysis in Generation Planning," *IEEE Transactions on Power Apparatus and Systems,* vol. PAS-102, pp. 1331-1339, 1983.

[27] T. Jen-Hao and Y. Chin-Ling, "Assessments for the Impacts and Benefits of Wind Farm Placement," in *TENCON 2005 2005 IEEE Region 10*, 2005, pp. 1-6.

[28] S. Roy, "Optimal planning of wind energy conversion systems over an energy scenario," *IEEE Transactions on Energy Conversion,* vol. 12, pp. 248-254, 1997.

[29] R. Billinton and W. Wangdee, "Reliability-Based Transmission Reinforcement Planning Associated With Large-Scale Wind Farms," *IEEE Transactions on Power Systems,* vol. 22, pp. 34-41, 2007.

[30] M. Behnke and A. Ellis, "Reactive power planning for wind power plant interconnections," in *Power and Energy Society General Meeting - Conversion and Delivery of Electrical Energy in the 21st Century, 2008 IEEE*, pp. 1-4, 2008.

[31] S. X. Chen and H. B. Gooi, "Capacitor planning of power systems with wind generators and PV arrays," in *TENCON 2009 - 2009 IEEE Region 10 Conference*, 2009, pp. 1-5.

[32] A. Uehara*, et al.*, "Study on optimum operation planning of wind farm/battery system using forecasted power data," in *Power Electronics and Drive Systems, 2009. PEDS 2009. International Conference on* 2009, pp. 907-912.

[33] L. Soder, "Reserve margin planning in a wind-hydro-thermal power system," *IEEE Transactions on Power Systems,* vol. 8, pp. 564-571, 1993.

[34] D. R. Joshi and S. H. Jangamshetti, "A Novel Method to Estimate the O&M Costs for the Financial Planning of the Wind Power Projects Based on Wind Speed-A Case Study," *IEEE Transactions on Energy Conversion,* vol. 25, pp. 161-167.

[35] S. Roy, "Market Constrained Optimal Planning for Wind Energy Conversion Systems over Multiple Installation Sites," *Power Engineering Review, IEEE,* vol. 22, pp. 67-67, 2002.

[36] W. Yuan-Kang and H. Jing-Shan, "A literature review of wind forecasting technology in the world," in *Power Tech, 2007 IEEE Lausanne*, pp. 504-509, 2007.

[37] B. Ernst*, et al.*, "Predicting the Wind," *Power and Energy Magazine, IEEE,* vol. 5, pp. 78-89, 2007.

[38] L. Landberg, "Short-term prediction of the power production from wind farms," *Journal of Wind Engineering and Industrial Aerodynamics,* vol. 80, pp. 207-220, 1999.

[39] M. S. M. Milligan, Y.-H. Wan, "Statistical Wind Power Forecasting Models: Results for U.S. Wind Farms," in *Wind Power 2003*, Austin, Texas, 2003.

[40] J. W. Taylor*, et al.*, "Wind Power Density Forecasting Using Ensemble Predictions and Time Series Models," *IEEE Transactions on Energy Conversion,* vol. 24, pp. 775-782, 2009.

[41] G. Sideratos and N. D. Hatziargyriou, "An advanced statistical method for wind power forecasting," *IEEE Transactions on Power Systems,* vol. 22, pp. 258-265, Feb 2007.

[42] G. N. Kariniotakis*, et al.*, "Wind power forecasting using advanced neural networks models," *IEEE Transactions on Energy Conversion,* vol. 11, pp. 762-767, Dec 1996.

[43] I. G. Damousis*, et al.*, "A fuzzy model for wind speed prediction and power generation in wind parks using spatial correlation," *IEEE Transactions on Energy Conversion,* vol. 19, pp. 352-361, Jun 2004.

[44] C. W. Potter and M. Negnevitsky, "Very short-term wind forecasting for Tasmanian power generation," *IEEE Transactions on Power Systems,* vol. 21, pp. 965-972, 2006.

[45] M. A. Mohandes*, et al.*, "Support vector machines for wind speed prediction," *Renewable Energy,* vol. 29, pp. 939-947, 2004.

[46] A. S. R. Samsudin and P. Saad, "A Comparison of Time Series Forecasting using Support Vector Machineand Artificial Neural Network Model," Journal of Applied Sciences, pp. 950-958, 2010.

[47] F. Shu*, et al.*, "Forecasting the Wind Generation Using a Two-Stage Network Based on Meteorological Information," *IEEE Transactions on Energy Conversion,* vol. 24, pp. 474-482, 2009.

[48] M. C. Alexiadis*, et al.*, "Wind speed and power forecasting based on spatial correlation models," *IEEE Transactions on Energy Conversion,* vol. 14, pp. 836-842, Sep 1999.

[49] L. Soder, "Reserve Margin Planning in a Wind-Hydro-Thermal Power-System," *IEEE Transactions on Power Systems,* vol. 8, pp. 564-571, May 1993.

[50] B. Kuri and F. R. Li, "Generation Scheduling in a system with Wind Power," presented at the Transmission and Distribution Conference and Exhibition: Asia and Pacific, 2005 IEEE/PES 2005.

[51] R. Billinton and W. Wangdee, "Reliability-based transmission reinforcement planning associated with large-scale wind farms," *IEEE Transactions on Power Systems,* vol. 22, pp. 34-41, Feb 2007.

[52] R. Karki and J. Patel, "Transmission system adequacy evaluation considering wind power," in *Electrical and Computer Engineering, 2005. Canadian Conference on* 2005, pp. 490-493.

[53] A. Fabbri, *et al.*, "Assessment of the Cost Associated With Wind Generation Prediction Errors in a Liberalized Electricity Market," *IEEE Transactions on Power Systems,* vol. 20, pp. 1440-1446, 2005.

[54] J. L. Rodriguez-Amenedo, *et al.*, "Automatic generation control of a wind farm with variable speed wind turbines," *IEEE Transactions on Energy Conversion,* vol. 17, pp. 279-284, Jun 2002.

[55] H. Banakar, *et al.*, "Impacts of wind power minute-to-minute variations on power system operation," *IEEE Transactions on Power Systems,* vol. 23, pp. 150-160, Feb 2008.

[56] P. Kundur, *Power System Stability and Control*. New York: McGraw-Hill, 1994.

[57] I. Egido, *et al.*, "Evaluation of Automatic Generation Control (AGC) regulators by performance indices using data from real operation," *IET Generation Transmission & Distribution,* vol. 1, pp. 294-302, Mar 2007.

[58] D. N. Ewart, "Automatic Generation Control Performance Under Normal Conditions-Systems Engineering for Power: Status and Prospects," pp. 1-14, 1975.

[59] M. R. Stambach and D. N. Ewart, "Dynamics of Interconnected Power Systems: A Tutorial for System Dispatchers and Plant Operators," Electric Power Research Institute Report EL6360-L, 1989.

[60] *Control Performance Criteria Training Document*. North American Electric Reliability Council (NERC), Aug. 1996.

[61] N. Jaleeli, *et al.*, "Understanding automatic generation control," *IEEE Transactions on Power Systems,* vol. 7, pp. 1106-1122, 1992.

[62] R. P. Schulte, "An automatic generation control modification for present demands on interconnected power systems," *IEEE Transactions on Power Systems,* vol. 11, pp. 1286-1291, Aug 1996.

[63] L. P. Kumar and D. P. Kothari, "Recent philosophies of automatic generation control strategies in power systems," *IEEE Transactions on Power Systems,* vol. 20, pp. 346-357, Feb 2005.

[64] N. Jaleeli and L. S. VanSlyck, "NERC's new control performance standards," *IEEE Transactions on Power Systems,* vol. 14, pp. 1092-1099, 1999.

[65] "NERC Performance Subcommittee, & Control Criteria," Task Force meeting minutes 1991 to date.

[66] N. Jalceli and L. S. VanSlyck, "Control Performance Standards and Procedures for Interconnected Operation," April, 1997.

[67] R. P. Schulte*, et al.*, "Modified Automatic Time Error Control and Inadvertent Interchange Reduction for the Wscc Interconnected Power-Systems," *IEEE Transactions on Power Systems,* vol. 6, pp. 904-913, Aug 1991.

[68] (2005). *Standard BAL-001-Control Performance Standard*. Available: http://standard.nerc.net/

[69] P. Bak, C. Tang, and K. Wiesenfeld, "Self-Organized Criticality: An Explanation of 1/f Noise. Phys," *Physical Review Letters,* vol. 59, pp. 381-384, 1987.

[70] H. J. Jensen, *Self-Organized Criticality*: Cambridge University, 1998.

[71] B. A. Carreras*, et al.*, "Initial evidence for self-organized criticality in electric power system blackouts," in *System Sciences, 2000. Proceedings of the 33rd Annual Hawaii International Conference on* 2000.

[72] Kim Christensen and Nicholas R. Moloney, *Complexity And Criticality*: Imperial College Press, 2005.

[73] P. Bak, *How Nature Works: The Science of Self-Organized Criticality*. New York: Springer-Verlag, 1996.

[74] I. Dobson, *et al.*, "A probabilistic loading-dependent model of cascading failure and possible implications for blackouts," in *System Sciences, 2003. Proceedings of the 36th Annual Hawaii International Conference on* 2003.

[75] I. Dobson, *et al.*, "Branching Process Models for the Exponentially Increasing Portions of Cascading Failure Blackouts," in *System Sciences, 2005. HICSS '05. Proceedings of the 38th Annual Hawaii International Conference on* 2005, pp. 64-64.

[76] J. Chen, *et al.*, "Cascading dynamics and mitigation assessment in power system disturbances via a hidden failure model," *International Journal of Electrical Power & Energy Systems,* vol. 27, pp. 318-326, May 2005.

[77] R. Baldick, *et al.*, "Initial review of methods for cascading failure analysis in electric power transmission systems," in *IEEE Power & Energy Society General Meeting,* pp. 52-59, 2008.

[78] D. P. Nedic, *et al.*, "Criticality in a cascading failure blackout model," *International Journal of Electrical Power & Energy Systems,* vol. 28, pp. 627-633, Nov 2006.

[79] S. W. Mei, *et al.*, "Blackout model based on OPF and its self-organized criticality," in *2006 Chinese Control Conference,* pp. 758-763, 2006.

[80] A. Gonzalez, *et al.*, "The role of hydrogen in high wind energy penetration electricity systems: The Irish case," *Renewable Energy,* vol. 29, pp. 471-489, Apr 2004.

[81] D. Weisser and R. S. Garcia, "Instantaneous wind energy penetration in isolated electricity grids: concepts and review," *Renewable Energy,* vol. 30, pp. 1299-1308, Jul 2005.

[82] G. Hassan, "Study into the impacts of increased levels of wind penetration on the Irish electricity systems: First Interim Report," University College Cork, 2002.

[83] C. L. Luo*, et al.*, "Estimation of wind penetration as limited by frequency deviation," *IEEE Transactions on Energy Conversion,* vol. 22, pp. 783-791, Sep 2007.

[84] E. Vittal*, et al.*, "Wind penetration limited by thermal constraints and frequency stability," in *2007 39th North American Power Symposium,* pp. 353-359, 2007.

[85] I. D. Margaris*, et al.*, "Methods for evaluating penetration levels of wind generation in autonomous systems," in *PowerTech, 2009 IEEE Bucharest*, 2009, pp. 1-7.

[86] H. T. Le and S. Santoso, "Analysis of Voltage Stability and Optimal Wind Power Penetration Limits for a Non-radial Network with an Energy Storage System," in *Power Engineering Society General Meeting,* pp. 1-8, 2007.

[87] S. A. Papathanassiou and N. G. Boulaxis, "Power limitations and energy yield evaluation for wind farms operating in island systems," *Renewable Energy,* vol. 31, pp. 457-479, Apr 2006.

[88] A. I. Tsouchnikas and N. D. Hatziargyriou, "Probabilistic analysis of isolated power systems with wind power penetration limitations," in *2006 International Conference on Probabilistic Methods Applied to Power Systems,* pp. 73-78, 2006.

[89] J. W. Park*, et al.*, "Instantaneous Wind Power Penetration in Jeju Island," in *2008 IEEE Power & Energy Society General Meeting,* pp. 4063-4069, 2008.

[90] *Global Wind 2008 Report*. Available: http://www.gwec.net/index.php?id=153

[91] (Oct. 2008). *Danish Annual Energy Statistics 2007*. Available: http://www.ens.dk/graphics/UK_Facts_Figures/Statistics/yearly_statistics/2007/energy%20statistics%202007%20uk.pdf.

[92] (Feb 2, 2009). *Spain wind power firms see steady growth in 2009*. Available: http://www.reuters.com/article/idUSTRE51136D20090202

[93] (Nov. 10, 2009). *Spain's wind turbines supply half of the national power grid*. Available: http://business.timesonline.co.uk/tol/business/industry_sectors/natural_resources/article6910298.ece

[94] (Jan. 04, 2010). *China ranks third in worldwide wind energy - Alternative energy news*. Available: http://www.instalbiz.com/news/3-full-news-cn-china-ranks-third-in-worldwide-wind-energy_129.html.

[95] E. Golding, *The Generation of Electricity by Wind Power*. New York: Halsted Press, 1976.

[96] A. Balouktsis, *et al.*, "A nomogram method for estimating the energy produced by wind turbine generators," *Solar Energy,* vol. 72, pp. 251-259, 2002.

[97] S. H. Jangamshetti and V. G. Rau, "Site matching of wind turbine generators: A case study," *IEEE Transactions on Energy Conversion,* vol. 14, pp. 1537-1543, Dec 1999.

[98] R. B. Corotis, *et al.*, "Probability Models of Wind Velocity Magnitude and Persistence," *Solar Energy,* vol. 20, pp. 483-493, 1978.

[99] A. Garcia, *et al.*, "Fitting wind speed distributions: A case study," *Solar Energy,* vol. 62, pp. 139-144, Feb 1998.

[100] P. M. Anderson and A. Bose, "Stability simulation of wind turbine systems," *IEEE Transactions on Power Apparatus and Systems,* pp. 3791-3795, 1983.

[101] Z. Lubosny, *Wind Turbine Operation in Electric Power Systems – Advanced modelling*: Springe Verlag, 2003.

[102] T. Sun*, et al.*, "Voltage recovery of grid-connected wind turbines with DFIG after a short-circuit fault," in *Pesc 04: 2004 IEEE 35th Annual Power Electronics Specialists Conference, Vols 1-6, Conference Proceedings*, pp. 1991-1997, 2004.

[103] V. Akhmatov and A. H. Nielsen, "A small test model of the transmission grid with a large offshore wind farm for education and research at technical university of Denmark," in *2006 IEEE/PES Power Systems Conference and Exposition. Vols 1-5*, pp. 650-654, 2006.

[104] G. Giebel, G. Kariniotakis, and R. Brownsword, (July 2003). *The State-Of-The-Art in Short-Term Prediction of Wind Power: A literature overview*. Available: http://anemos.cma.fr

[105] G. Kariniotakis, *et al.*, "What performance can be expected by short-term wind power prediction models depending on site characteristics," in *European Wind Energy Association Conference, (EWEC'04)*, London, UK, 2004.

[106] N. H. Chan, *Time series – Applications to Finance (Wiley Series in Probability and Statistics)*: Wiley-Interscience, 2002.

[107] N. E. Huang, *et al.*, "The empirical mode decomposition and the Hilbert spectrum for nonlinear and non-stationary time series analysis," in *Proceedings of the Royal Society A: Mathematical, Physical and Engineering Sciences 454*, 1998, pp. 903-995.

[108] Z.Wu and N. E. Huang, "Ensemble empirical mode decomposition: a noise-assisted data analysis method," *Advances in Adaptive Data Analysis,* vol. 1, pp. 1-41, 2009.

[109] Z.Wu and N. E. Huang, "Ensemble empirical mode decomposition: a noise-assisted data analysis method," Centre for Ocean-Land-Atmosphere Studies,Technical Report2005.

[110] V. N. Vapnik, *The Nature of Statistical Learning Theory*. New York: Springer-Verlag, 1995.

[111] H. W. Kuhn and A. W. Tucker, "Nonlinear programming," in *Proc. 2th Berkeley Symp. Mathematical Statistics and Probabilistics*, Berkeley, CA: Univ, 1951, pp. 481 - 492.

[112] A. K. Johan, *Least Squares Support Vector Machines*: NJ: World Scientific, 2002.

[113] Y. T. Zhang, K. W. Chan, P. Zhang, D. Y. Yang and G.W. Cai, "Short-term Wind Forecasting Based on EMD and Statistical Models," presented at the 16th International Conference on Electrical Engineering, Busan Korea, 2010.

[114] R. Doherty and M. O'Malley, "Quantifying reserve demands due to increasing wind power penetration," in *Power Tech Conference Proceedings, 2003 IEEE Bologna*, 2003.

[115] R. Billinton and R. N. Allan, *Reliability Evaluation of Power System*: Springer, 1996.

[116] R. Piwko*, et al.*, "Wind energy delivery issues [transmission planning and competitive electricity market operation]," *Power and Energy Magazine, IEEE,* vol. 3, pp. 47-56, 2005.

[117] S. Heier, *Grid Integration of Wind Energy Conversion Systems*: John Wiley & Sons, 1998.

[118] M. Shengwei, *et al.*, "An Improved OPA Model and Blackout Risk Assessment," *IEEE Transactions on Power Systems,* vol. 24, pp. 814-823, 2009.

[119] J.P.Morgan, *RiskMetrics-Technical Document*. New York, 1996.

[120] P. Artzner, F. Delbaen, Jean-Marc Eber and David Heath, "Coherent Measures of Risk," *Mathematical Finance,* vol. 9, pp. 203-228, 25 Dec 2001.

[121] R.T. Rockafellar and S. Uryasev, "Optimization of Conditional Value-at-risk," *Journal of Risk,* vol. 2, pp. 21-41, 2000.

[122] S. A. Blumsack, "Network Topologies and Transmission Investment under Electric-Industry Restructuring," Ph.D. dissertation, Carnegie Mellon. University, May 2006.

[123] A. Feliachi and D. Rerkpreedapong, "NERC compliant load frequency control design using fuzzy rules," *Electric Power Systems Research,* vol. 73, pp. 101-106, Feb 2005.

[124] "Policy 1—Generation Control and Performance in Operating Manual," North American Electric Reliability Council (NERC), Dec. 1996.

[125] "Control Performance Standard Limits (1997)," North American Electric Reliability Council (NERC),1998.

[126] D. X. Wang, "Study of CPS standard in East China Power Grid," *Automation of Electric Power Systems,* vol. 24, pp. 41-44, 2000.

[127] G. Gross and J. W. Lee, "Analysis of load frequency control performance assessment criteria," *IEEE Transactions on Power Systems,* vol. 16, pp. 520-525, Aug 2001.

[128] T. Sasaki and K. Enomoto, "Statistical and dynamic analysis of generation control performance standards," *IEEE Transactions on Power Systems,* vol. 17, pp. 476-481, May 2002.

[129] T. Sasaki and K. Enomoto, "Dynamic analysis of generation control performance standards," *IEEE Transactions on Power Systems,* vol. 17, pp. 806-811, Aug 2002.

[130] M. Yao*, et al.*, "AGC logic based on NERC's new control performance standard and disturbance control standard," in *Power Engineering Society Summer Meeting, 2000. IEEE*, 2000.

[131] N. B. Hoonchareon*, et al.*, "Feasibility of decomposing (ACE)over-bar(1) to identify the impact of selected loads on CPS1 and CPS2," *IEEE Transactions on Power Systems,* vol. 17, pp. 752-756, Aug 2002.

[132] (Nov. 1996). *Control Performance Standard and Disturbance Control Standard Frequently Asked Questions*.

[133] Z. H. Gao, X. L. Teng, and L. Q. Tu, "Hierarchical AGC mode and CPS control strategy for interconnected power systems," *Automation of Electric Power Systems,* vol. 28, pp. 78-81, 2004.

[134] Z. H. Gao, X. L. Teng, and X. B. Zhang, "CPS control strategy for interconnected power systems," *Automation of Electric Power Systems,* vol. 19, pp. 40-44, 2005.

[135] J. Michalakes, S. Chen, J. Dudhia, L. Hart, J. Klemp, J. Middlecoff, W. Skamarock, "Development of a Next Generation Regional Weather Research and Forecast Model," in *Developments in Teracomputing: Proceedings of the Ninth ECMWF Workshop on the Use of High Performance Computing in Meteorology*, Singapore, 2001, pp. 269-276.

[136] NCEP FNL Operational Model Global Tropospheric Analyses Data [Online]. Available: http://dss.ucar.edu/datasets/ds083.2/

[137] M. Gibescu*, et al.*, "Statistical wind speed interpolation for simulating aggregated wind energy production under system studies," in *2006*

International Conference on Probabilistic Methods Applied to Power Systems, Vols 1 and 2, pp. 1101-1107, 2006.

[138] T. Yu, L. Chen, and G. L. Cai, "CPS Statistic Information Self-learning Methodology Based Adaptive Automatic Generation Control," in *Proceedings of CSEE*, pp. 45-49, May 2008.

[139] V. Kola, A. Bose, and P. M. Anderson, "Power Plant Models for Operating Training Simulators," *IEEE Transactions on Power Systems,* vol. 4, pp. 559-565, May 1989.

[140] K. Methaprayoon*, et al.*, "An integration of ANN wind power estimation into UC considering the forecasting uncertainty," in *Industrial and Commercial Power Systems Technical Conference, 2005 IEEE*, pp. 116-124, 2005.

[141] M. Yao, R. R. Shoults, R. Kelm, "AGC Logic Based on NERC's New Control Performance Standard and Disturbance Control Standard," *IEEE Transactions on Power System,* vol. 15, pp. 855-857, 2000.

[142] "The Operation Mode of China Southern Power Grid in 2010," China Southern Power Grid Co. Ltd.

[143] M. Ahlstrom, L. Jones, R. Zavadil, and W. Grant, "The future of wind forecasting and utility operations," *Power and Energy Magazine, IEEE* , vol.3, no.6, pp. 57- 64, Nov.-Dec. 2005.

[144] E. Vittal, M. O'Malley, A. Keane , "A Steady-State Voltage Stability Analysis of Power Systems With High Penetrations of Wind," *IEEE Transactions on Power Systems*, vol.25, no.1, pp.433-442, Feb. 2010.

[145] I. Erlich, K. Rensch, F. Shewarega, "Impact of large wind power generation on frequency stability," *Power Engineering Society General Meeting, 2006. IEEE,* pp. 8.

[146] S. A. Papathanassiou, F. Santjer, "Power-quality measurements in an autonomous island grid with high wind penetration," *IEEE Transactions on Power Delivery*, vol.21, no.1, pp. 218- 224, Jan. 2006.